1-1-1985

Age and Structural Relations of Granites, Stony Creek Area, Connecticut

McLellan, Eileen L.

Stockman, Stephanie

AGE AND STRUCTURAL RELATIONS OF GRANITES, STONY CREEK AREA, CONNECTICUT

Eileen L. McLellan and Stephanie Stockman
University of Maryland

INTRODUCTION

The Stony Creek gneiss dome of coastal Connecticut is a possible diapiric structure containing four distinct granitic (sensu latu) units. These show variably concordant to discordant contacts to associated Pre-Cambrian metasediments. The field trip will offer an opportunity to discuss the origins (intrusive, extrusive or anatectic) and ages (Pre-Cambrian? Acadian? Alleghanian?) of the granitic units, and their relations to the metamorphic and structural history of the area. In particular, discussion will center on:

(i) possible polymetamorphism and associated melting of basement material, and

(ii) possible relations between melt segregation and shear deformation.

This roadlog presents preliminary petrographic, structural and chemical data. Rb/Sr dating of the various granitic units is in progress, and results should be available at the time of the field trip.

A sketch map showing approximate locations of stops is shown in Fig. 1.

REGIONAL SETTING

The Stony Creek gneiss dome lies at the intersection of two major structural trends (Fig. 2). It is the westernmost of a series of gneiss domes extending E-W along the Connecticut coast from just east of New Haven to the Rhode Island border. It also lies on the southernmost extension of the Bronson Hill Anticlinorium.

Rocks in the core of the Stony Creek dome have been mapped as intermixed Sterling Plutonic Group and Plainfield Formation (Dale, 1923). This interpretation implies correlation with rocks in the core of the Lyme dome to the east, and this in turn is correlated with the Hope Valley terrain of southwestern Rhode Island (Loughlin, 1910). The Hope Valley terrain is ~ 600m.y. in age (Hermes et al., 1981; Gromet and O'Hara, this volume). In support of possible correlation, Hills and Dasch (1972) obtained a 616m.y. Rb/Sr whole-rock age on the Stony Creek. However, the interpretation of this age presents some difficulty in view of the large error (± 78m.y.) and poorly-controlled sampling.

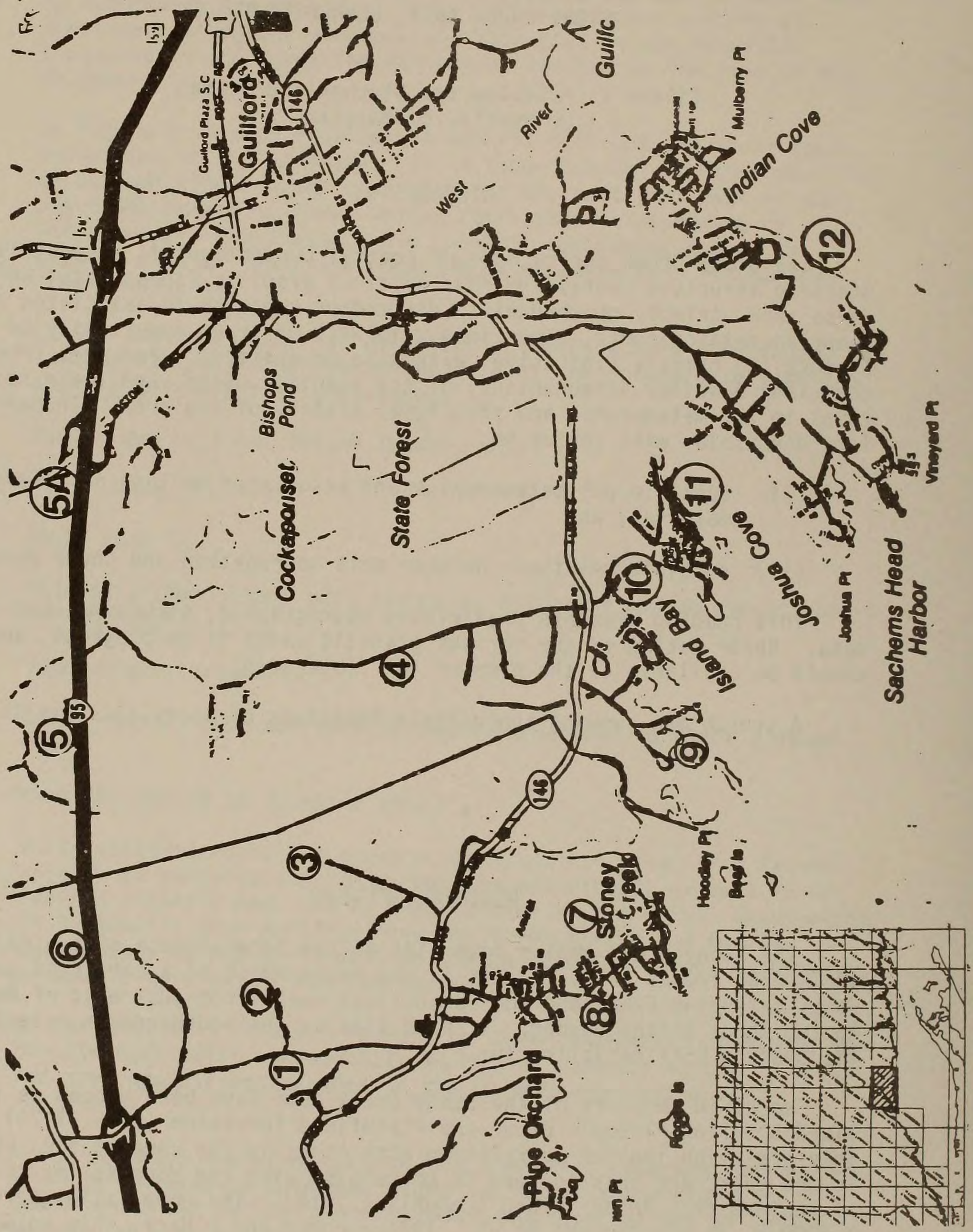

Figure 1. Location of field trip stops.

Rocks of the Lyme dome and Hope Valley terrain are separated from Siluro-Devonian rocks of Merrimack Synclinorium affinity by the Honey Hill Fault. The significance of this structure is unclear; movement on the fault is known to have occurred ~ 250m.y. ago (O'Hara and Gromet, 1983) but it is not known whether this movement was an Alleghanian suturing event or local basement-cover sliding on an existing (?Taconic ?Acadian) suture. Mylonites of the Honey Hill Fault are deformed by the Lyme dome (Lundgren and Ebbin, 1972) suggesting the Lyme dome to be a late Alleghanian feature. However, the Honey Hill Fault cannot be traced west of the Lyme dome, and no major tectonic discontinuity can be traced between the Stony Creek rocks and overlying Siluro-Devonian strata.

Hall and Robinson (1982) suggest correlation of units in both the Stony Creek and Lyme domes with the ~ 560m.y. (Naylor et al., 1975) Dry Hill Gneiss in the Pelham Dome of the Bronson Hill Anticlinorium. Domes in the Bronson Hill are generally considered to be of Acadian age (c.f. the Alleghanian Lyme dome) (Hall and Robinson, 1982). It has been suggested that ~ 600m.y. rocks of Pelham-Stony Creek-Lyme-Hope Valley affinity were already sutured to the North American continent by the time of Taconic (Hall and Robinson, 1982) or Acadian (Naylor, 1975; Osberg, 1978) orogeny. An attempt to reconcile apparently conflicting evidence in terms of successive docking of discrete fragments of a dispersed terrain is presented by Gromet and O'Hara (1983 and this volume).

There are no studies of the grade or timing of metamorphism in the Stony Creek area. The role of Alleghanian metamorphism in eastern Connecticut is very difficult to determine. Dallmeyer (1982) has reported ~ 250m.y. K/Ar and $^{40}Ar/^{39}Ar$ ages across the Hope Valley terrane and into an area of eastern Connecticut traditionally viewed as having been subject only to Acadian events. Similarity of biotite (~248-240m.y.) and hornblende (~ 260-255m.y.) $^{40}Ar/^{39}Ar$ ages argues for this being a discrete Alleghanian thermal pulse, rather than slow post-Acadian cooling. No data are yet available from as far west as Stony Creek.

In the interpretation of their Rb/Sr data, Hills and Dasch (1972) note localised remobilisation of Rb on a scale ~ 0.3m; on this scale data could be fitted to a ~ 250m.y. isochron. Hills and Dasch therefore suggested Alleghanian metamorphism as a possible explanation, but noted that "earlier redistribution of Rb and Sr cannot be disproven".

Two problems therefore arise:

(i) can the Stony Creek rocks be correlated with any or all of the Pelham dome, Lyme dome or Hope Valley sequences?

(ii) what was the timing of suturing of Stony Creek rocks to the North American continent--Taconic, Acadian or Alleghanian?

STRATIGRAPHIC FRAMEWORK

Some discussion of stratigraphy in the Stony Creek area may be found in Mikami and Digman (1957), Bernold (1962) and Sanders (1968). The litho-stratigraphic sequence proposed by the author is shown in Table 1, and the

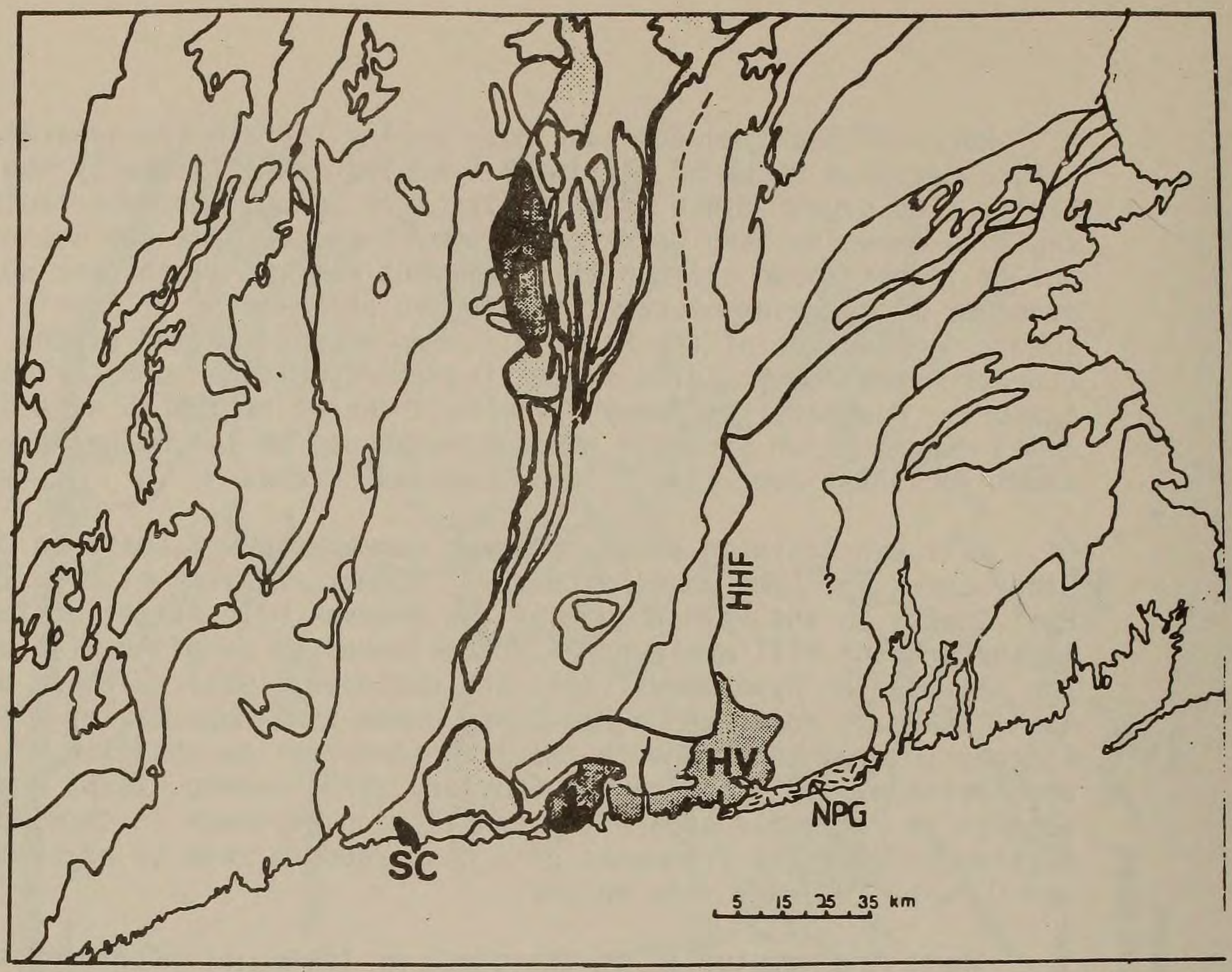

Figure 2. Geologic setting of the Stony Creek Dome. (a) Location of Stony Creek, Lyme and Pelham Domes, Hope Valley terrane and other major structures.

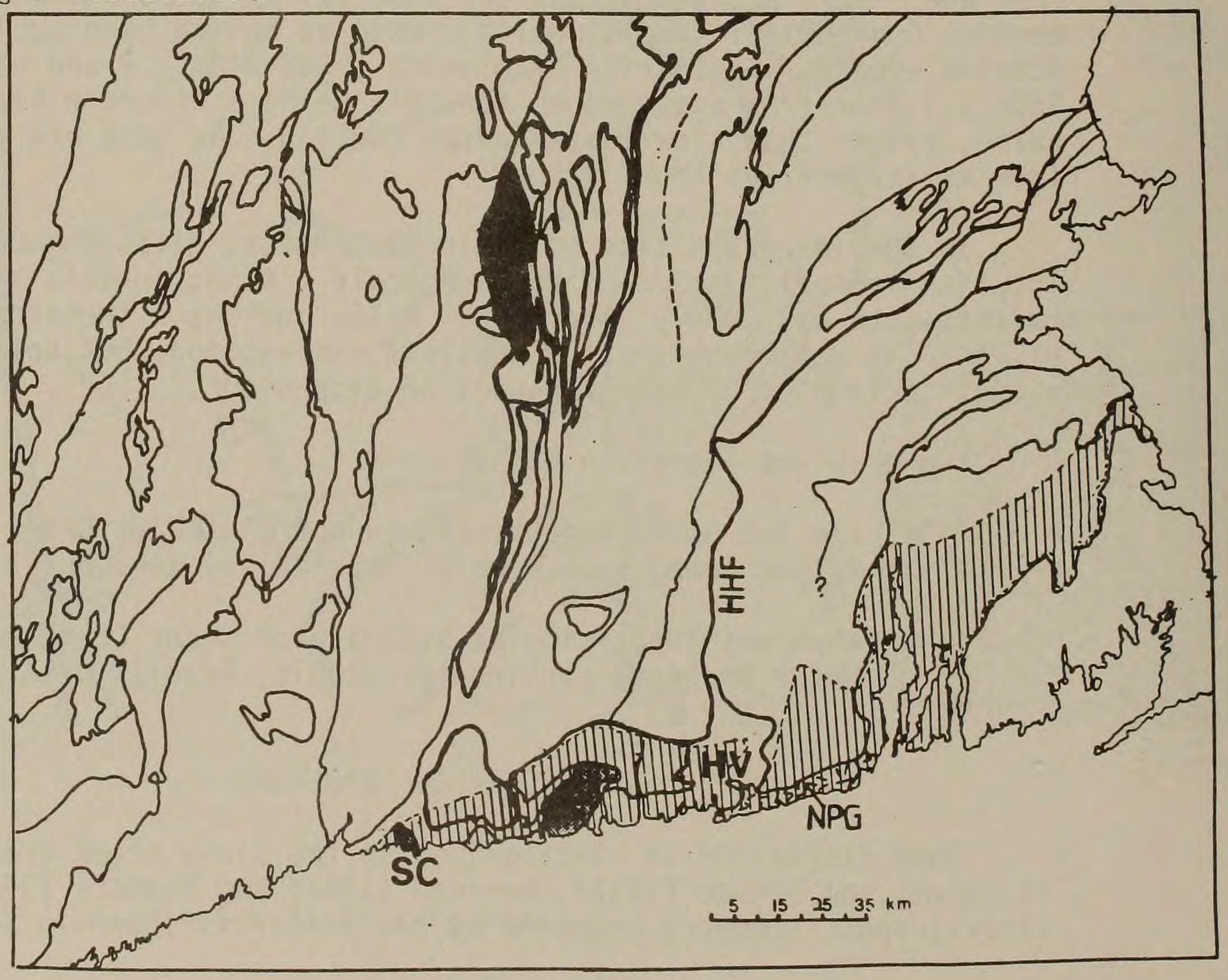

(b) Regions of PreCambrian and Alleghanian metamorphism, from Robinson (1984).

distribution of the various units is shown in Fig. 3. This sequence is similar to that of the above authors, and to that of Goldsmith (1967) for the Lyme dome, with the following additional information.

The core of the dome is dominated by gneisses and amphibolites, identified as part of the Lower Plainfield by the abundance of garnet-bearing lithologies. The amphibolites are typically coarse-grained and massive. They may have a spotty appearance in outcrop (e.g. STOP 12) due to the irregular distribution of plagioclase crystals, and they are usually extensively veined by subpegmatitic tonalite veins. The majority of the Lower Plainfield gneisses are dark bi-plag-qz-gt ± amph gneisses, with very pronounced gneissic banding on a scale of ~ 2cm. Garnet selvedges are very common along the contacts to associated granites (STOP 11). The Middle Plainfield is very heterogeneous. Quartzites occur at several different levels within the Plainfield, but only the Upper Plainfield is dominated by quartzite and only at this level is the rock massive. This massive quartzite marks the top of the Plainfield.

Mamacoke and Monson gneisses are relatively easily distinguished by the abundance of very dark, hb-bearing lithologies in the latter, together with its more massive character. The Mamacoke is commonly layered on a scale 1-2cm., and often weathers with a distinctive red-and-green striped appearance.

STRUCTURAL FRAMEWORK

Interpretation of the Stony Creek structure as a dome follows from the approximately concentric disposition of lithostratigraphy (Fig. 3) with a core of older units (Lower Plainfield) and a margin of younger units (Mamacoke and Monson). Basement domes in the southern and central Appalachians have been variously attributed to thrusts, diapirs and refolded nappes (Hatcher, 1984; Muller and Chapin, 1984). Gneiss domes in the Bronson Hill Anticlinorium, of which the Stony Creek dome is the southern extension, are considered diapiric (Hall and Robinson, 1982). The Lyme dome may be a basement ramp (Losh and Bradbury, 1984). The alternative possibilities can be evaluated by careful search for the characteristic thrusts, strain distributions and cross-folds.

No major thrusts have been recognized in the Stony Creek dome or at its contact to overlying strata. The mapped distribution of Upper Plainfield strata reveals the existence of a north-plunging overturned anticline, the Sachem's Head anticline (Sanders, 1968), the axis of which is almost coincident with one axis of the dome (Fig. 3). Other, more minor, folds parallel to this axis may also be recognized. However, the cross-folds which would be necessary to warp the linear anticline into the observed dome shape have not been observed.

Much of the evidence is suggestive of a diapiric origin. Foliation (phase layering in SCGI and biotite selvedges in SCGII) is flat-lying in the core of the dome and steepens gradually outward to ~70^{o} at the margins (Fig. 4, STOP 6). Lineation (defined by feldspar shape aggregates in SCGI and SCGII and by feldspar augen and biotite stringers in SCGII) likewise shows a transition from flat-lying in the core to steeper in the margins (Fig. 4). This lineation is not strictly a downdip lineation--it is often

UNITS IN STONY CREEK DOME

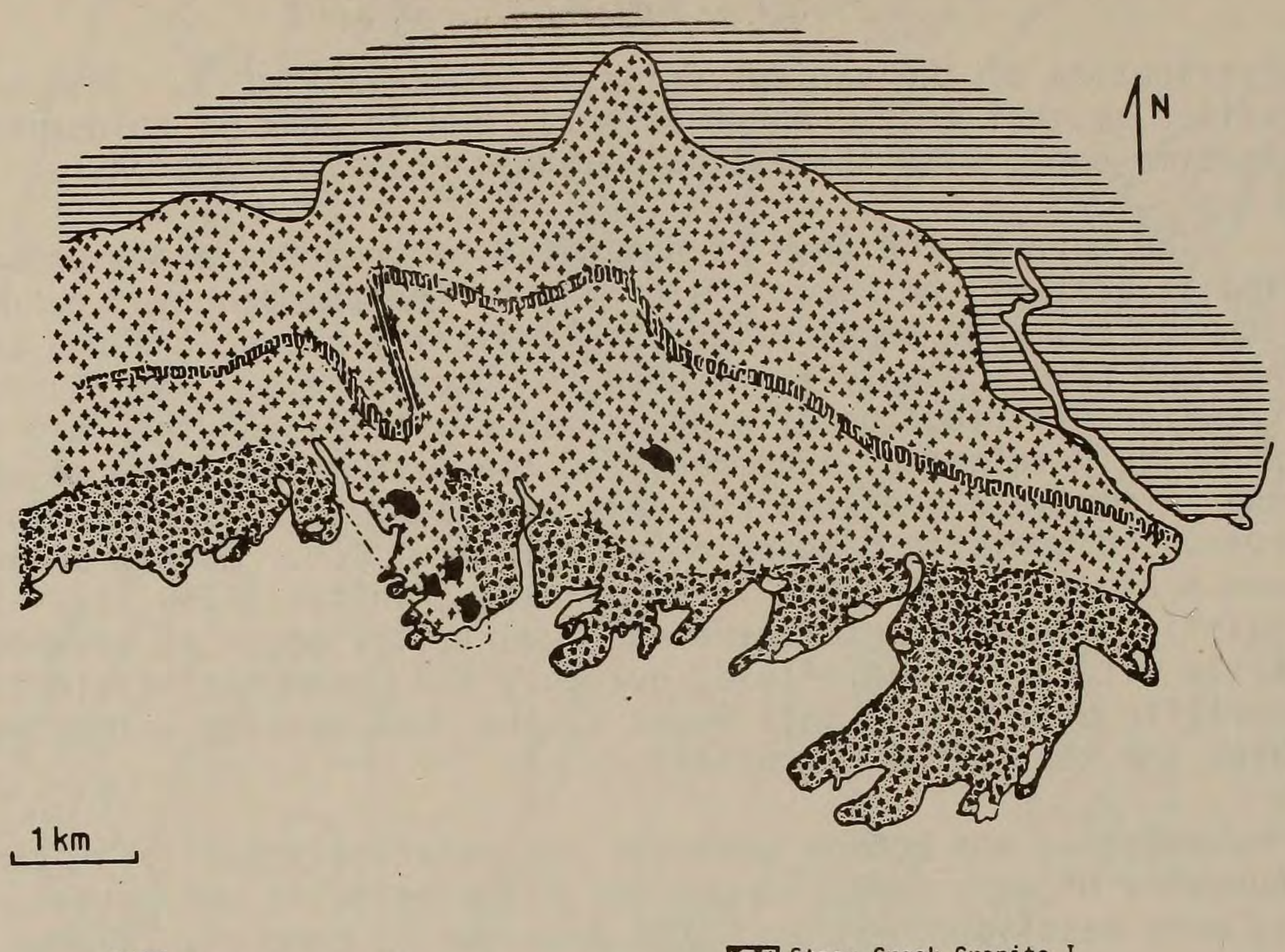

Figure 3. Geological sketch map of Stony Creek Dome.

FOLIATIONS AND LINEATIONS WITHIN THE DOME

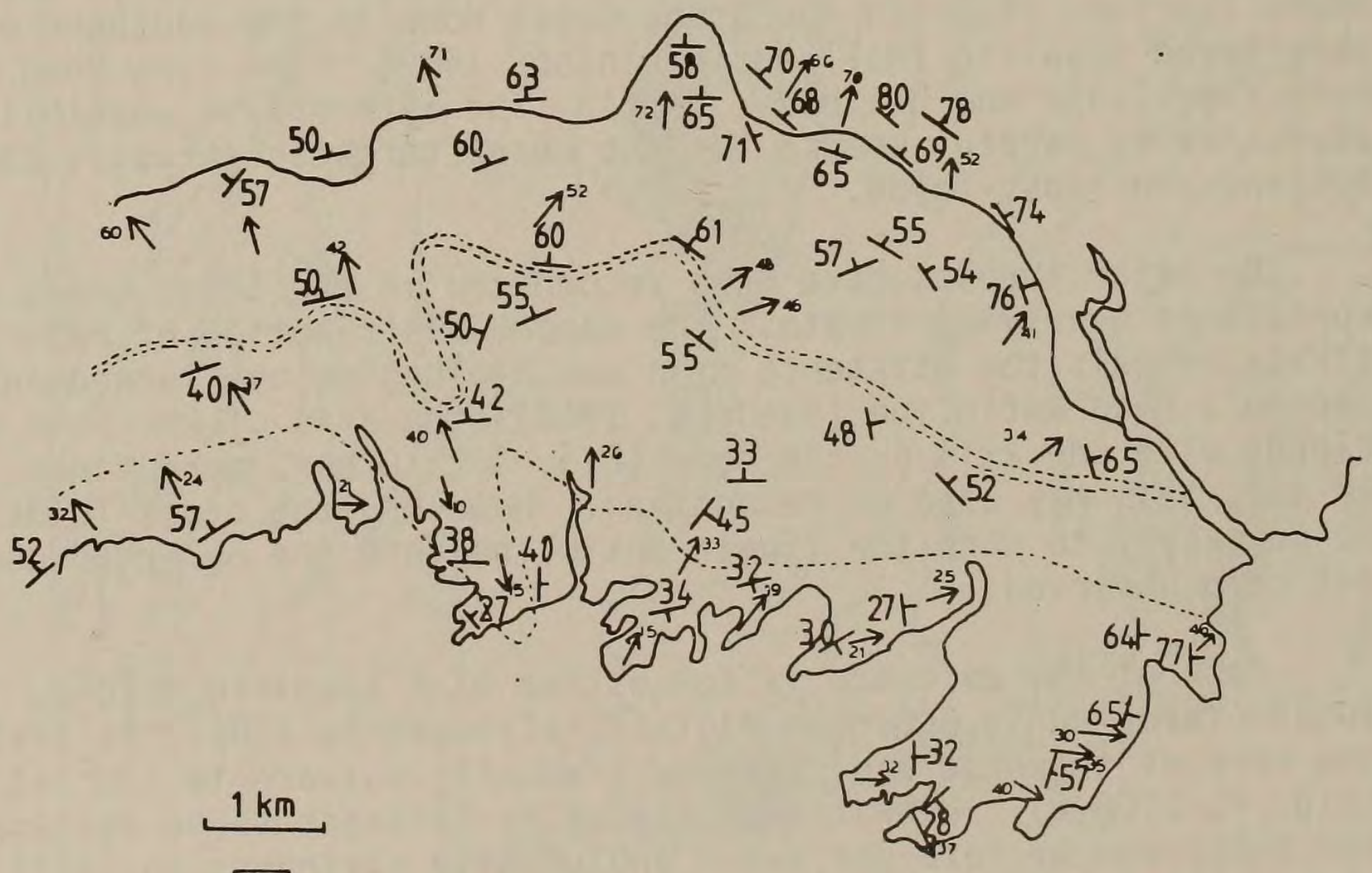

Figure 4. Foliations and lineations in Stony Creek Dome.

more steeply dipping than foliation, possibly suggestive of non-coaxial deformation. L-fabrics are strongly developed in the core of the dome, whereas margin fabrics are LS or S type. The concentric foliations, radial lineations and change outward from L to S fabrics are more suggestive of an origin by diapirism than by multiple folding.

An estimate of variations in strain across the dome is shown in Fig. 5(a). Strain estimates are from:

(i) R_f/ϕ analysis of grain aggregates in SCGI and SCGII (only R_f shown on Fig. 5(a))

(ii) direct measurements of axial ratios (X:Z) of enclaves in SCGI.

Not surprisingly, enclave measurements suggest greater ellipticity (higher strains) than do grain aggregate measurements. This may be due to originally higher ellipticity (R_i), indicated by the tendency of biotite schists to have higher ratios than do (presumably more isotropic) amphibolites or quartzites from the same area. Only values for quartzites are shown on Fig. 5(a), to allow for comparability. Alternatively and/or additionally, if SCGI is intrusive then the greater ellipticity of enclaves than of granite fabrics may indicate that enclaves are in fact xenoliths deformed more strongly than the enclosing granite, due either to syntectonic intrusion of SCGI or to preintrusion deformation of the country rock. Compatible with this latter suggestion is the truncation of folded fabrics in the enclaves at their contacts with SCGI (STOP 2). Comparison of the strains recorded in SCGI and SCGII is complicated by their spatial separation; it is not clear whether the differences in strain magnitude (SCGI more strained than SCGII) are due to real differences in strain history (SCGI predates SCGII) or are due to variations in strain across the dome.

On a Flinn diagram (Fig. 5(b)) data are clearly suggestive of near-plane strain in the core of the dome and increasing flattening in the margins. Plane strain near the core of the dome is compatible with the diapir models of Dixon (1975) which predict a neutral surface (K=1) where vertical extension in the "stalk" passes into horizontal extension in the "cap" of a mushrooming diapir. Similar strain distributions have been reported by various workers (Holder, 1979 ; Ramsay, 1979) for plutons infilled by ballooning; however, the apparently diapiric strains extend well beyond the regions of possible intrusion (SCGI outcrops).

If the Stony Creek dome is indeed a diapir, this may imply a structural history more similar to the Pelham dome than to the Lyme. This, in turn, would by implication suggest Acadian-age diapirism, i.e. Stony Creek basement would have been already sutured to North America by the Acadian.

Both foliations and lineations are deformed by shear zones (Plate 8). These typically dip gently to the NW (STOP 3) or N (STOP 12). They are the last penetrative deformational event seen. SCGIII and SCGIV are closely associated with these shear zones and commonly are concentrated within them (Fig. 20).

Any proposed structural history for the Stony Creek dome must take account of the above, and must also answer the following:

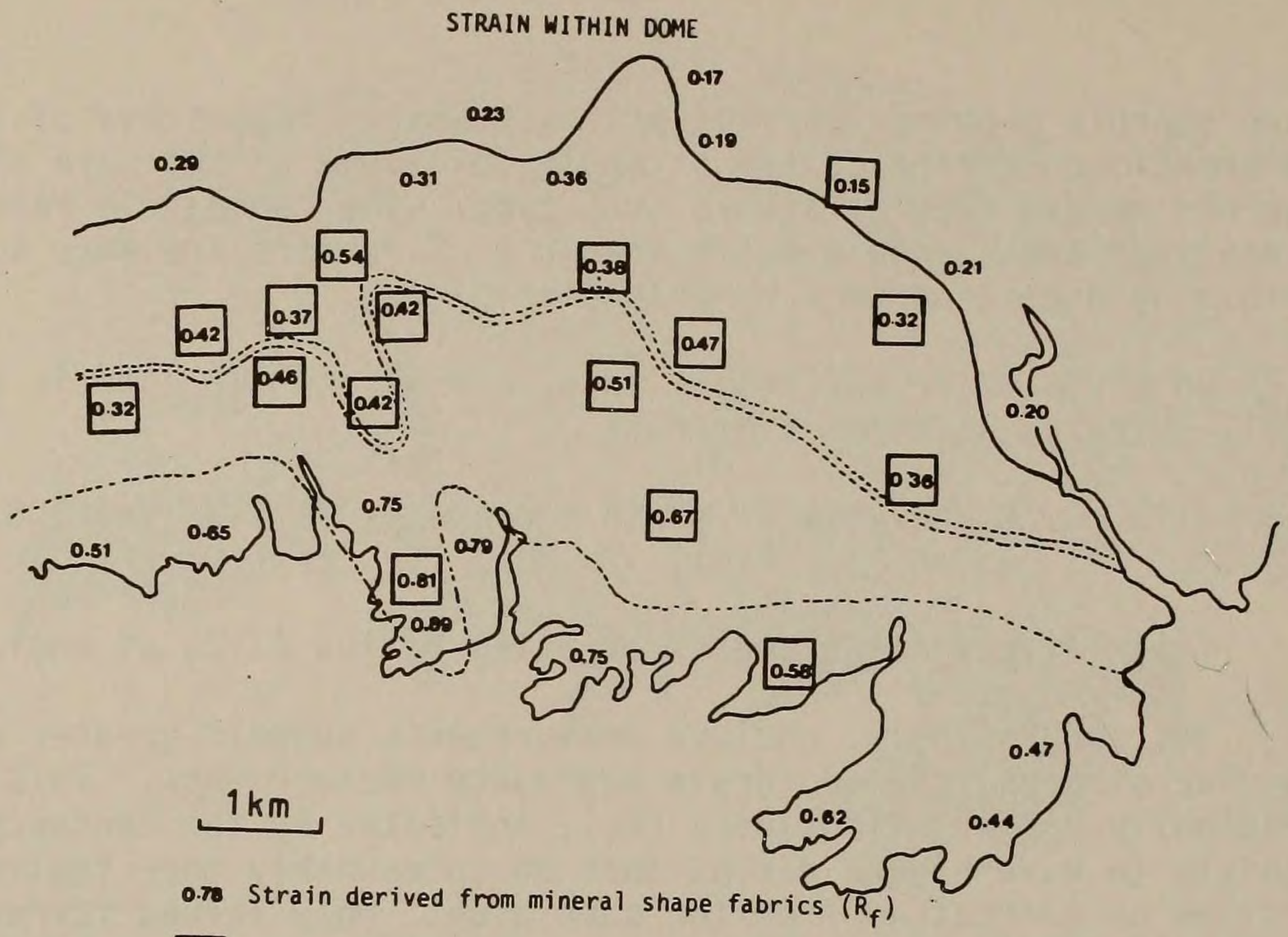

Figure 5 (a). Strain within the Stony Creek Dome.

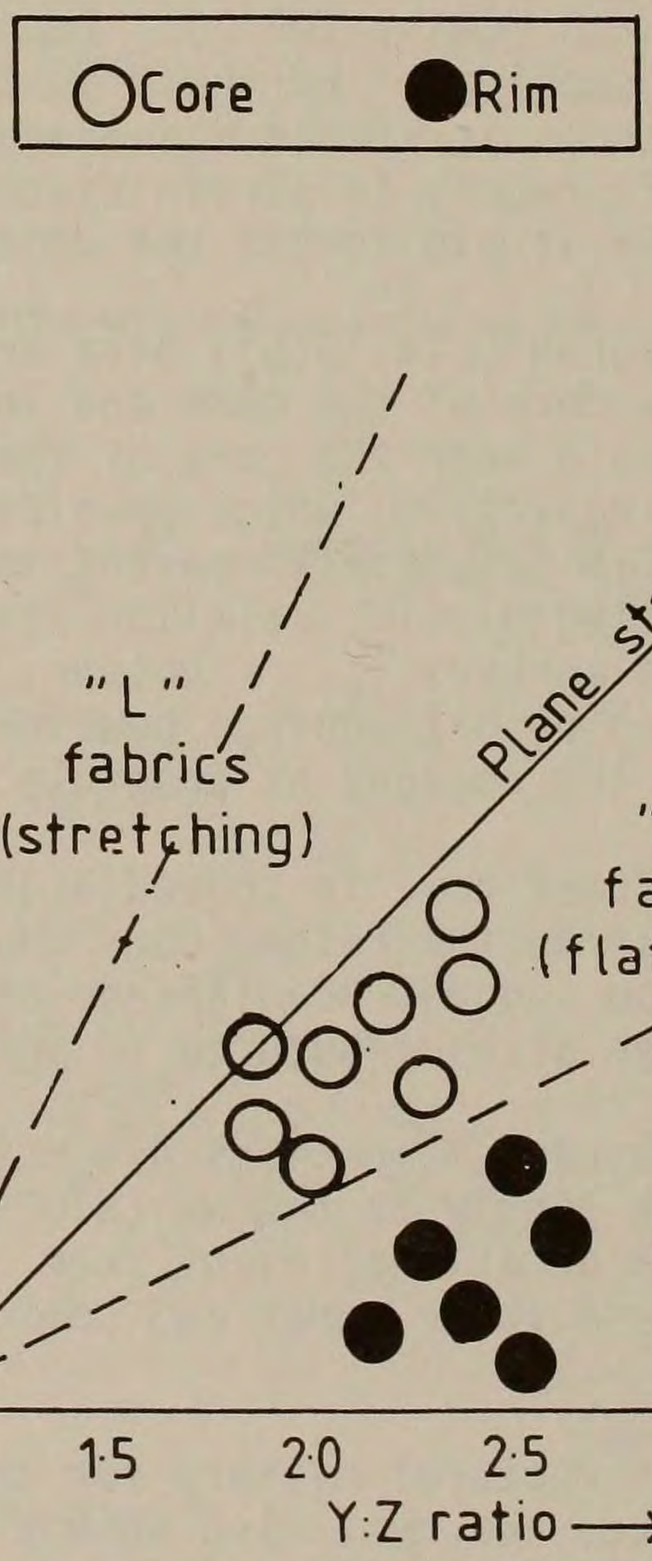

(b) Flinn diagram of enclave measurements.

(i) what is the timing of diapirism?

(ii) what is the relative timing of SCGI and SCGII formation, and of this compared to formation of the Sachem's Head Anticline? Can SCGI develop in a pre-existing fold (possibly by lit-par-lit injection, STOPS 3 and 6)? Alternatively, could the fold develop on a large scale without producing small-scale fabrics in the granite?

(iii) what is the timing of folding seen in enclaves of Plainfield within SCGI? Do these folds relate to the Sachem's Head Anticline, or are they an earlier, possibly PreCambrian (the Hills and Dasch (1972) date, if accepted) event?

(iv) does the occurrence of SCGIII and SCGIV in shear zones indicate the segregation of melt into shear zones, or the localisation of strain in relatively low-strength melt areas? Why do SCGIII and SCGIV lack fabrics--was melt crystallisation post-tectonic, but melt-segregation syn-tectonic? If SCGIII is ~ 250m.y. (as implied by Hills and Dasch (1972)) then these shears must be of Alleghanian age.

METAMORPHIC FRAMEWORK

Only limited geobarothermometric data is presently available. Further work to detail (i) possible variations in P and T within the dome and (ii) changes in P and T with time is planned. Deduced metamorphic conditions are plotted on Fig. 6 together with curves for the beginning of melting of granite (Johannes, 1984) and of peraluminous granite (Clemens and Wall, 1981).

Ternary Feldspars

Compositions of coexisting feldspars are plotted in Fig. 7, where they are compared to the isotherms of Whitney & Stormer (1977) for low-structural state feldspars. The calculated temperatures are slightly P-dependent, and maximum recorded temperatures range from ~ 680°C at 5kb to ~ 720°C at 10kb. Most temperatures are lower than this due to re-equilibriation. The maximum recorded temperatures are likewise under-estimates of maximum attained temperatures, due to possible re-equilibration.

Garnet-biotite

Due to the generally high Al and Ti contents of the biotites, the formulation of Ferry and Spear (1977) gave anomalously high temperatures. Recalculation using the equation of Indares and Martignole (1985) suggests temperatures in the range 730°C to 770°C. These temperatures are for garnet-biotite pairs from the Lower Plainfield and work is in progress to obtain thermal data from other units.

Qz-Plag-As-Gt

Using the equation of Ghent (1976) a pressure of 8.1 was obtained from this geobarometer; this estimate appears too high in view of the absence of kyanite from the Stony Creek rocks (although this may be a bulk composition

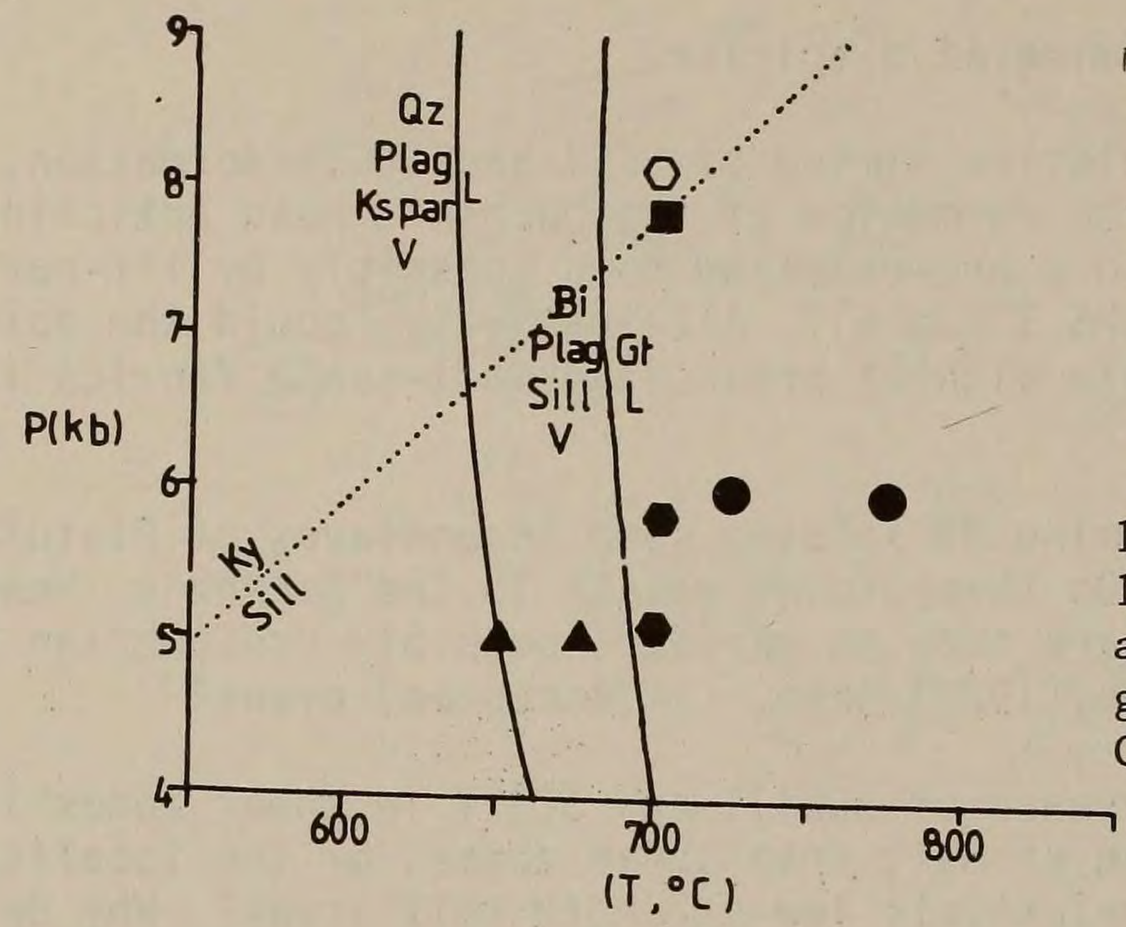

Figure 6. Metamorphic conditions in the Stony Creek Dome. Temperatures: ● from garnet-biotite geothermometry (Indares and Martignole, 1985), ▲ from feldspar geothermometry (Whitney and Stormer, 1977). Pressures from qz-plag-AS-gt ⬡ T=700 (Ghent, 1976), ⬢ (Newton and Haselton, 1981), ■ GRAIL T=700 (Bohlen, 1984). Curves for granite melting are from Johannes (1984) and for garnet-granite melting from Clemens and Wall (1981).

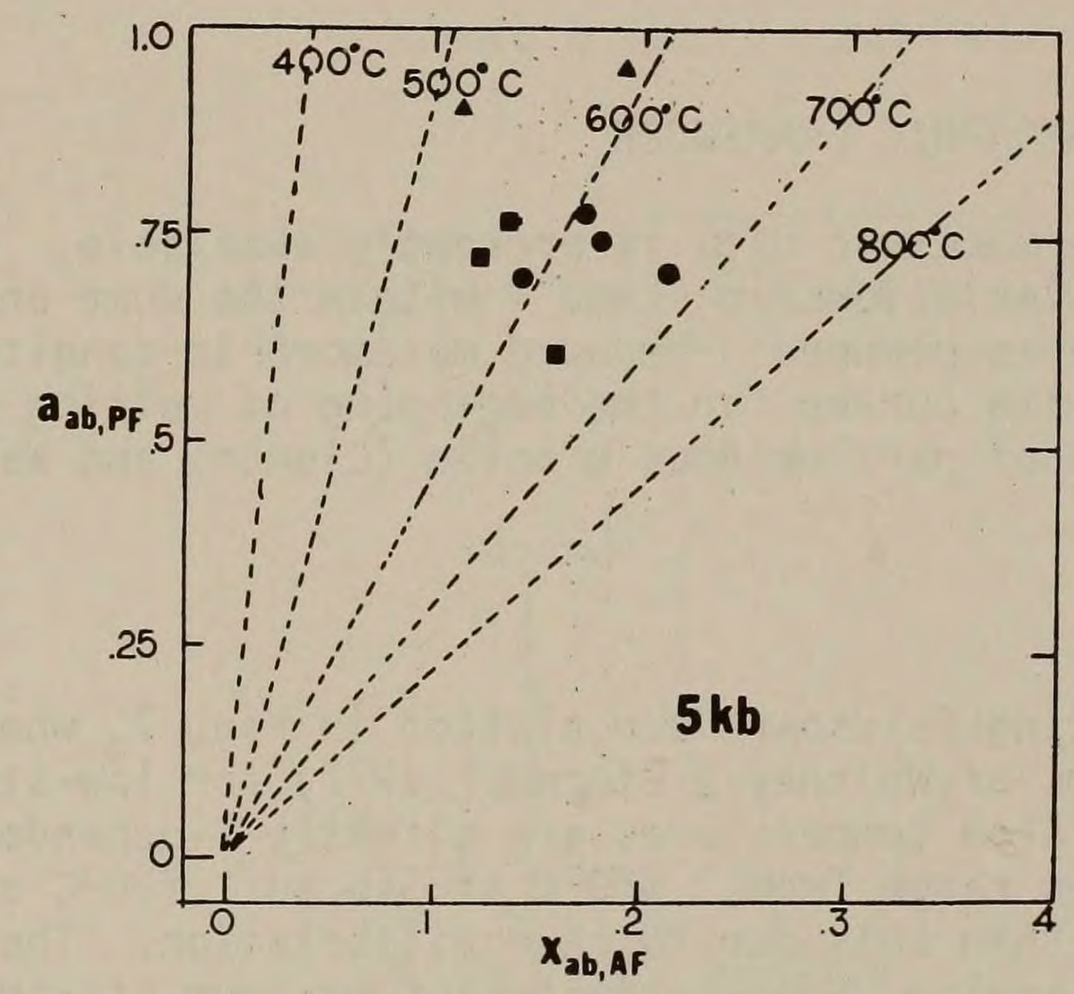

Figure 7. Compositions of ternary feldspars. Isotherms are from Whitney and Stormer (1977).

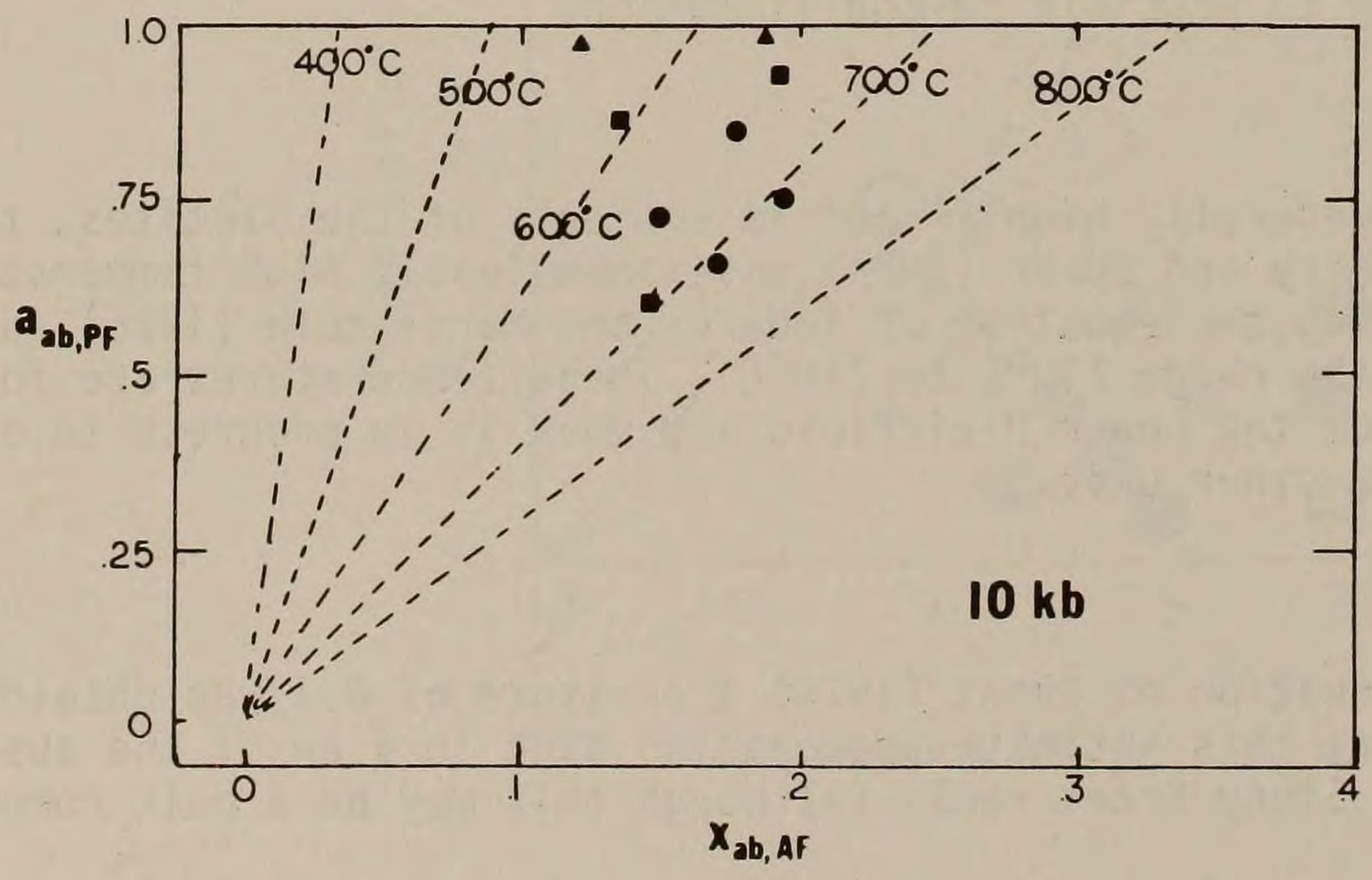

problem). The method of Newton and Haselton (1981) gives pressures of 5.2kb to 5.8kb from the core and rim of a garnet respectively. These values may be low, but the relative increase in pressure from core to rim appears real.

GRAIL

One sample from the Lower Plainfield Formation contains rutile in the core of the garnet and ilmenite in the rim (note that this implies P decrease during garnet growth, the opposite to that noted above). Using the data of Bohlen (1984), the assemblage gt-rutile-sill-ilm-qz in this rock implies P ~ 7.8kb. This appears high in view of the lack of kyanite.

Bi-Kspar-Mt

Using the equilibrium:

$$\text{Annite} + O_2 = \text{Sanidine} + \text{Mt} + H_2O$$

and assuming T ~ 700°C, $a_{H_2O} = 1$, we obtain a value of log f_{O_2} for samples of SCGIII ranging from -20 to -22 (NNO to QFM) (Eugster & Wones, 1962).

Possible polymetamorphism

Complex garnet zoning (Fig. 8) may be interpretable in terms of polymetamorphism; further work is needed to constrain possible pressure variations noted above. Evidence for polymetamorphism would clearly be of great significance for the tectonic evolution of the Stony Creek dome.

GRANITIC UNITS

In addition to the stratigraphic sequence outlined above a variety of granitic (s.l.) units can be recognised (Fig. 3, Plates 1-3, 5-8). Modal and bulk chemical analyses of three of these units can be found in Tables 2 and 4. The amount of granitic material is greatest in the core of the dome, where outcrops of homogeneous granite occur, and decreases outward. Granite is very much more abundant in the Plainfield Formation than in the overlying Mamacoke and Monson, where it is typically restricted to cross-cutting pegmatites (Fig. 9). Four distinct granitic units (Stony Creek Granite I-IV (SCGI-IV)) can be recognised on the basis of mineralogy and relations to structural chronology.

Field Relations

The first of these units, referred to as Stony Creek Granite I (SCGI) is most abundant in the northern part of the dome. It was the subject of the local quarrying industry and is the type referred to in the literature as "Stony Creek Granite". It is a medium-grained (3-5mm), granular-weathering biotite-granite. A garnet-bearing facies of SCGI is developed locally (STOP 7) (Plate 3) where it appears gradational to the more normal type. This rock type is also found to the west of Stony Creek where it has been mapped as the Branford Quartz Monzonite (Mikami and Digman, 1957). SCGI can be seen to wedge into disrupted country rock (STOPS 3 and 5) and to assimilate xenoliths of Plainfield Formation (STOPS 3 and 5). Large blocks of resistant quartzite from the Upper Plainfield form a series of

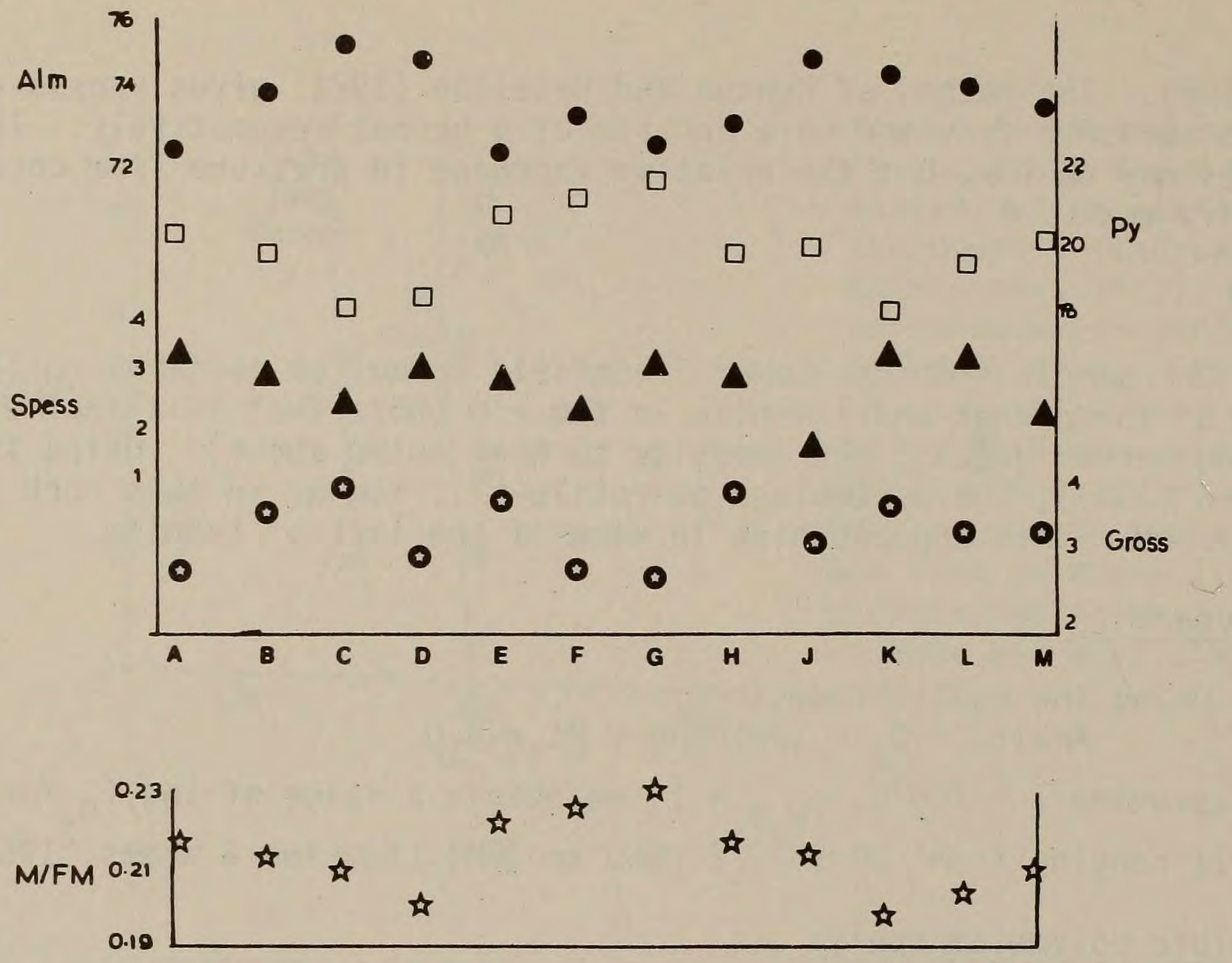

Figure 8. Zonation in country rock garnet.

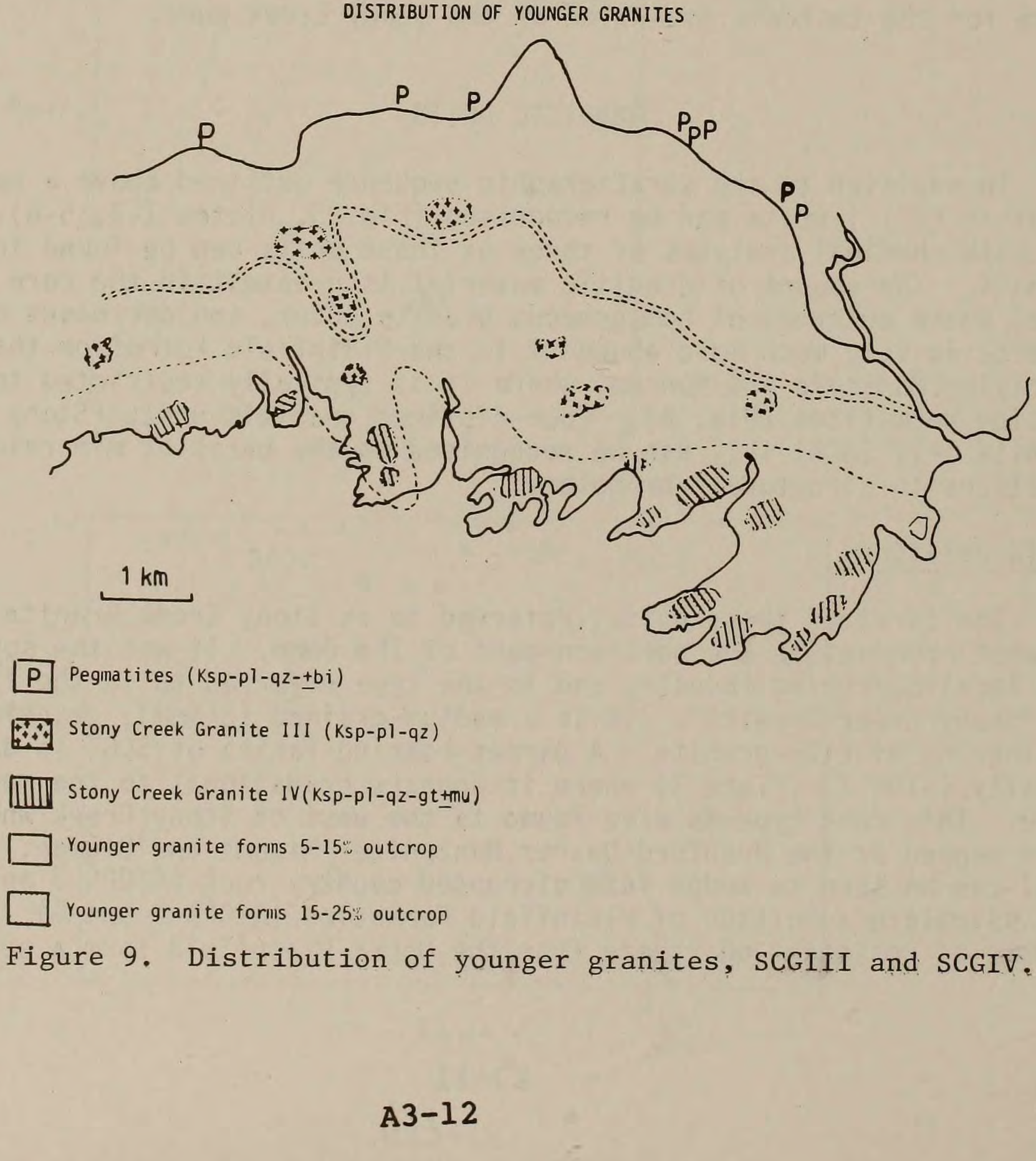

Figure 9. Distribution of younger granites, SCGIII and SCGIV.

raft trains near the outer margin of the body. Xenoliths are most common near the outer edges of the dome. There is a gradual transition in granite: host proportions over a distance ~ 400m. from country rock with veins (STOP 1) to masses of SCGI with occasional xenoliths (STOP 2). Fabrics within xenc-liths are truncated at xenolith margins (STOP 2). SCGI shows pronounced phase layering, marked by the development of Kspar-rich and qz+plag-rich bands. This phase layering is parallel to locally abundant biotite schlieren (STOPS 3 and 6) (Plate 1). Both features were attributed by Mikami and Digman (1957) to filter pressing during melt crystallization.

The second granitic unit, SCGII, is a relatively fine-grained (1-3mm.) garnet- and locally muscovite-bearing granite. It is found in lit-par-lit association with the Lower Plainfield Formation. Layers of SCGII may be very thick, up to 10m. across; many outcrops contain several such units separated by thin layers of Lower Plainfield (STOP 9). Fragments of Lower Plainfield can be traced out into surrounding SCGII as biotitic clots and stringers of tiny garnets (STOPS 9 and 11). SCGII shows a well-developed lineation (Plate 5) formed both by biotite and garnet stringers (Plate 6) and by elongate aggregates of qz and feldspar. Kspar augen are common (STOPS 9 and 12).

The third granitic unit (SCGIII) is typically very closely associated with SCGI (STOPS 3 and 4). Rocks apparently correlative to SCGIII can be found as pegmatitic veins cutting the Plainfield, Mamacoke and Monson Formations (STOPS 5a and 6). Where associated with SCGI, SCGIII may form 5-15% of the outcrop and may occur either as veins (~ 3-20cm. wide) cutting layering in SCGI, or as subpegmatitic to pegmatitic (grain size 5-10mm.) patches. Such patches range in size from ~ 3x3cm. to ~ 40x40cm. Pegmatitic patches of SCGIII merge into host SCGI by a decrease in grain size and by a decrease in the proportion of Kspar. The high Kspar content of those patches renders them more distinctly pink than the host. Veins are more sharply bounded than patches and often have a ~ 1cm. wide selvedge rich in bi + plag. Neither veins nor pegmatitic patches have an internal fabric (Plate 2). Coarse garnet-bearing veins in the garnetiferous facies of SCGI (STOP 7) may be a garnetiferous facies of SCGIII and will be treated as such below.

SCGIV occurs as pods and veins at a high angle to the lineation in SCGII. Proportions of SCGIV to SCGII in outcrops vary from ~ 5:95 to 20:80 (STOPS 9 and 12). SCGIV is often concentrated in shear zones (Plate 8) within SCGII (STOP 12); such pods can be traced several m. across the outcrop. SCGIV lacks the fabric of the enclosing SCGII, and contains garnets which are both coarser and more abundant than those in SCGII.

Petrography

Modes of units SCGI-III are shown in Table 2 and Fig. 10. With the exception of a few samples of SCGII (which are classified as quartz monzo-nites) samples of all units lie in the granite field of Streckeisen (1976). Shown on Fig. 10 for comparison are modes of granitic rocks from possibly correlative Sterling Plutonic Group sequences, i.e. the Hope Valley alaskites of Rhode Island and alaskites and gneisses from the Lyme dome. Data from the Stony Creek samples are more Kspar-rich than the field of Hope Valley alaskite samples. Material from the Lyme dome is represented by only 2 samples; how-ever, these samples lie in the center of the field defined by the Stony Creek

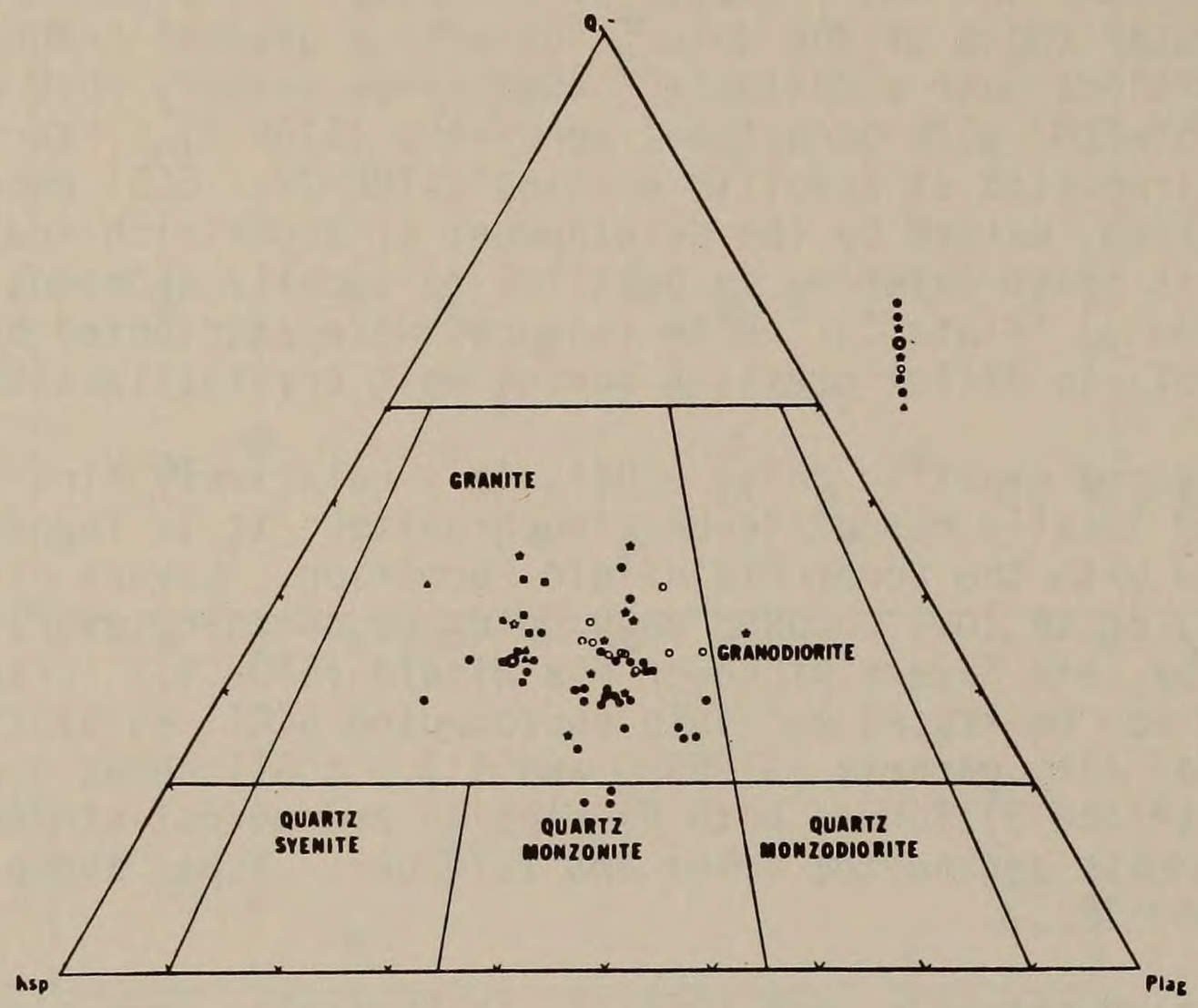

Figure 10. Modes of SCGI■, SCGII●, SCGIII▲, in Qz-Ab-Or. Other data: Westerly ✸ and Narragansett Pier Granites ❋ from Hermes et. al. (1981) and Quinn (1972); Hope Valley alaskites ★ and Ten Rod Granite Gneiss ○ from Day et. al. (1980); Lyme alaskite ✪ and biotite-granite-gneiss ✰ from Goldsmith (1967).

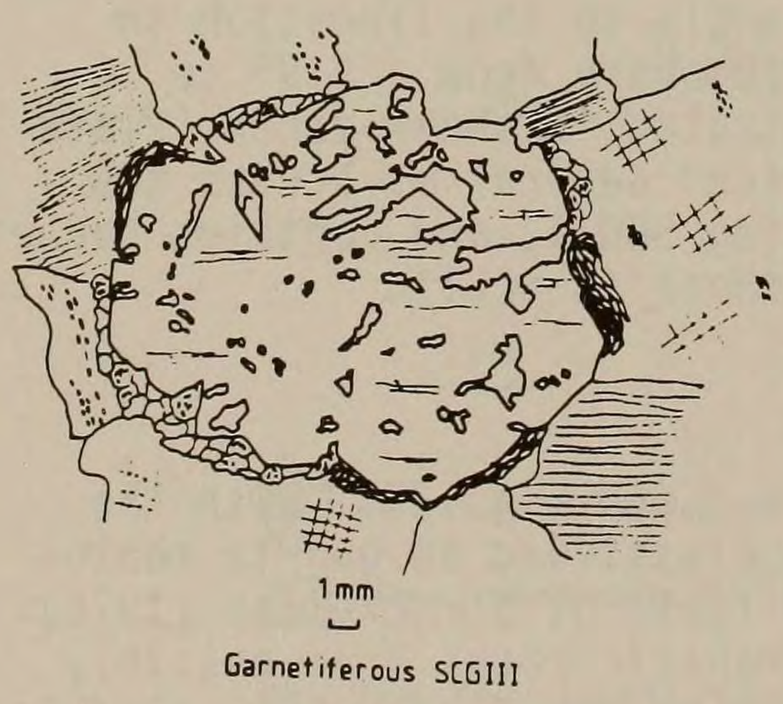

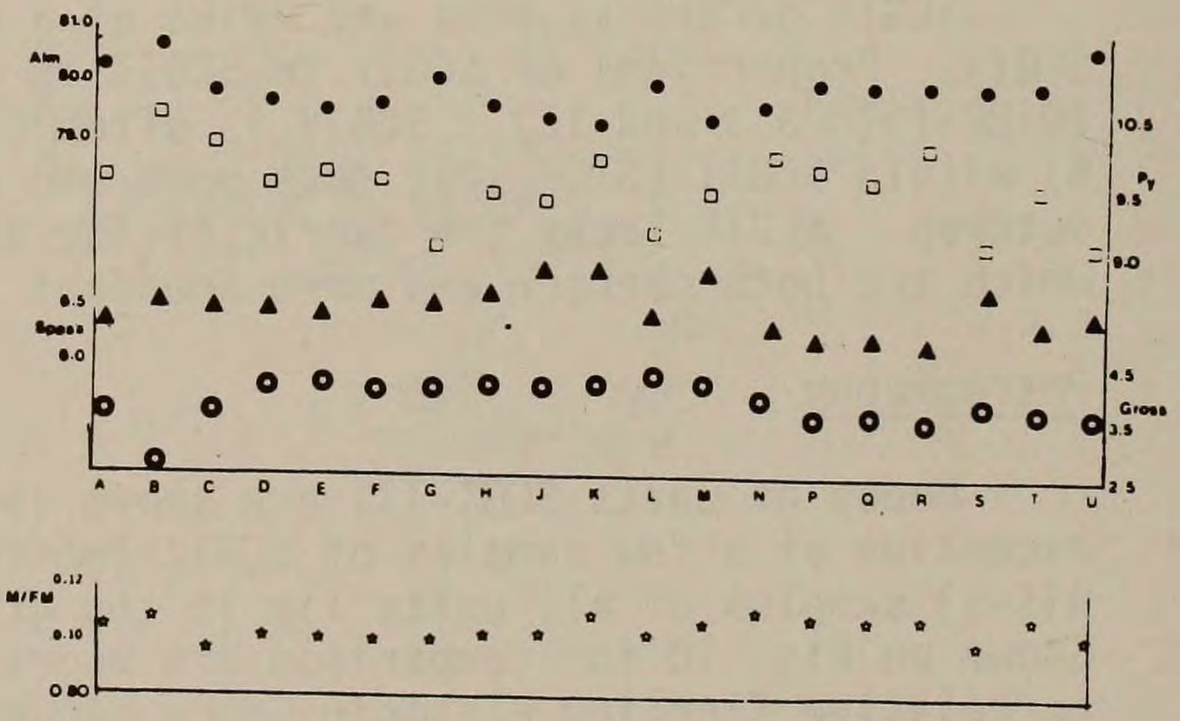

Figure 11. Gernet from SCGIII sample 7, showing (a) qz inclusions and rim of sillimanite, together with (b) zoning.

data. Also shown on Fig. 10 are modes of the Alleghanian-age Naragansett Pier and Westerly Granites. Coarse material of SCGIII type has previously been interpreted as pegmatites of Narragansett Pier Granite; however, Fig. 10 shows that the fields of SCGIII and of Narragansett Pier Granite are different.

SCGI samples in thin section show very highly strained quartz; grain contacts are extensively sutured and subgrains are abundant. In some samples local production of smaller, more equant, strain-free quartz grains has occurred. The samples have therefore been deformed at temperatures where recovery and recrystallisation was possible (~ 400°C). Work to characterise quartz c-axis fabrics in terms of temperature and strain-rate is planned. No relict igneous textures can be recognised; all Kspar is microcline. SCGI samples contain abundant accessory sphene, zircon and magnetite.

The garnetiferous facies of SCGI (STOP 7) looks texturally like the garnet-free SCGI, with evidence of recovered and recrystallised quartz. Biotite flakes define a layering.

SCGII samples in thin section show textures very similar to SCGI, with no relic igneous textures and with abundant recovered and recrystallised quartz grains. Ribbons of sutured quartz are very common, and elongate aggregates of feldspar (interpreted as the products of recrystallisation of highly deformed feldspar) occur. Both shape fabrics and phase layering are more obvious in SCGII than in SCGI. Apatite is an abundant accessory in SCGII; magnetite and zircon occur sporadically.

SCGIII samples in thin section are highly inequigranular, with Kspar much coarser than the other species. Kspar grains are often perthitic, and often contain plagioclase and quartz inclusions. Myrmekitic intergrowths of plagioclase and quartz often invade Kspar. Some Kspar is microcline. Kspar grains often show brittle fractures, which locally displace perthite lamellae and/or microcline twins. Plagioclase is occasionally Carlsbad-twinned, and may show discontinuous zoning to more sodic rim compositions. Quartz occurs as strained grains with abundant fluid inclusion trails. These fluid inclusions will be examined in a later stage of this project. There is no sign of recrystallisation in quartz. Accessory minerals are represented by large grains of magnetite.

Veins of garnetiferous SCGIII are texturally similar to non-garnetiferous SCGIII, with large and ragged Kspar containing quartz inclusions and being invaded by myrmekite. Garnets in these veins are often partially atolled (see also Fig. 11), with concentric inclusions of quartz. These garnets are mantled by sillimanite ± biotite, now partially altered to muscovite and chlorite. Myrmekitic intergrowths of plagioclase and quartz, together with tiny anhedral grains of Kspar, surround the sillimanite ± biotite rim (Fig 11). Quartz in the garnetiferous facies of SCGIII is highly strained but not recrystallised.

Diagrammatic sketches to illustrate the textures of SCGI-III are presented in Fig. 12. The above descriptions indicate that SCGIII (both garnet-bearing and garnet-free) contains relict igneous textures which have been destroyed by high-temperature deformation in SCGI and SCGII. This fits with field observations (above) that SCGIII cross-cuts fabrics in SCGI and SCGII.

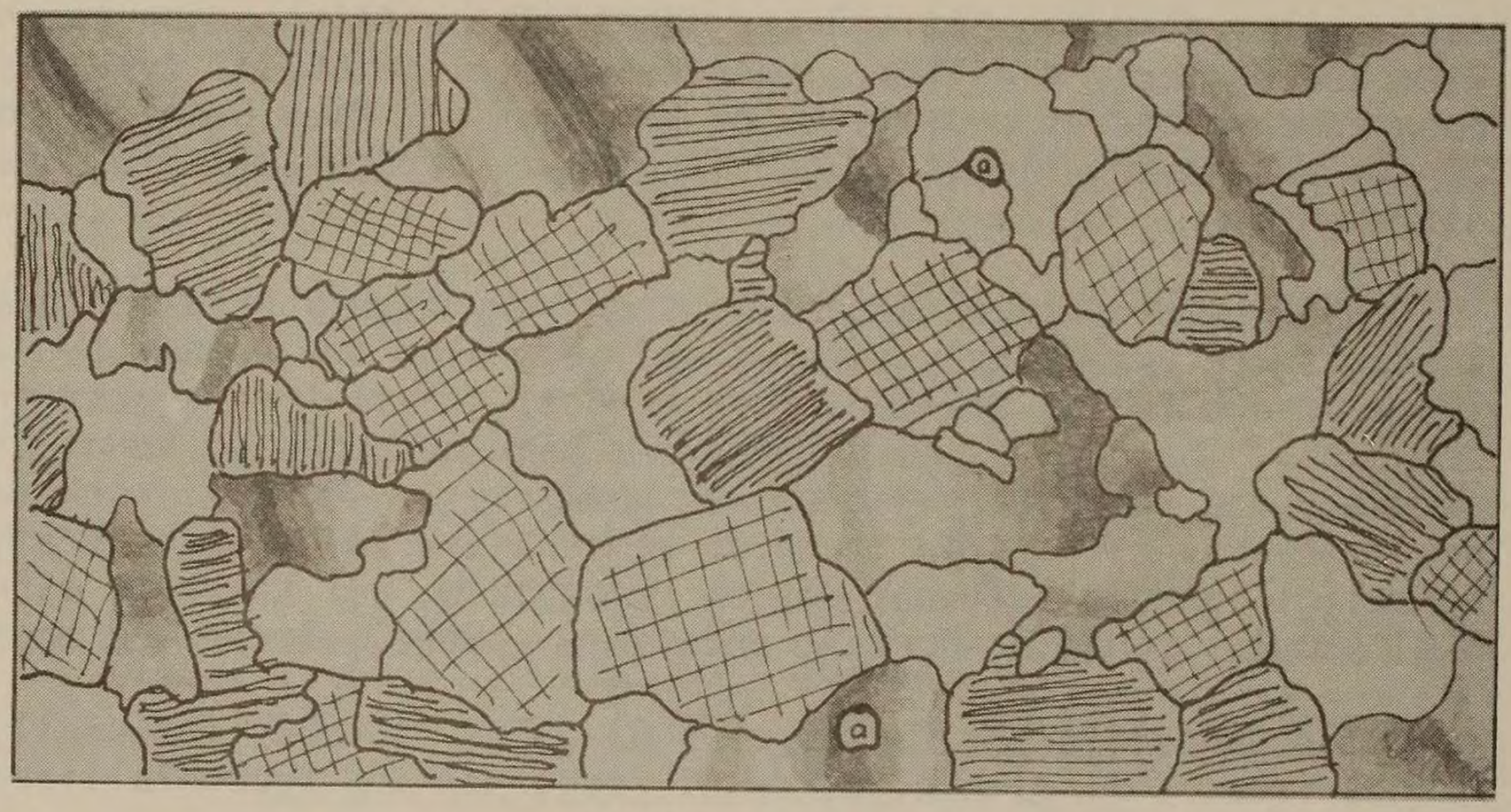

SCGI ⌊⌋

Figure 12. Schematic thin section sketches (a) SCGI, (b) SCGII, (c) SCGIII.

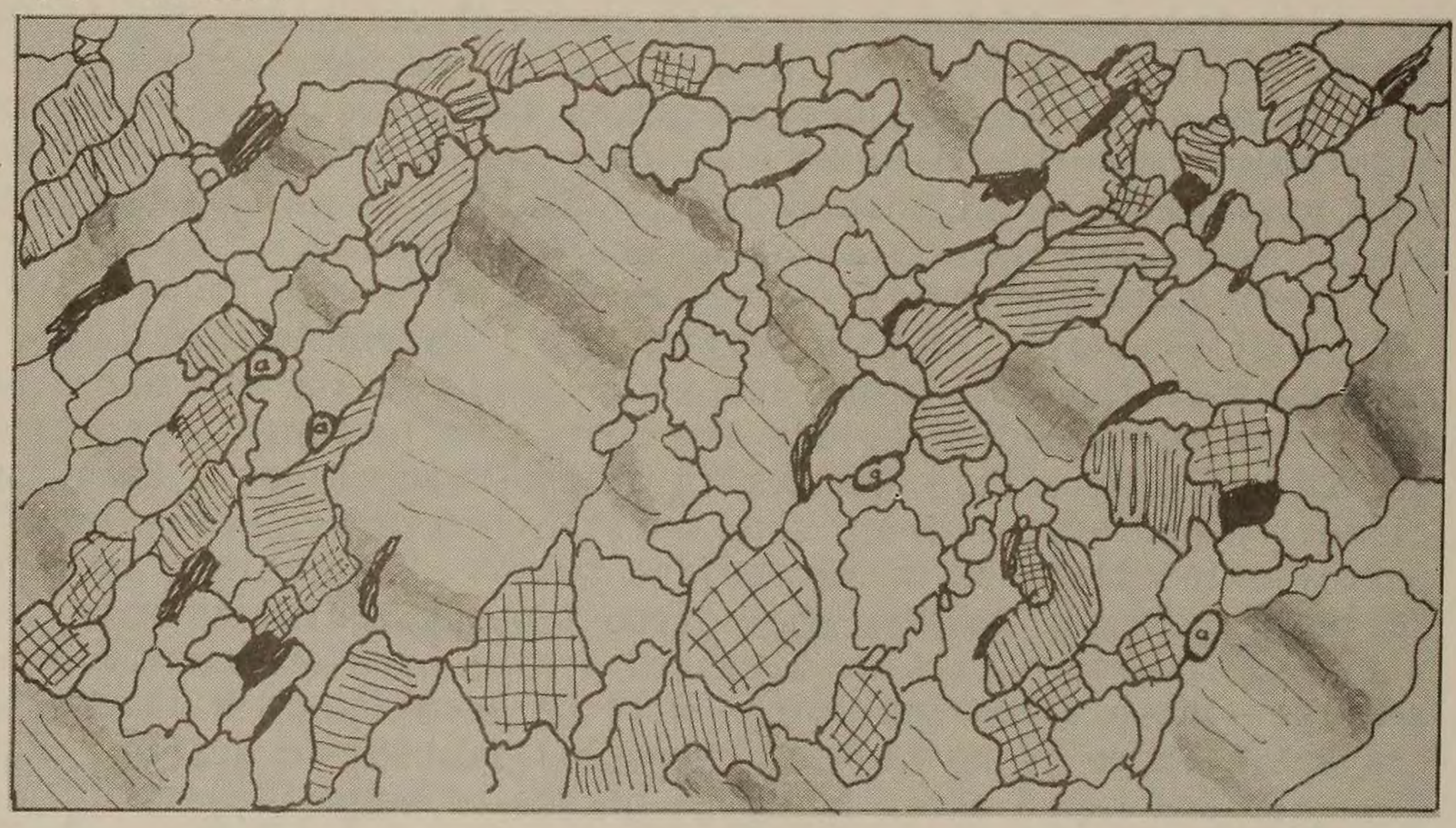

SCGII ⌊⌋

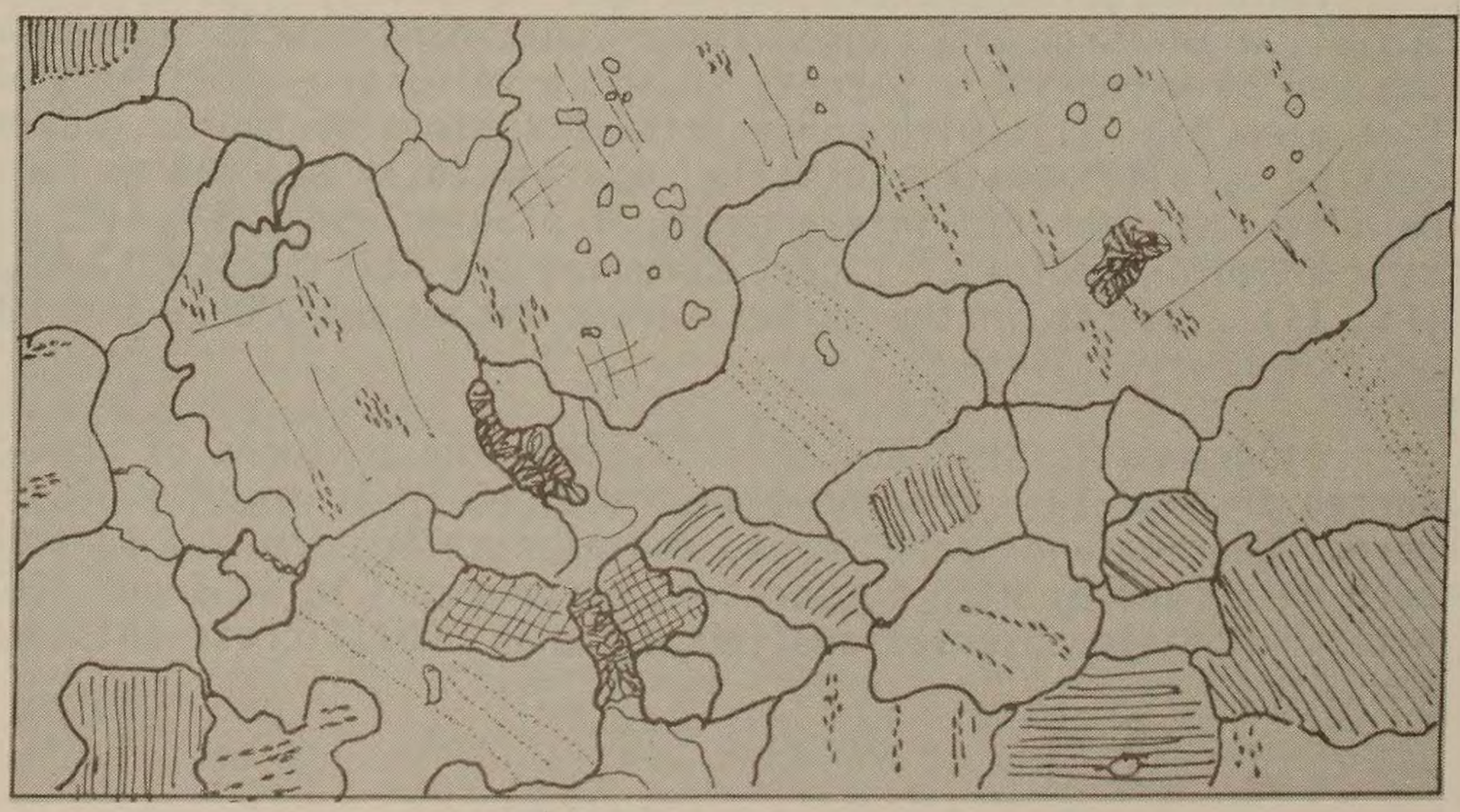

SCGIII ⌊⌋

Mineral Chemistry

Feldspars

Representative feldspar compositions (obtained by microprobe analysis with a 20μ beam) from samples of SCGI-SCGIII are shown in Table 3 and plotted on Fig. 7. Ternary feldspar isotherms on Fig. 7 are from Whitney & Stormer (1977) for low structural state feldspars. Peak temperatures (obtained from the most sodic Kspar in a sample) range from ~ 680°C (at P = 5kb) to ~ 720°C (at P = 10kb). These temperatures are minimum estimates due to the possibility of re-equilibration. In general, peak temperatures from SCGIII samples (including the garnetiferous SCGIII sample no. 7) are ~ 100°C higher than the peak temperatures from SCGI and SCGII samples. This difference is probably more apparent than real; rather than indicating any real temperature gradient between the different groups (which is physically implausible) it probably reflects variations in the extent of post-peak re-equilibration. All of the analysed samples show some evidence of resetting to lower temperatures (~ 500°C), as shown by the occurrence of grains of less sodic Kspar. The difference in peak temperatures between groups SCGI, SCGII and SCGIII probably relates to more extensive solid-state homogenisation in the former. This interpretation is supported by the textural differences noted above, whereby SCGI and SCGII have solid-state deformation textures whereas SCGIII retains igneous textures.

Consistent zoning of plagioclase was noted only in samples V and 3 of group SCGIII, where zoning ranged from Ab_{78} to Ab_{94} (core to rim) and from Ab_{74} to Ab_{86} (core to rim) respectively.

Garnet

The typical composition of garnets in garnetiferous SCGIII veins is $Py_{9.5}$ Alm_{80} Gr_4 $Sp_{6.5}$; for comparison, garnet in metagreywackes of the Plainfield Formation averages Py_{20} Alm_{75} Gr_3 Sp_2 (Table 3). Thus garnets in the veins are notably richer in CaO and MnO than those in the country rock. Vein garnets have considerably lower M/FM (0.106) than country rock garnets (0.211).

Comparative zoning profiles of vein and country rock garnets are shown in Figs. 7 and 11. Country rock garnets have very complex zoning whereas vein garnets are essentially unzoned. This cannot be an effect of diffusive homogenisation which would preferentially homogenise the smaller (country rock) garnets, contrary to observation. Thus it appears that vein garnets are not xenocrysts of country rock.

Allen and Clarke(1981) separate xenocrystic garnets from magmatic garnets in the South Mountain Batholith of Nova Scotia by composition, $Py_{9.5}Alm_{80}Gr_{1.3}Sp_{6.6}$ vs. $Py_6Alm_{76}Gr_2Sp_{16}$. Similarly spessartine-rich compositions ($Py_{3.5}$ $Alm_{61.5}$ $Gr_{2.5}$ $Sp_{32.5}$) characterise magmatic garnets in the Ruby Mountains (Kistler et al., 1981). Not all magmatic garnets are so spessartine-rich; for example, samples from the Kinsman Quartz Monzonite of New Hampshire (Clark, 1977) average Py_{22} Alm_{73} Gr_2 Sp_2. Thus spessartine content alone may not discriminate magmatic and metamorphic garnets, and the relatively low spessartine content (6.5%) of sample 7 garnets does not necessarily imply a non-magmatic origin.

The abundant quartz inclusions in the SCGIII garnets are compatible with synchronous crystallisation of garnet and quartz from a melt. Garnet-biotite tie-lines for sample 7 are shown in AFM projection in Fig. 13 in comparison to tie-lines for garnet-biotite pairs in surrounding metamorphic rocks. The crossing tie-lines for rocks of similar grade are suggestive of very different modes of origin, i.e. magmatic vs. metamorphic.

Abbott and Clarke (1979) present a variety of AFM liquidus topologies to allow crystallisation of garnet from granitic liquids; these are shown below as Fig. 14. Topologies A and B of Fig. 14 allow crystallisation of both garnet and sillimanite from liquid, and may allow the observed mantling of garnet by sillimanite in sample 7. Both topologies require T > 700^{o}C; A (cordierite-absent) is favoured over B at P > 7kb. These conditions (P > 6kb, T > 700^{o}C) were apparently attained in the Stony Creek area (see "Metamorphic Framework" section). It is therefore plausible that the garnets in SCGIII crystallised from a melt.

Biotites

Representative biotite compositions from SCGII and SCGIII are shown in Table 3. The high (~ 3.2%) TiO_2 contents suggest that even in strongly deformed SCGII much original igneous mineral chemistry is retained. Particularly striking is the very low M/FM of biotites from sample 7 (which contains garnet interpreted as igneous). Biotites of peraluminous granites are characterised by tetrahedral Al contents of 2.5-2.8 per 22 oxygens, and by MgO/MgO + FeO ~ 0.6-0.8 (Clarke, 1981). Only biotite from sample 7 (SCGIII group) fits both criteria.

Bulk Chemistry

XRF analyses of samples from units SCGI-SCGIII are presented in Table 4, together with published analyses of Narragansett Pier Granite, Hope Valley alaskite and Pelham dome gneiss (Dry Hill Gneiss) for comparison. Also shown for comparison are published analyses of a peraluminous garnet-granite from the Ruby Mountains and of a metamorphosed rhyolite from the Adirondacks. Previously published analyses of Stony Creek Granite (here ≡ SCGI) and Branford Quartz Monzonite (≡ garnetiferous SCGI) are also shown in Table 4.

There is very little difference between SCGI samples and SCGII samples; marginally higher Na_2O in SCGII may be more apparent than real. Some SCGI samples have very high K_2O (~7%). To test proposed correlations of Stony Creek basement with Pelham Dome basement and Hope Valley basement, published analyses of these are shown. Only partial analysis of the Dry Hill Gneiss was reported (Hodgkins, 1983). The Dry Hill Gneiss is clearly richer in Fe_{total} and poorer in CaO (and possibly Na_2O) than Stony Creek samples. Hope Valley alaskites (this study and Day et al., 1980) are typically higher in SiO_2 and lower in Al_2O_3, CaO and Fe_{total} than SCGI and SCGII. Similarly the Adirondack metarhyolite (which is chemically similar to Hope Valley alaskite) is higher in SiO_2 and lower in Al_2O_3, CaO and Fe_{total} than SCGI and SCGII.

Surprisingly, the garnetiferous SCGI sample no. 6 shows very little difference from garnet-free SCGI. Published analyses of Branford Quartz Menzonite, however, show markedly higher Al_2O_3: (Na_2O + CaO + K_2O) consistent with the presence of garnet. Analyses of these show similarities to the garnet-2-mica granite from the Ruby Mountains.

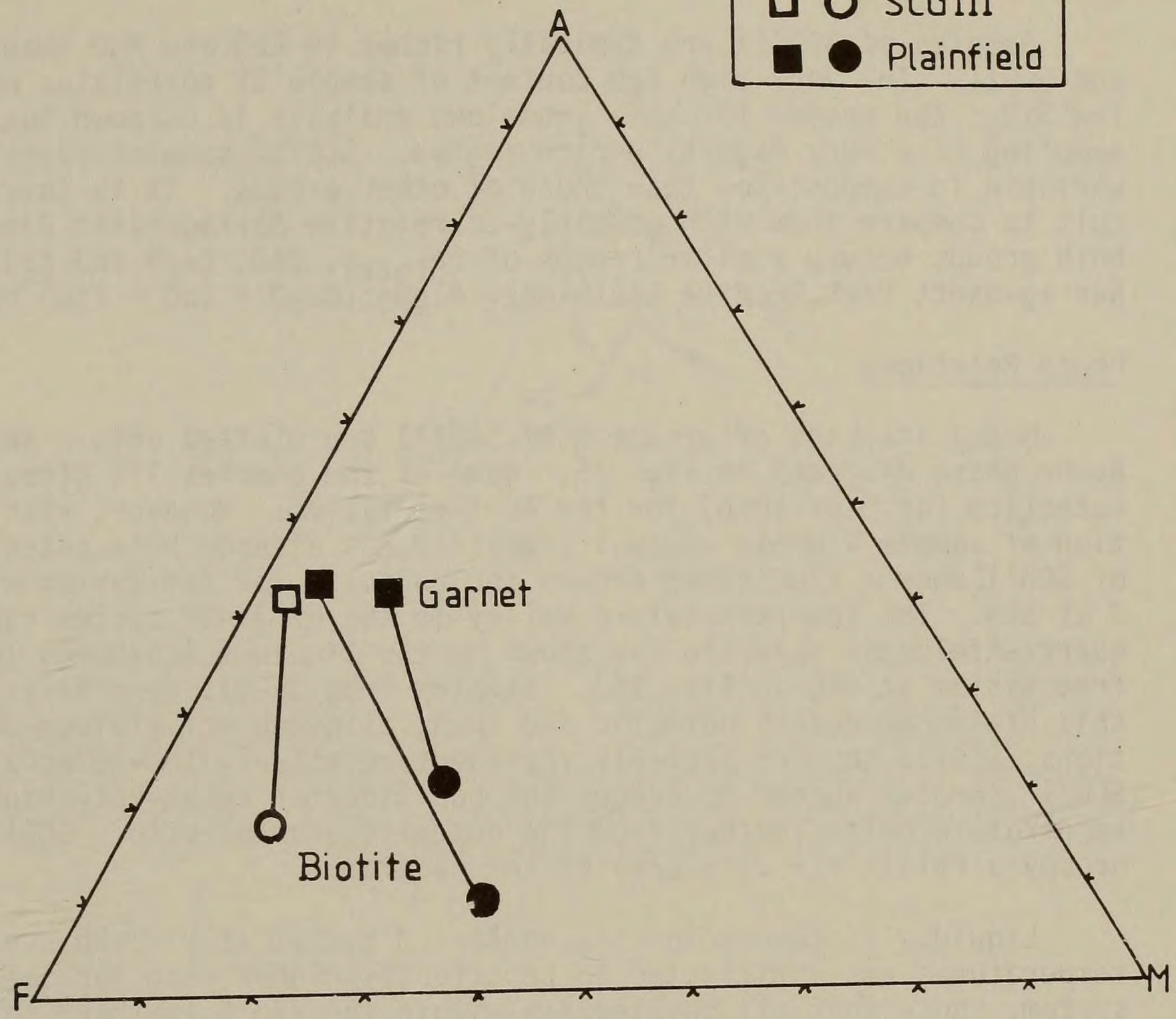

Figure 13. AFM projection of garnet-biotite tielines for 2 country-rock samples and for SCGIII sample 7.

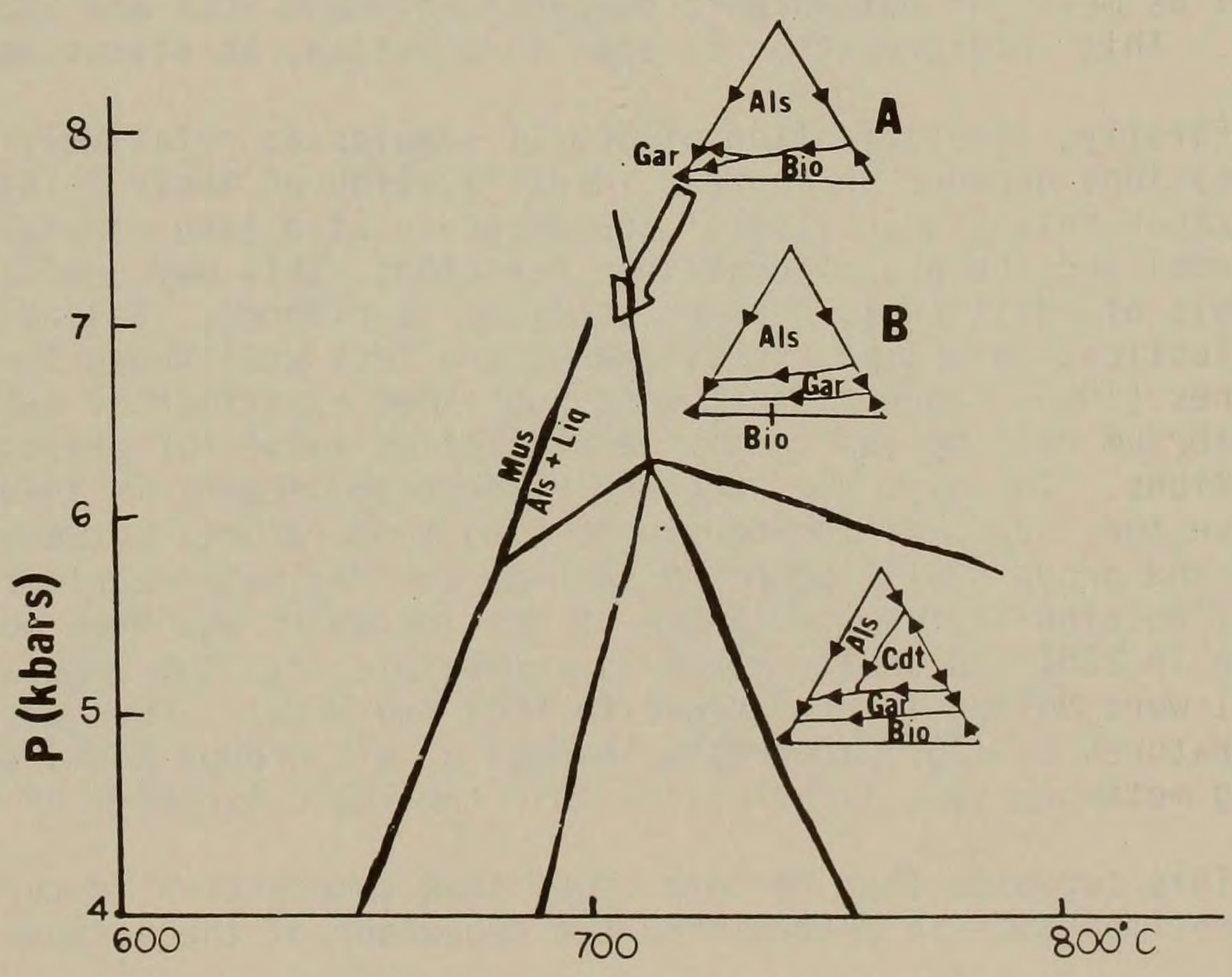

Figure 14. AFM liquidus topologies for garnet-bearing melts, from Abbott and Clarke (1979).

Samples of SCGIII are typically richer in FeO and MgO than are SCGI and SCGII. The very high FeO content of sample 5V correlates with very low SiO_2; the reason for this anomalous analysis is unknown but may reflect sampling of a very magnetite-rich region. SCGIII samples appear more variable in composition than those of other groups. It is therefore difficult to compare them with possibly-correlative Narragansett Pier Granite; both groups occupy similar ranges of Fe_{total}, CaO, Na_2O and K_2O. However, Narragansett Pier Granite has higher Al_2O_3:(Na_2O + CaO + K_2O) ratios.

Phase Relations

Modal analyses of groups SCGI-SCGIII are plotted onto a series of Qz-Ab-Or phase diagrams in Fig. 15. None of the samples lie close to the eutectics (at 5 or 10kb) for the An-free system. However, with the exception of sample V whose unusual chemistry has already been noted, samples of SCGIII show a clustering around the eutectic for the system with Ab/An = 3 at 5kb. The low-temperature valley in the Qz-Ab-Or system runs along the quartz-Kfeldspar cotectic (as shown by the liquidus isotherms for the An-free system at 5kb in Fig. 15). Samples from SCGIII generally lie along this Kfeldspar-quartz cotectic and thus, although not minimum-melt compositions, SCGIII samples probably represent relatively low-temperature melts. SCGII samples appear to occupy the positions of relatively higher-temperature melts further from the eutectic and cotectic. SCGI samples occupy a relatively wide area of the diagram.

Liquidus isotherms for the Ab/An = 3 system at P = 5kb are unknown; temperatures are anticipated to be slightly higher than for the An-free system. Note that all samples lie within the 740°C isotherm for the An-free system at P = 5kb; temperatures in the An_{25} system are unlikely to be more than about 25°C higher (Johannes, 1985). It seems likely therefore that groups SCGI-SCGIII all lie within the 760°C isotherm; this is near the upper limit of temperatures recorded by metamorphic assemblages in the area. The data is consistent with, but does not demand, occurrence of SCGIII as melts at metamorphic temperatures where SCGI and SCGII were not melts. This interpretation is open to question, as discussed below.

Firstly, identification of SCGIII samples as relatively low-melting compositions depends on correct identification of their relatively higher plag:Kspar ratios. In view of coarse grain size (and consequent sampling problems) and the use of unstained sections, this may need further revision; analysis of additional, stained sections is planned. Secondly, the locations of eutectics, cotectics and isotherms are less well-known than Fig. 15 implies. Johannes (1985) suggests that most published experimental data are for disequilibrium melting and so may be of limited value for petrogenetic interpretations. Thirdly, the accuracy of geothermometers is inadequate to resolve the ~ 20°C difference in melting temperatures between group SCGI + SCGII and group SCGIII proposed in Fig. 15. As noted earlier ("Petrography") SCGIII retains textural evidence of melting which has been lost during deformation in SCGI and SCGII. This is compatible with the suggestion above that SCGIII were molten in preference to SCGI and SCGII. However, if metamorphic temperatures of 770°C are real, samples of all groups would have been molten during metamorphism, as all lie within the 760°C isotherm of Fig. 15.

This suggests that factors other than composition in terms of Qz:Ab:An:Or were important in determining the behaviour of the various granitic units.

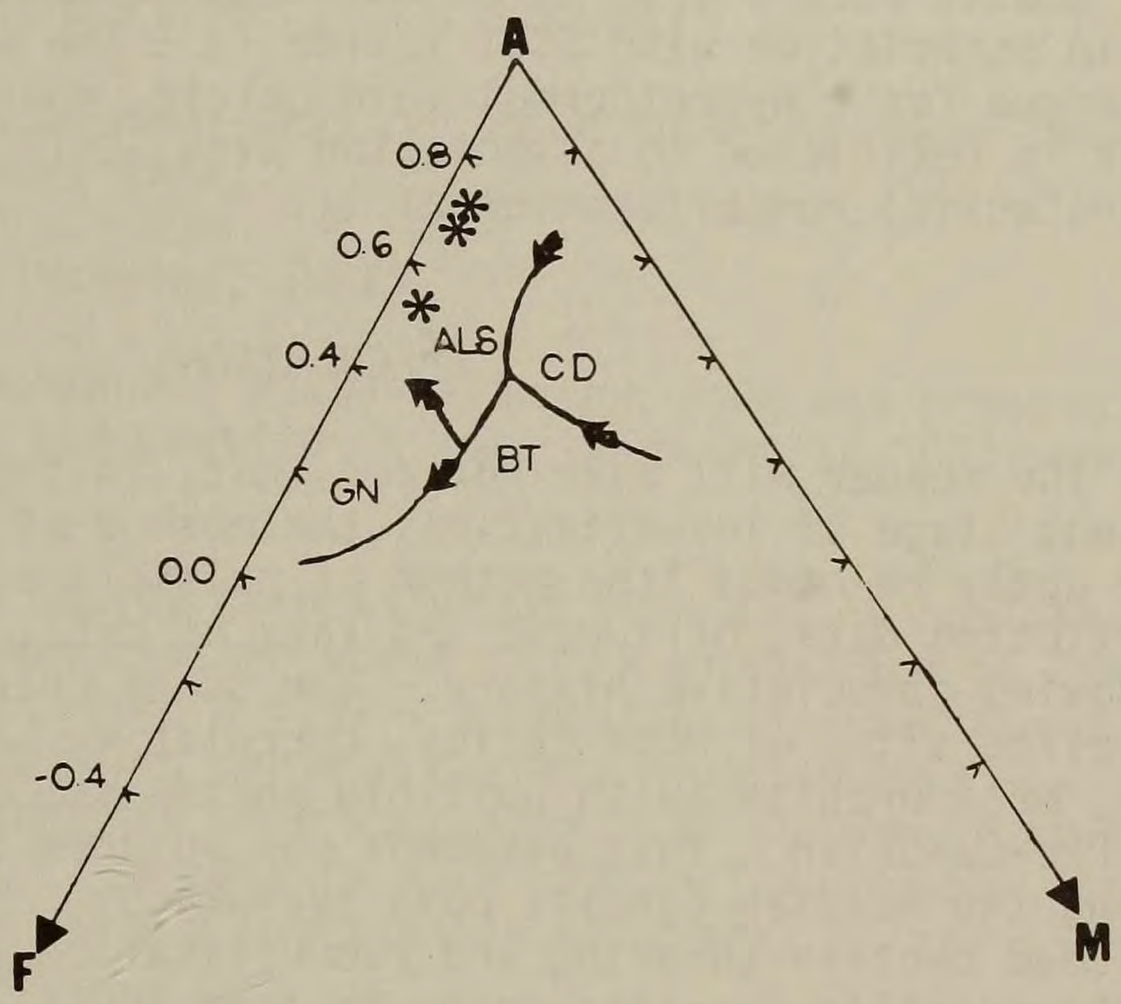

Figure 16. AFM projection of SCGIII samples compared to liquidus fields or sill. and gt. from Abbott and Clarke (1979).

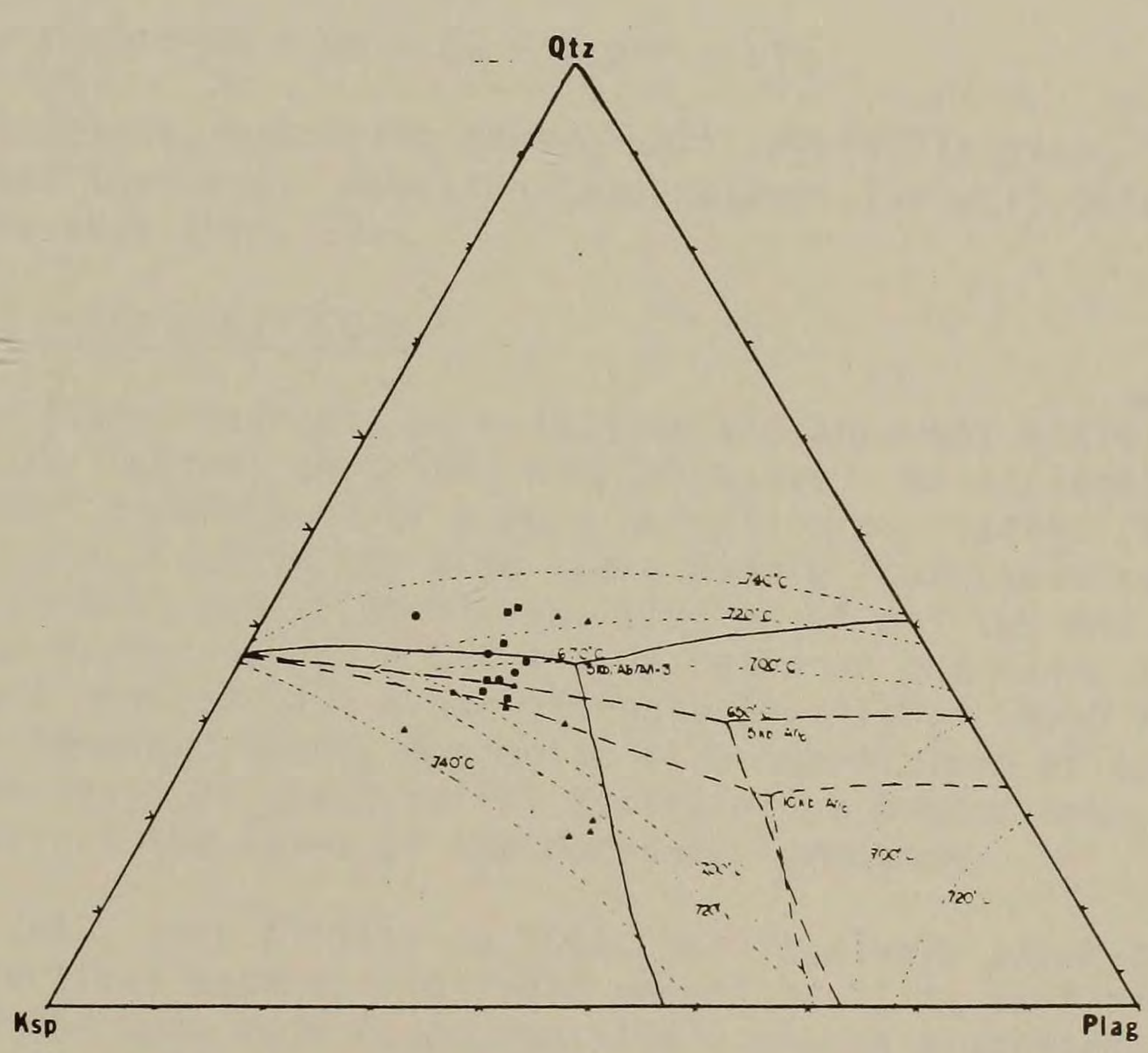

Figure 15. Modes of SCGI-SCGIII in Qz-Ab-Or compared to experimental data. Eutectics for An at 5 and 10 kb from Johannes (1985); eutectic for Ab/An^{o} = 3 from Winkler (1976). Liquidus contours for 5 kb from Luth and Tuttle (1964).

SCGIII occurs both as pegmatites outside the envelope of Plainfield and in association with SCGI inside it. The wide range of compositions may argue for a hydrothermal-vein origin, possibly derived from SCGI. SCGIV is restricted to association with SCGII and may form by (hydrothermal or anatectic) remobilisation of it.

SPECULATIONS

The reader will have noticed that, in the Stony Creek dome, at the present stage of investigation, the method of multiple hypothesis may be more aptly re-named "the method of multiple confusion". Undeterred by conflicting data, or indeed the lack of data, we present for amusement the following speculative history. The Stony Creek dome represents a far-travelled slice of Hope Valley--correlative basement, subject to deformation, metamorphism (with possible anatexis-SCGII) and intrusion (SCGI) in the Pre-Cambrian. This basement was sutured to North America before or during the Acadian (gneiss dome tectonics). Subsequent Alleghanian effects included ductile shearing and remobilisation (hydrothermal or anatectic) of the existing granitic units to form SCGIII and SCGIV. We look forward to animated discussions!

Possible factors favouring melts of SCGII include:

(i) higher MgO and/or FeO--this has been shown to lower the solidus by ~ 30°C (Naney, 1983)

(ii) higher B or F (Manning, 1981)

(iii) higher P_2O_5 (Johannes, 1985)--although P_2O_5 was present in only trace amounts, and apatite is more abundant in SCGII than in SCGIII.

Bulk analysis of one SCGIII garnetiferous vein and of published analyses of the Branford Quartz Monzonite are shown in AFM projection in Fig. 16. Also shown are Abbott and Clarke's (1979) schematic liquidus fields for P > 5kb, T > 700°C. All samples contain garnet, none contain Al_2SiO_5 (although sample no. 7, which is otherwise identical to the plotted sample, does contain sillimanite). All samples plot within the Al_2SiO_5 liquidus field. Boundaries in Fig. 16 are not well-constrained, so the significance of this is unknown.

Sample no. 7 contains textures suggestive of reaction of the form Gt + Liq → Sill ± Bi; this is incompatible with Abbott and Clarke's topologies. However, Clemens and Wall (1981) note that at temperatures ~ 700°C the reactions:

$$Bi + Plag + AS + V = Gt + Liq$$

and

$$Bi + Plag + AS + Qz = Gt + Kspar + Liq$$

can occur. Such reactions, operating during melt crystallisation, could generate the observed textures. Reaction temperatures lie well below peak temperatures for the area (Fig. 6).

Possible Origins of Units SCGI-SCGIV

Field evidence (the cross-cutting relations and apparent assimilation of xenoliths) strongly suggest that SCGI was intrusive. No explanation can be given for the local development of a more garnetiferous facies (STOP 7). This is restricted to a level in the dome where Middle Plainfield assimilation might be anticipated, and so local assimilation of pelites and consequent raising of the Al_2O_3: (Na_2O + CaO + K_2O) ratio of the magma might be postulated. Sample 6 however gave a surprisingly low Al_2O_3: (Na_2O + CaO + K_2O ratio). If the Branford Quartz Monzonite is a correlative of garnetiferous SCGI, the hypothesis of preferential assimilation breaks down; the Branford masses occur at the level of the Mamacoke Formation.

SCGII is chemically very similar to SCGI, but is always layer-conformable and is of limited vertical extent. In field relation, it is very similar both to the alaskites of the Lyme dome (Lundgren, 1967) and to alaskites of the Adirondacks (Carl and van Diver, 1975). The latter are interpreted as metamorphosed rhyolites. Chemically, SCGII is distinct from these (lower SiO_2, higher Al_2O_3, CaO and Fe_{total}). The association with migmatised lower Plainfield Formation and the occurrence of possibly restitic garnet stringers is consistent with formation by anatexis. This will be investigated further.

TABLE 1

STRATIGRAPHY

MONSON GNEISS

Massive or, less commonly, layered gneisses. Dark grey, medium-grained qz-pl-bi-hb gneisses, probably intrusive.

MAMACOKE FORMATION

Massive or layered, fine-grained, light grey, qz-pl-bi±hb gneisses. "Striped" appearence in outcrop. Rare garnetiferous gneisses.

PLAINFIELD FORMATION

Upper — Well-bedded massive quartzite, minor calc-silicates and amphibolites.

Middle — Foliated grey pelitic gneisses, often migmatitic. Very variable; minor quartzite.

Lower — Highly migmatitic garnetiferous gneisses, garnetiferous amphibolites.

TABLE 2

MODAL ANALYSIS

SCGI Samples

	SCGI/1	SCGI/2	SCG/1	SCG/2	7/3
Qz	38	28	33	35	41
Plag	20	24	23	24	28
Kspar	33	38	40	39	25
Bi	8	9	3	1	6
Mt	1	1	tr.	1	tr.
Ap	tr.	tr.	1	tr.	tr.
Others	tr.	tr.	tr.	tr.	-

SCGII Samples

	19/1	19/2	20/1	20/2
Qz	31	34	35	39
Plag	21	21	21	14
Kspar	35	39	33	43
Bi	9	4	5	2
Mt	3	2	4	2
Ap	1	tr	2	tr.
Others	tr.	tr.	tr.	tr.

SCGIII Samples

	2	3/1	3/2	6/1	6/2	6/3	V/1	V/2	V/3	7/1	7/2
Qz	28	32	28	32	36	39	18	17	19	27	26
Plag	18	25	18	23	22	22	39	37	40	23	28
Kspar	51	39	39	42	36	31	37	40	37	35	32
Bi	2	3	10	3	4	6	3	2	2	3	3
Mt	1	1	3	-	1	tr.	3	3	2	tr.	tr.
Ap	tr.	tr.	2	-	tr.	tr.	-	1	tr.	tr.	tr.
Others	tr.	-	tr.	-	(Gt)1	(GT)1	-	-	tr.	12	11

TABLE 3

MINERAL COMPOSITIONS

KFeldspar

	SCGI[1]	SCG[1]	6[1]	19[2]	20[2]
SiO_2	64.20	66.24	65.78	63.13	63.98
Al_2O_3	18.75	18.83	18.78	18.54	18.29
CaO	0.04	0.02	0.08	0.02	0.01
Na_2O	1.30	1.62	1.21	1.09	2.03
K_2O	14.99	13.27	14.15	14.05	14.26
Total	99.27	99.98	100.00	99.99	98.56
Or	87.7	85.5	88.6	89.6	82.3
Ab	11.3	15.5	11.4	10.4	17.6
An	-	-	-		-

	2[3]	3[3]	V[3]	7[4]
SiO_2	64.56	64.74	64.78	63.93
Al_2O_3	19.14	18.13	18.53	19.28
CaO	0.10	0.06	0.04	0.05
Na_2O	2.71	1.74	1.34	1.92
K_2O	13.38	13.47	15.42	14.77
Total	99.89	98.14	100.11	100.00
Or	73.7	83.5	87.1	83.2
Ab	23.4	16.5	11.6	16.5
An	2.9	-	1.3	0.2

Plagioclase

	SCGI[1]	SCG[1]	6[1]	19[2]	20[2]
SiO_2	61.98	62.94	63.41	63.13	64.07
Al_2O_3	24.18	23.84	22.91	22.42	21.78
CaO	4.89	4.82	3.93	3.22	3.38
Na_2O	8.94	8.72	8.95	9.38	9.69
K_2O	0.35	0.26	0.74	0.40	0.28
Total	100.34	100.59	100.94	98.54	99.19
Or	1.8	1.5	4.1	2.2	1.6
Ab	75.5	75.5	77.1	82.3	82.6
An	22.7	23.0	18.8	15.5	15.8

	2[3]	3[3]	V[3]	7[4]
SiO_2	61.82	62.40	62.93	64.08
Al_2O_3	24.16	23.67	23.12	22.50
CaO	4.93	4.95	4.20	3.95
Na_2O	8.55	8.61	9.06	9.06
K_2O	0.47	0.34	0.27	0.38
Total	99.30	99.98	99.58	100.00
Or	2.5	2.0	1.4	2.2
Ab	73.9	74.5	78.5	78.9
An	23.6	23.5	20.1	18.9

Biotite

	SCGI[1]	19[2]	V[3]	7[4]
SiO_2	31.85	39.28	37.24	35.46
TiO_2	4.37	3.46	2.91	5.00
Al_2O_3	13.70	13.30	14.06	16.00
FeO	26.09	20.56	22.76	26.13
MnO	-	0.11	0.09	0.07
MgO	10.17	10.30	9.25	4.65
CaO	0.05	0.05	-	0.17
Na_2O	0.02	0.03	-	0.19
K_2O	10.19	9.99	10.24	9.40
H_2O	3.00	3.00	3.00	3.00
Total	99.44	100.08	100.05	100.07

Ions to 24(O,OH)

	SCGI[1]	19[2]	V[3]	7[4]
Si	5.51	6.44	6.29	5.99
Al^4	2.49	1.55	1.71	2.01
Al^6	0.30	1.02	1.05	1.18
Ti	0.57	0.42	0.36	0.63
Fe	3.77	2.82	3.17	3.69
Mn	-	0.01	0.01	0.01
Mg	2.62	2.52	2.29	1.17
Ca	-	-	-	0.03
Na	-	-	-	0.06
K	2.36	2.09	2.17	2.03
M/FM	41.0	47.2	41.9	24.1

1 SCGI
2 SCGII
3 SCGIII
4 SCGIII garnet-bearing

TABLE 4

BULK CHEMISTRY

SCGI Samples

	5C	32C	SCGI	6
SiO_2	68.68	74.23	71.24	70.25
Al_2O_3	16.20	14.49	14.43	15.11
Fe_{total}	1.64	2.19	2.29	2.22
MgO	0.09	0.10	0.22	0.01
CaO	1.55	1.33	2.36	1.63
Na_2O	4.20	2.29	4.67	5.09
K_2O	7.31	4.97	4.36	5.11
TiO_2	0.28	0.28	0.32	0.28
MnO	0.01	0.02	0.03	0.06
Al/Alk	1.24	1.68	1.27	1.27

Possible correlatives to SCGI

	SCG[1]	TRG[2]	BQM[3]	BQM[3]	RM[4]
SiO_2	70.19	73.00	74.29	72.47	73.60
Al_2O_3	15.66	13.60	14.74	14.78	14.00
Fe_2O_3	0.72	2.98	0.20	0.57	0.80
FeO	0.81		0.65	2.00	1.40
MgO	0.24	0.56	0.15	0.34	0.18
CaO	1.23	1.51	0.80	1.27	0.92
Na_2O	2.87	3.21	2.70	4.03	2.90
K_2O	7.41	4.47	4.62	4.53	4.70
TiO_2	0.15	0.31	0.10	-	0.06
MnO	0.01	0.07	0.06	0.48	0.01
Al/Alk	1.36	1.48	1.82	1.50	1.64

SCGII Sample

	20
SiO_2	70.71
Al_2O_3	14.48
Fe_{total}	1.89
MgO	0.07
CaO	1.63
Na_2O	5.29
K_2O	5.34
TiO_2	0.41
MnO	0.12
Al/Alk	1.18

Possible correlatives to SCGII

	HVA[5]	DH[6]	A[7]	HVA[8]	HVA[8]	HVA[8]	HVA[8]
SiO_2	73.61	n.a.	76.51	76.08	76.70	76.10	72.85
Al_2O_3	15.25	n.a.	10.60	11.09	11.06	12.99	13.12
Fe_2O_3	0.87	3.42	2.71	0.62	0.47	1.03	1.02
FeO				1.58	1.34	0.57	0.56
MgO	0.04	0.08	0.18	0.10	0.07	0.04	0.32
CaO	1.08	0.67	0.62	0.79	0.60	0.75	0.89
Na_2O	3.98	2.73	3.53	2.96	2.98	3.98	3.56
K_2O	4.98	4.42	4.40	5.28	5.41	5.03	4.83
TiO_2	0.14	n.a.	-	0.21	0.17	0.12	0.29
MnO	0.06	n.a.	0.01	0.07	0.05	0.02	0.05
Al/Alk	1.53	n.a.	1.24	1.23	1.23	1.33	1.41

SCGIII Samples

	2	5V	32V	61V	V
SiO_2	70.83	57.38	71.32	70.35	71.66
Al_2O_3	14.57	15.89	14.78	16.20	17.57
Fe_{total}	2.27	7.81	1.54	2.54	2.45
MgO		0.09	0.11	0.10	0.08
CaO	1.78	1.55	1.24	1.66	2.63
Na_2O	5.10	3.77	4.53	3.69	1.57
K_2O	5.00	9.13	5.97	5.02	3.65
TiO_2	0.42	0.57	0.25	0.31	0.35
MnO	0.03	0.05	0.02	0.09	0.04
Al/Alk	1.22	1.09	1.26	1.56	2.24

Possible correlatives to SCGIII

	NPG[9]	NPG[10]	NPG[10]	NPG[10]	NPG[11]	NPG[11]
SiO_2	70.37	71.96	70.45	70.59	74.30	74.89
Al_2O_3	15.75	14.26	14.09	15.76	15.18	14.71
Fe_2O_3	2.04	0.86	0.79	1.13	0.39	0.01
FeO		1.29	0.96	0.69	0.26	0.21
MgO	0.13	0.49	0.34	0.42	0.18	0.07
CaO	1.77	1.58	1.18	1.14	1.05	0.77
Na_2O	4.62	3.37	3.55	4.08	3.27	3.75
K_2O	4.93	5.06	5.13	4.99	4.35	4.88
TiO_2	0.39	0.45	0.24	0.29	0.11	0.08
MnO	0.03	0.03	0.02	0.03	0.01	0.01
Al/Alk	1.39	1.42	1.43	1.54	1.75	1.56

1. Stony Creek Granite from Mikami & Digman (1957)
2. Ten Rod Granite Gneiss from Day et al. (1980)
3. Branford Quartz Monzonite from Mikami & Digman (1957)
4. Ruby Mountains 2-mica-granet granite from Kistler et al. (1981)
5. Hope Valley Alaskite, this study
6. Dry Hill Gneiss (Pelham Dome) from Hodgkin (1981)
7. Adirandack alaskite from Carl & von Diver (1980)
8. Hope Valley Alaskite, from Day et al. (1980)
9. Narragansett Pier Granite, this study
10. Narragansett Pier Granite, Hermes et al. (1981)
11. Muscovite-garnet Narragansett Pier Granite, Hermes et al. (1981)

PLATE CAPTIONS

PLATE 1
SCGI from STOP 3, showing phase layering and biotite schlieren.

PLATE 2
Close-up of SCGII from STOP 3, showing lack of internal fabric.

PLATE 3
Veins of garnetiferous (?) SCGII in garnetiferous(?) SCGI, STOP 7.

PLATE 4
Migmatised Lower-Plainfield from STOP 8. Note marginal selvedges, very open folds and cross-cutting pegmatite.

PLATE 5
SCGIII from STOP 9, showing very strong L fabric; flattened aplitic layer parallels this.

PLATE 6
Close-up of SCGIII at STOP 9, showing garnet + biotite stringers.

PLATE 7
SCGIII from STOP 12, with feldspar augen forming strong L fabric, warped into shear zone.

PLATE 8
SCGIII from STOP 12, deformed in shear zones; SCGIV concentrated in these.

PLATE 9
Migmatised Lower Plainfield with pegmatite, possibly equivalent to SCGII, STOP 12.

REFERENCES

ABBOTT, R.N. & CLARKE, D.B., (1979), "Hypothetical liquidus relationships in the subsystem Al_2O_3-FeO-MgO projected from quartz, alkali-feldspar + plagioclase for $a_{H_2O} \leq 1$", Can. Mineral., 17, 549-560.

ALLAN, B.L. & CLARKE, D.B., (1981), "Occurrence and origin of garnets in the South Mountain batholith, Nova Scotia", Can. Mineral., 19, 19-24.

BERNOLD, S., (1962), "Structural geometry and tectonics of gneiss doming, Guilford, Connecticut", GSA Spec. Paper, 73, 115-116.

BOHLEN, S.J., (1984), "Geobarometry in granulites", In "Kinetics and Equilibrium in Mineral Reactions", ed. Saxena, S.K., Springer-Verlag.

CARL, J.D. & von DIVER, B.B., (1975), "PreCambrian Grenville alaskite bodies as ashflow tuffs, northwest Adirondacks, New York", Bull. Geol. Soc. Am., 86, 1691-1707.

CLARK, R.G., (1977), "Garnet-rich rocks in the Kinsman Quartz Monzonite, south-central New Hampshire", GSA Abs. with Progs., (1977), 252.

CLARKE, D.B., (1981), "The mineralogy of peraluminous granites: a review", Can. Mineral., 19, 3-17.

CLEMENS, J.D. & WALL, V.J., (1981), "Origin and crystallisation of some peraluminous (S-type) granitic magmas", Can. Mineral., 19, 111-131.

DALE, T.N., (1923), "The commercial granites of New England", U.S.G.S. Bull. 738.

DALLMEYER, R.D., (1982), "$^{40}Ar/^{39}Ar$ ages from the Narragansett Basin and southern Rhode Island basement terrane: their bearing on the extend and timing of Alleghanian tectonothermal events in New England", Bull. Geol. Soc. Am., 93, 118-1130.

DAY, H.W., BROWN, V.M. & ABRAHAM, K., (1980), "Pre Cambrian(?) crystallisation and Permian(?) metamorphism of hypersolvus granite in the Avalonian terrane of Rhode Island", Bull. Geol. Soc. Am., 91, 389-391.

DIXON, J.M., (1975), "Finite strain and progressive deformation in models of diapiric structures", Tectonophysics, 28, 89-124.

EUGSTER, H.P. & WONES, D.R., (1962), "Stability relations of the ferruginous biotite, annite", J. Petrol., 3, 82-125.

FERRY, J.M. & SPEAR, F.S., (1978), "Experimental calibration of the partitioning of Fe and Mg between biotite and garnet", Contr. Mineral. Petrol, 66, 113-117.

GHENT, E.D., (1976), "Plagioclase-garnet-Al_2SiO_5-quartz: a geothermometer-geobarometer", Am. Mineral, 61, 710-714.

GOLDSMITH, R., (1976), "Pre-Silurian stratigraphy of the New London area, south-eastern Connecticut", In "Contributions to the Stratigraphy of New England", ed. Page, L.R., G.S.A. Mem., 148, 211-275.

GROMLET, L.P. & O'HARA, K.D., (1984), "Two distinct late PreCambrian terranes within the "Avalon Zone", S.E. New England, and their late Palaeozoic juxtaposition", GSA Abs. with Progs., (1984), 20.

HATCHER, R.D., (1984), "Southern and central Appalachian basement massifs", GSA Spec. Paper, 194, 149-153.

HALL, L.M. & ROBINSON, P., (1982), "Stratigraphic-Tectonic sub-divisions of southern New England", Geol. Ass. Canada Spec. Paper 24.

HERMES, O.D., GROMET, L.P. & ZARTMAN, R.E., (1981), "Zircon geochronology and petrology of plutonic rocks in Rhode Island", In Guidebook for Field Trips in Rhode Island and Adjacent Areas", NEIGC at Univ. of R.I., Kingston, R.I., pp. 315-338.

HILLS, F.A. and DASCH, E.J., (1972), "Rb/Sr study of the Stony Creek granite, southern Connecticut: a case for limited remobilisation", Geol. Soc. Am. Bull., 83, 3457-3464.

HODGKINS, C., (1983), "Major element geochemistry and petrology of the Dry Hill Gneiss, Pelham dome, central Massachusetts", GSA Abs. with Progs., (1983), 141.

HOLDER, M.T., (1979), "An emplacement mechanism for post-tectonic granites and its implications for their geochemical features", In "Origin of Granite Batholiths: Geochemical Evidence", ed. Atherton, M.P. & Tarney, J.; Shiva Publishing.

INDARES, A. & MARTIGNOLE, J., (1985), "Biotite-garnet geothermometry in the granulite facies: the influence of Ti and Al in biotite", Am. Mineral., 70, 272-279.

JOHANNES, W., (1984), "Beginning of melting in the granite system, Qz-Or-Ab-An-H_2O", Contr. Mineral. Petrol., 86, 264-274.

JOHANNES, W., (1985), "The significance of experimental studies for the formation of migmatites", In "Migmatites" ed. Ashworth, J.R.; Blackie & Son, Glasgow.

KISTLER, R.W., GHENT, E.D. & O'NEIL, J.R., (1981), "Petrogenesis of garnet two-mica granites in the Ruby Mountains, Nevada", J. Geophys. Res., 86, 10591-10606.

LOSH, S. & BRADBURY, H.J., (1984), "Late Palaeozoic deformation within the Honey Hill-Lake Char fault zone, southern New England", GSA Abs. with Progs., (1984), 48.

LOUGHLIN, G.F., (1910), "Intrusive granites and associated metamorphic sediments in S.W. Rhode Island", Amer. J. Sci., 29, 447-457.

LUNDGREN, L.W. & EBBLIN, D., (1972), "Honey Hill Fault in eastern Connecticut: regional relations", Bull. Geol. Soc. Am., 83, 2773-2794.

LUTH, W.C. & TUTTLE, O.F., (1969), "The hydrous vapour phase in equilibrium with granite and granitic magmas", GSA Mem. 115, 513-548.

MANNING, D.A.C., (1981), "The effect of fluorine on liquidus phase relationships in the system Qz-Ab-Or with excess water at 1kb", Contr. Mineral. Petrol., 76, 205-215.

MIKAMI, H.M. & DIGMAN, R.C., (1957), "Bedrock geology of the Guilford 15-minute quadrangle", State Geol. and Nat. Hist. Surv. of Connecticut, Bull. 86.

MULLER, P.D. & CHAPIN, D.A., (1984), "Tectonic evolution of the Baltimore Gneiss anticlines, Maryland", GSA Spec. Paper 194, 127-148.

NANEY, M.T., (1983), "Phase equilibria of rock-forming ferromagnesian silicates in granitic systems", Amer. J. Sci., 283, 993-1033.

NAYLOR, R.S., (1975), "Age provinces in the northern Appalachians", Ann. Rev. Earth Planet. Sci., (1975), 387-400.

NEWTON, R.C. & HASELTON, H.T., (1981), "Thermodynamics of the garnet-plagioclase-Al_2SiO_5-quartz geobarometer", In "Thermodynamics of Minerals and Melts" ed. Newton, R.C., Navrotsky, A. & Wood, B.J.; Springer-Verlag.

O'HARA, K.D. & GROMET, L.P., (1983), "Textural and Rb-Sr isotopic evidence for late Palaeozoic mylonitisation within the Honey Hill Fault Zone, S.E. Connecticut", Amer. J. Sci., 283, 762-779.

O'HARA, K.D. & GROMET, L.P., (1984), "Identification, characterisation and ages of a ductile shear zone separating two late PreCambrian terranes, S.E. New England", GSA Abs. with Progs. (1984), 54.

OSBERG, P.H., (1978), "Synthesis of the geology of the north-east Appalachians", Geol. Surv. Canada Paper 78-13, 137-147.

QUINN, A.W., (1971), "Bedrock geology of Rhode Island", U.S.G.S. Bull. 1295.

RAMSAY, J.G., (1981), "Emplacement mechanics of the Chindamora batholith, Zimbabwe", J. Struct. Geol. 3, 93.

ROBINSON, P. (1984), "Realms of regional metamorphism in southern New England, with emphasis on the eastern Acadian metamorphic high", In "Regional Trends in the Geology of the Appalachian-Caledonian-Hercynian-Mauritanide Orogen", ed. Scherk, P.E.; NATO ASL Series C vol. 116; Reidel.

SANDERS, J.E., (1968), "Stratigraphy and structure of the metamorphic rocks of the Sachem's Head Anticline and related structural features, S.W. of Killingworth dome, south-central Connecticut", In "Guidebook For Fieldtrips in Connecticut", Connecticut Geol. and Nat. Hist. Surv. Guidebook no. 2, ed. Orvill, P.M.

STRECKEISEN, A., (1976), "To each plutonic rock its proper name", Earth Sci. Rev. 12, 1-33.

WHITNEY, J.A. & STORMER, J.C., (1977), "The distribution of $NaAlSi_3O_8$ between co-existing microcline and plagioclase and its effect on geothermometric calculations", Am. Mineral., 62, 687-691.

WINKLER, H.J.F., (1976), "Petrogenesis of Metamorphic Rocks", (4th ed.); Springer-Verlag.

ROAD LOG AND STOP DESCRIPTION

Assembly time: 8:00 a.m.

Assembly point: Branhaven Plaza, Branford.

If coming from New Haven and west, take exit 53 from I-95 (Connecticut Turnpike). Turn right on U.S. Rte 1 west - Branhaven Plaza is approximately 0.25mi on left.

If coming from New London, Rhode Island or most points east of New Haven, take exit 55 from I-95 (Connecticut Turnpike). Turn right at stop sign onto U.S. Rte 1 west, drive 2.8mi. Turn left at lights into Branhaven Plaza.

There will be an opportunity to buy lunch supplies between STOPS 4 and 5. Lunch is scheduled for the scenic attractions of STOP 9, but may be brought forward to STOP 7 (by a consensus of opinion) if hunger intervenes. Please consolidate vehicles as much as possible; many of the stops have extremely limited parking. We will be returning to Branhaven Plaza at the end of the trip to collect vehicles left there.

Mileage		
Interval	Total	
	0.0	Turn right out of plaza on U.S.1E and follow signs for I-95N.
0.3	0.3	Bear left: follow signs for I-95N.
0.8	1.1	Turn left at light for I-95N.
0.1	1.2	Turn right for I-95N (signed for "Rhode Island and East").
		Several outcrops of Branford Granite.
2.9	4.1	Take exit 56 off I-95N (signed for "Stony Creek").
0.3	4.4	Turn right at stop sign onto Thimble Island Road.
0.8	5.2	STOP 1

Turn left down Flat Rock Road and park. Walk back up Flat Rock Road, cross Thimble Island Road to low flat outcrops. We are here near the northwestern margin of the Stony Creek dome. The outcrop is dominated by units of the Upper Plainfield Formation, particularly the well-bedded quartzite member. Rafts of this,

several meters in length, are surrounded by anastomosing veins of granite belonging to the SCGI unit. The granite locally reaches 40 volume percent, and locally contains coarser subpegmatitic patches. Relict stratigraphy is preserved here.

The SCGI here shows a mineral shape fabric which wraps around enclaves of Upper Plainfield. Flattening strains here (discussed in the introduction) are attributed to ballooning during emplacement of SCGI.

Walk 0.3mi down Flat Rock Road past vehicles and up gentle hill. After 9th house on left, road forks; bear left and turn into first driveway on left. Walk to low flat outcrops behind house.

STOP 2.

Northwestern margin of Stony Creek dome. Enclaves of Upper Plainfield in SCGI. Upper Plainfield here is more varied than at STOP 1 and includes biotite-schists, amphibolites and semi-pelites together with quartzite. Granite: enclave ratio varies from 20:80 to 60:40. Some parts of the outcrop show relict stratigraphy as at STOP 1, and here foliations can be traced continuously from enclave to enclave. Elsewhere in the outcrop, however, internal fabrics cannot be traced continuously between enclaves; relative rotations of up to 60^{o} between adjacent blocks can be documented (see sketch below). Such rotation can apparently occur without disrupting the larger-scale stratigraphy. Towards the base of the outcrop both fabric and stratigraphy are disrupted, with various lithologies chaotically jumbled in apparently random orientation (see sketch). The extent of stratigraphic disruption does not seem to be solely controlled by the relative volumes of host and enclave.

Amphibolitic and biotitic enclaves contain aplitic layers which commonly show biotite-rich selvedges. These aplitic layers are folded, and the folds themselves are truncated at the margins of the enclaves (see sketch). Amphibolitic layers are commonly subequant (axial ratios ~ 1:1:1) whereas semi-pelitic enclaves are more tabular (axial ratios ~ 2:5:1:1). This is presumably due to variations both in original lithology and in competence contrast with the host.

The host is granite of SCGI type, here ~ 5mm in grain-size and without pronounced fabric. Locally coarser patches occur. Enclaves are commonly cut by small (~ 3cm.) veins of this coarser, undeformed SCGI.

We expect debate to focus on possible relations between the aplitic layers in the enclaves and the granite surrounding the enclaves. If these are gradational, why do the aplitic layers appear to define folds whilst the granite appears undeformed? Are the aplites mimetic after an earlier folded fabric? What is the significance of the biotite selvedge?

We also wish to discuss whether the enclaves are of tectonic origin (i.e. are boudins) or of magmatic origin (i.e. are xenoliths). Do the folds indicate intrusion of magma into previously-deformed rocks? Are folding and boudinage successive stages in a single, non-coaxial deformational event, or do they represent very different deformational events?

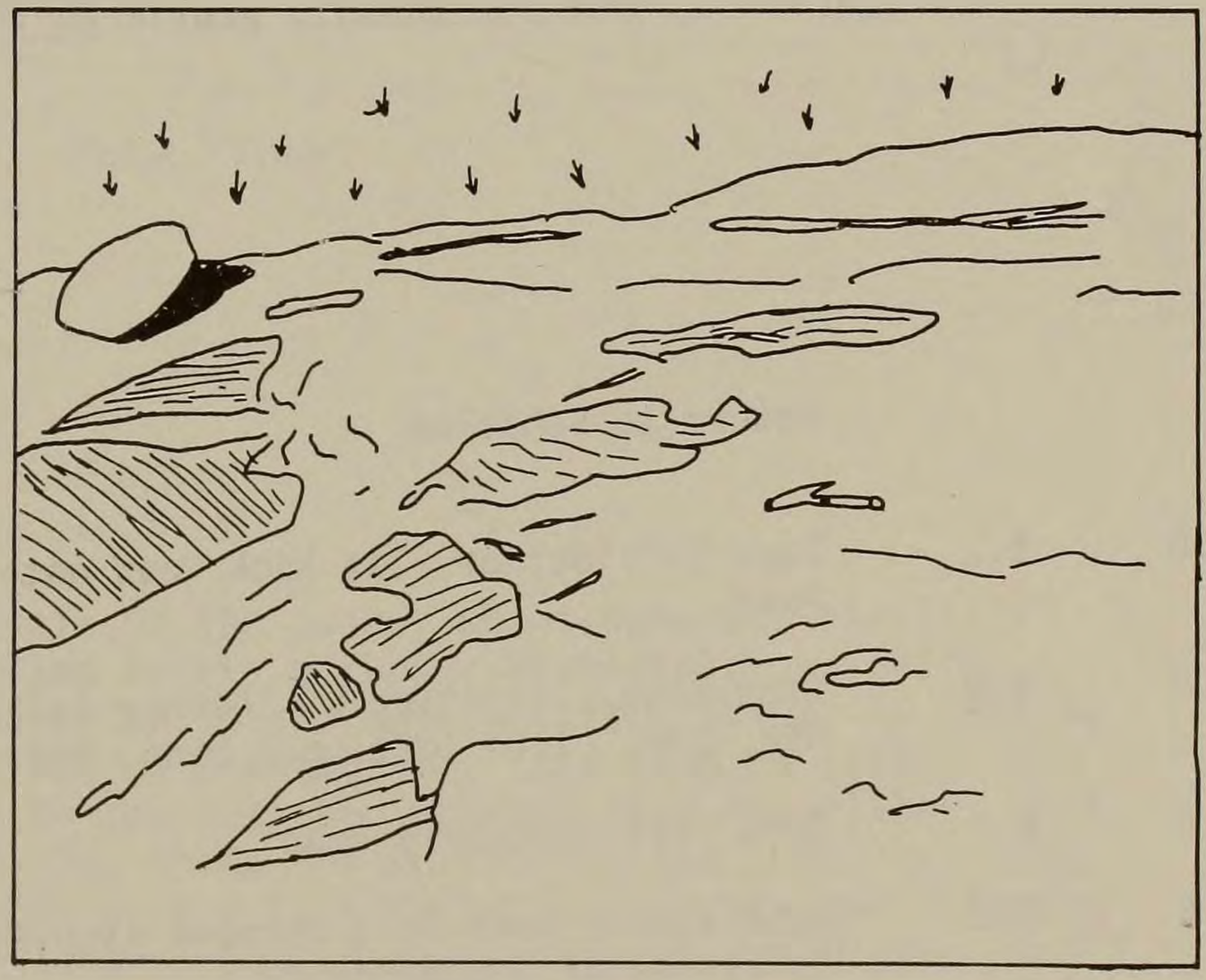

Fig. 17 STOP 2. Chaotic mixing of Upper Plainfield lithologic types in host of SCGI.

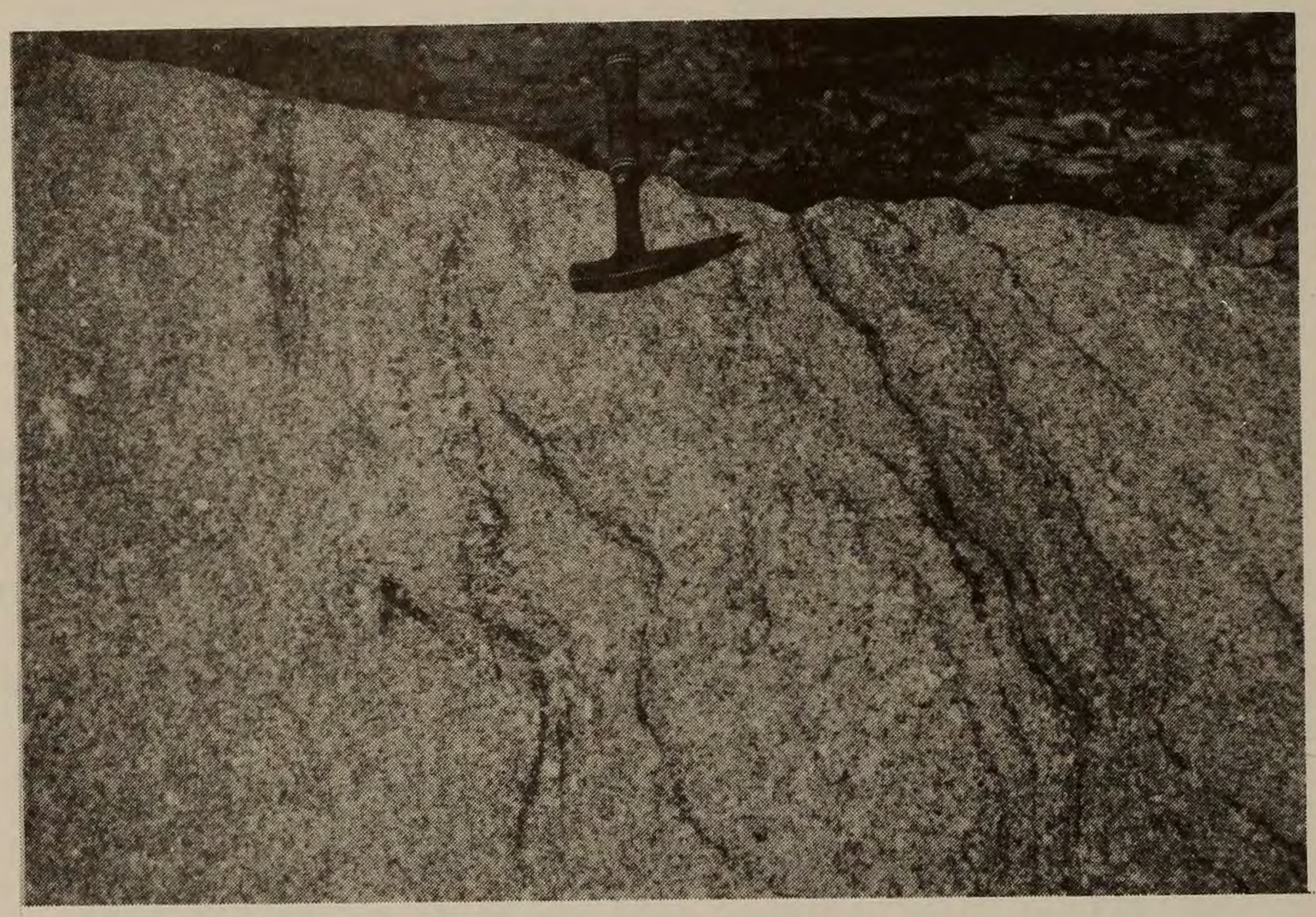

Plate 1 STOP 3. Biotite schlieren in SCGI from quarry.

Return to vehicles

0.0	5.2	Turn left out of Flat Rock Road onto Thimble Island Road.
0.8	6.0	Stop sign. Junction of Thimble Island Road and Conn. Rte. 146. Turn left onto Conn. Rte. 146.
0.6	6.6	Turn left on Quarry Road
0.6	7.3	Road forks; bear left through stop sign. (Gate here is closed at 3 p.m. daily.)
0.1	7.4	Large metal gate; closes at 3 p.m. daily. Continue through.
0.1	7.5	Park vehicles across from trailers. (If following this trip later, check in with quarry manager in large blue trailer.) Do not enter quarry without supervision,

i.e. after 3 p.m. or at weekends. Do NOT climb quarry faces and exercise great care when walking on loose blocks--not all of these are stable.

STOP 3.

The main working area of the quarry is to your left; follow track ~ 80m. towards working face. Examine the closer of the two faces striking NW-SE (see sketch).

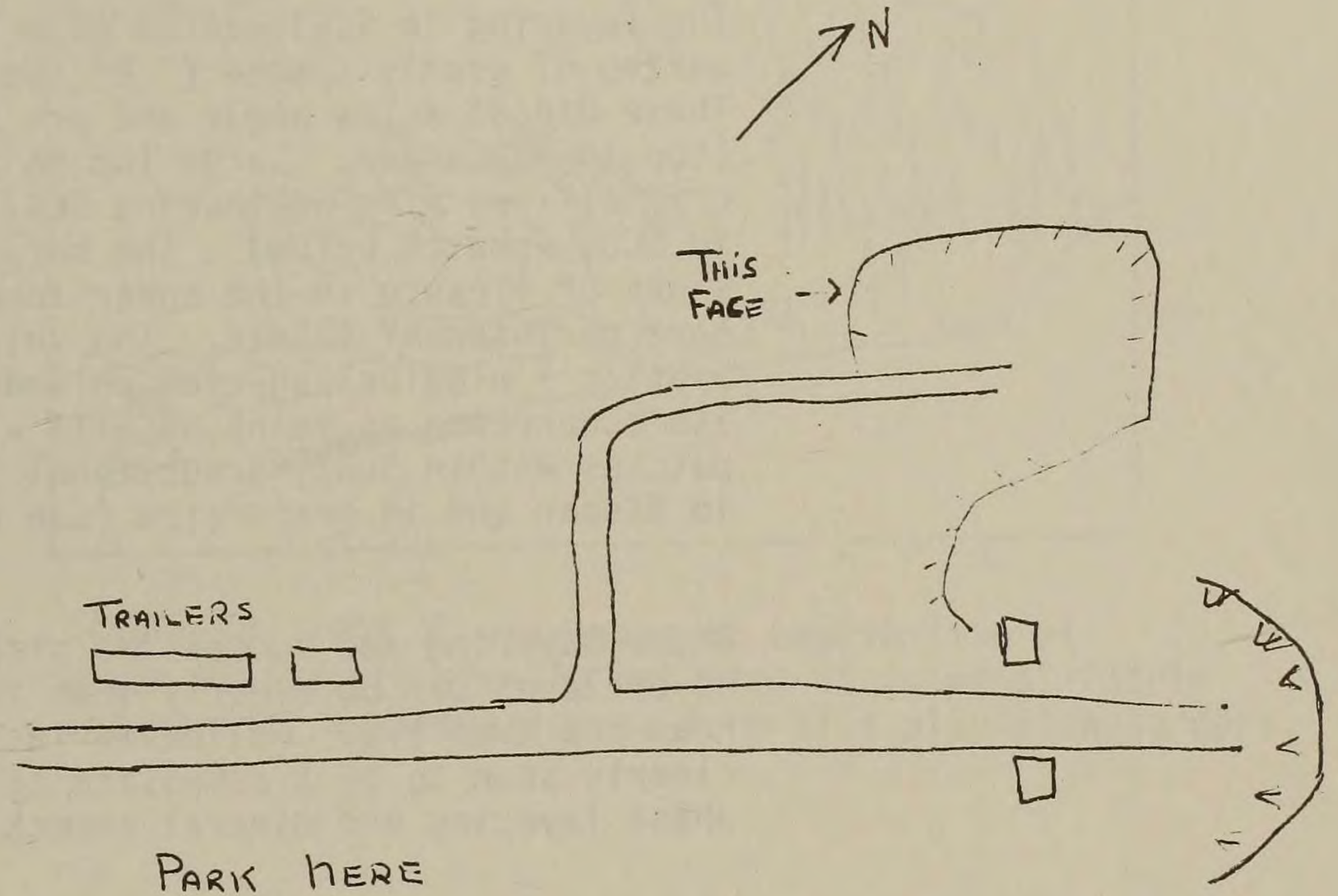

One wall of the quarry shows numerous partially digested blocks of Upper Plainfield quartzite, biotite schist and amphibolite. It was by tracing such relict stratigraphy that Sanders (1968) was able to map out the Sachem's Head Anticline. This wall also shows the well-developed phase layering of SCGI marked by alternating quartz- and feldspar-rich layers, attributed by Mikami and Digman (1957) to filter-pressing.

Sub-parallel to this are schlieren ~ 2" thick of more mafic material, predominantly biotite + plagioclase. These may either be the products of flow segregation

or highly flattened and assimilated xenoliths. If interpreted as xenoliths, their great lateral continuity would require extreme flattening: the blocky nature of observed enclaves may argue against such extreme flattening. However, such biotite + plagioclase-rich lithologies can be seen in the process of formation during assimilation of amphibolite xenoliths elsewhere in the quarry (Plate 1 and sketch below). This may support a xenolithic origin for the schlieren.

The layering in SCGI can be seen to be deformed by a series of evenly-spaced (~ 6" separation) shear zones. These dip at a low angle and are suggestive of dextral (top to NW) shear. Large (up to 18") veins of coarsely crystalline, pink-weathering SCGIII cut phase layering in SCGI (sketch below). The margins of these veins show signs of flexure in the shear zones; however, the veins have no internal fabric. The veins commonly have a biotite + plagioclase-rich selvedge. In addition to its occurrence as veins, SCGIII also occurs as irregular patches within SCGI, gradational into SCGI by a decrease in %Kspar and in grain size (see Plate 2).

Phase layering and successive stages in the assimilation of enclaves can be clearly seen in the gigantic blocks near the trailers. Foliation in SCGI (Plate 1) can be clearly seen to be a composite of biotite schlieren, phase layering and mineral aspect ratio.

If time permits, we will walk down the path to the right of the working area (the continuation of the entrance road) to the abandoned face. This face shows steeply dipping wedges of SCGI in the Upper Plainfield. This lit-par-lit structure, together with the assimilation so well displayed in blocks here, is suggestive of emplacement of SCGI by stoping which in turn implies a thermal contrast between granite and country rock and/or high-level intrusion. However, the flattening strains seen at the margin are more suggestive of diapirism, i.e. no thermal contrast and/or deep-level emplacement.

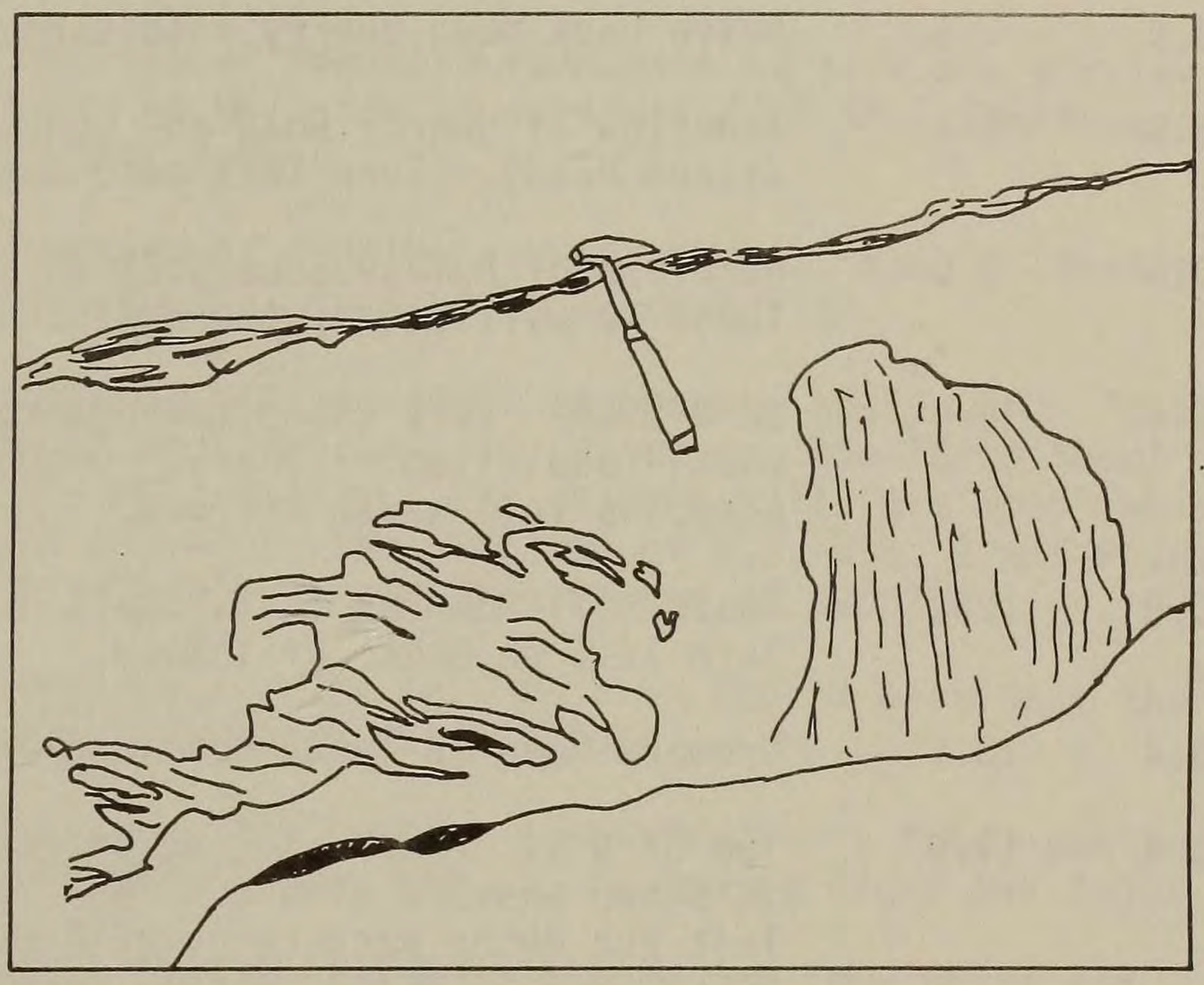

Figure 18 STOP 3. Enclaves of amphibolite of Upper Plainfield showing rotation of internal fabric and partial assimilation to form bi + plag-rich borders.

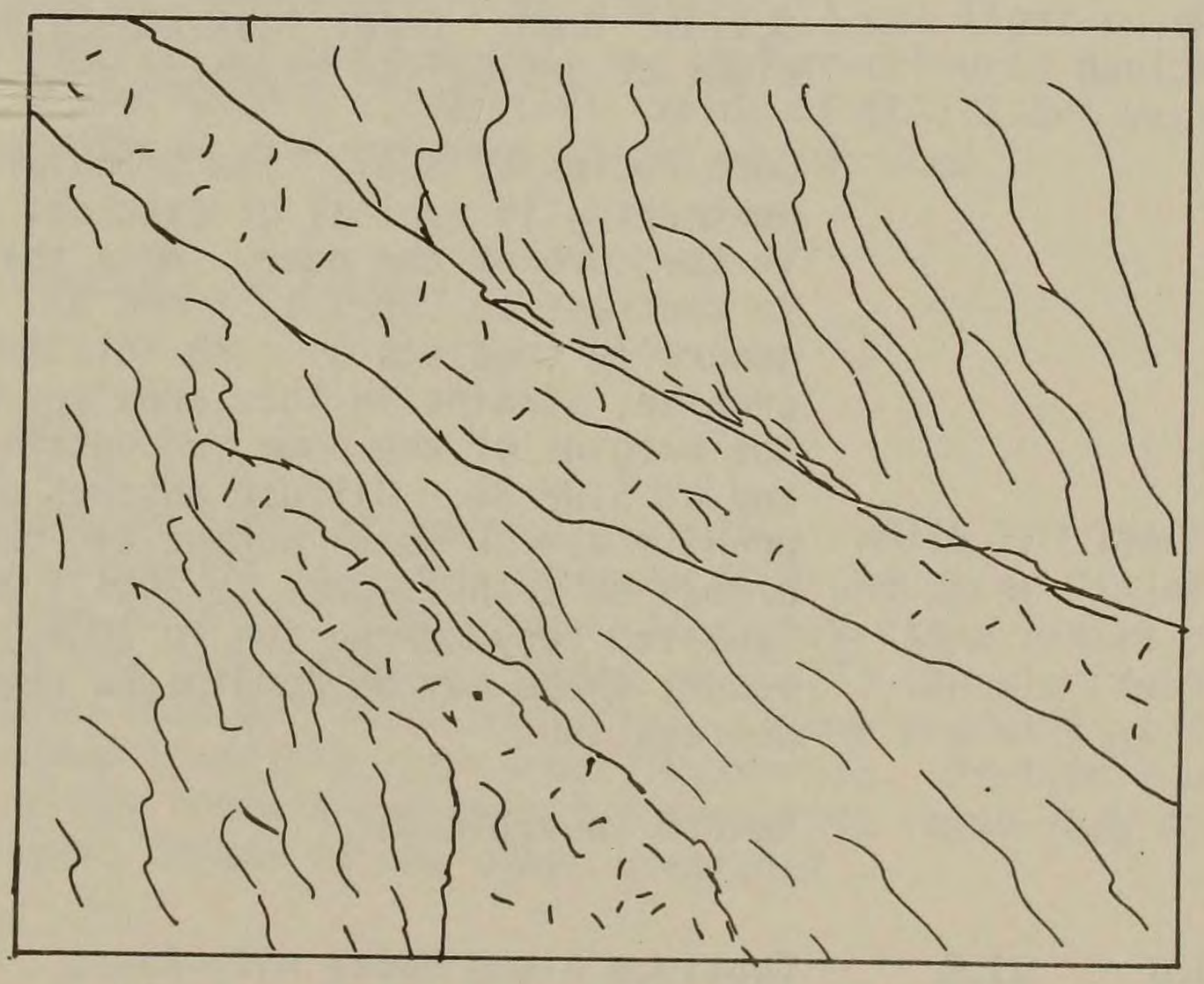

Figure 19 STOP 3. Veins of SCGIII cut phase layering in SCGI. Note selvedges.

Return to vehicles.

0.0	7.5	Drive back down quarry road through gates.
0.9	8.4	Junction of Quarry Road and Conn. Rte. 146 (Leetes Island Road). Turn left onto Conn. Rte. 146.
0.6	9.0	Outcrops of homogeneous SCGI on left are similar to those we will see at the next stop.
0.4	9.4	SLOW DOWN! Very sharp curve through railroad underpass, road often slippery. Oncoming traffic often occupies full width of road.
0.8	10.2	Moose Hill Road on left, Shell Beach Road on right. Turn left on Moose Hill Road.
0.4	10.6	Dromora Road on left; continue on Moose Hill Road.
0.4	11.0	Top of hill. Park at side of road, across from walled-in sheep pasture with conifers. Walk down drive at left and enter pasture by gate on left. (If doing this subsequent to NEIGC, please check with owner first.)

STOP 4

(If following this roadlog in winter, you will be able to detect the outcrops even through several inches of snow, by the simple expedient of kicking one's toes against them. Local inhabitants are accustomed to the sight of geologists brushing away snow in this pasture.)

Core Facies of SCGI. The granular appearance on weathering is typical of outcrops of homogeneous SCGI in the core of the dome. Note the lack of enclaves, in contrast to STOPS 1, 2 and 3. The core of the dome generally consists of such relatively clean, massive granite; strains in this area are much lower than at the margins of the dome (cf. grain shape fabrics here and at STOP 3). Diffuse patches of coarser-grained granite may be local pegmatitic segregations of SCGI, or may be transitional to SCGIII as seen at STOP 3. Isolated very coarse (up to 10cm.) Kspar crystals occur; these may be boudinaged pegmatites, or local segregations.

Return to vehicles.

0.0	11.0	Continue along Moose Hill Road.
0.8	11.8	Barker Hill Drive on left; continue on Moose Hill Road.

0.7	12.5	Stop sign. Continue straight. Note change of name of road to Peddler's Road. Do not turn left on Moose Hill Road.
0.1	12.6	Outcrops of Mamacoke Formation at left are similar to those we will see at optional STOP 5A. Continue on Peddler's Road.
1.4	14.0	Junction of Peddler's Road and U.S. Rte. 1 (Boston Post Road). Turn right at stop sign.
0.4	14.4	Shopping mall on right is stop to buy lunch. "Dairy Mart" provides basic supplies and the "Grog Shop" is self-explanatory. The "Bishop Hill Farm Shop" which you passed at the junction of U.S. Rte. 1 and Peddler's Road is also a possible source of supplies.
0.0	14.4	Leave mall, turn left on U.S. Rte. 1 back past the junction with Peddler's Road.
0.4	14.8	Junction of U.S. Rte. 1 and Peddler's Road--continue straight on U.S. Rte. 1, following signs for I-95S.
0.8	15.6	Turn right onto I-95S (signed for "New Haven and west").
0.2	15.8	OPTIONAL STOP 5A.

Park on right at edge of turnpike. WATCH FOR TRAFFIC. We will have a police escort for this section of the trip. Pegmatitic veins of SCGIII (marked on the State map as "Narragansett Pier Granite") cut light-coloured gneisses of the Mamacoke and darker-coloured gneisses of the Monson. Pegmatitic veins of SCGIII are very common on the northern margin of the dome.

Continue on I-95S.

STOP 5.

0.5	16.3	Park on right at edge of turnpike. WATCH FOR TRAFFIC. Lit-par-lit structure between SCGI and Upper Plainfield (see sketch). Again note relatively steep radial dips at the dome margins. Veins of SCGIII sharply cross-cut both SCGI and Upper Plainfield. Some pegmatitic patches carry (possibly retrograde) muscovite. Biotite schist layers contain qz+plag+Ksp+gt±sulfide veins--how do these relate to the other granites?

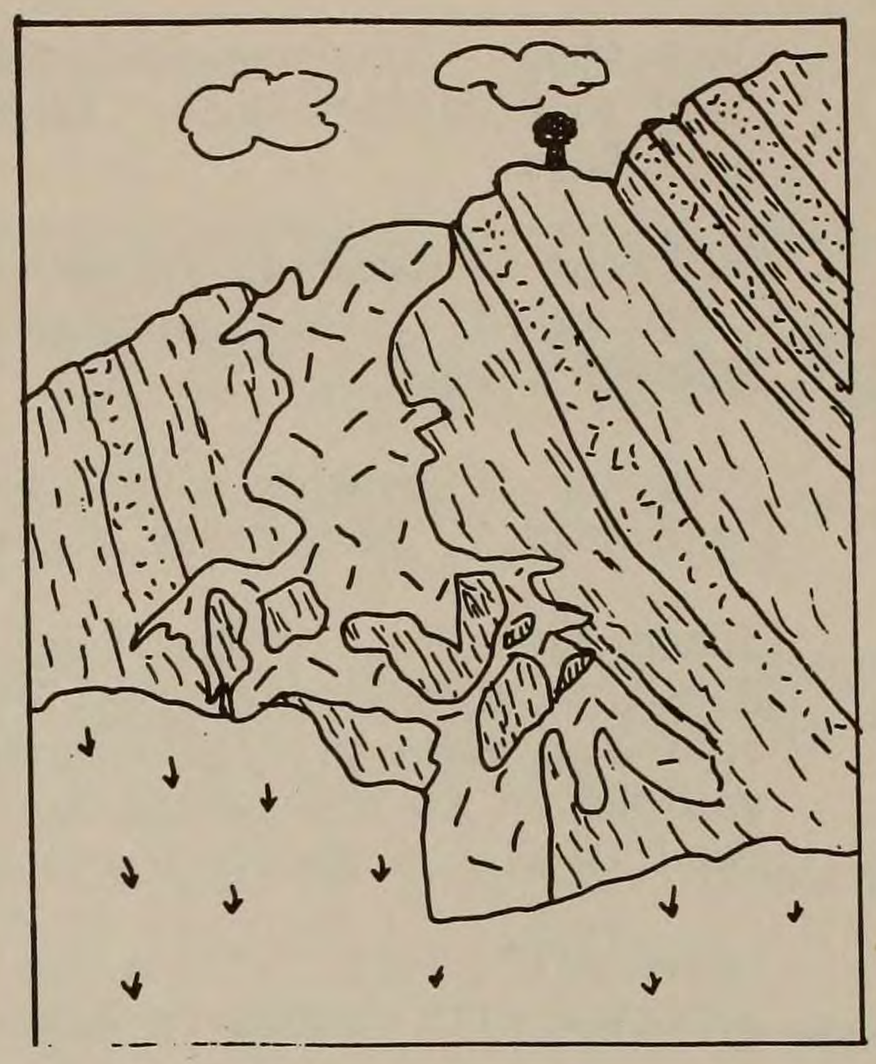

Figure 20 STOP 5. Lit-par-lit structures of SCGI and U.Pl.

Continue on I-95S.

1.3 17.6 STOP 6.

Park on right at edge of turnpike. WATCH FOR TRAFFIC. Walk ~ 100m. examining outcrop. Outcrop is predominantly SCGI with diffuse patches of SCGIII. This stop offers another opportunity to examine the assimilation of xenoliths and the biotite schlieren seen at STOP 3. Several very mafic blocks ~ 1m. in length show varying degrees of assimilation. These blocks appear to define a relict stratigraphy which is at an angle to the phase layering in SCGI. Plagioclase + biotite rims develop around the blocks at the contacts to granite. Local concentrations of mafics in SCGI appear to parallel the relict stratigraphy defined by the enclaves, and are likewise at an angle to phase layering. Moving W. along the outcrop (i.e. moving in from the dome margin) the dip of phase layering in SCGI can be seen to increase.

0.0 17.6 Return to vehicles and continue on I-95S.

1.3 18.9 Take exit 56 off I-95S. Turn left at stop sign onto Thimble Islands Road.

Continue on Thimble Islands Road past STOPS 1 and 2 to the junction of Thimble Islands Road and Conn. Rte. 146.

1.9	20.8	Junction of Thimble Islands Road and Conn. Rte. 146. Straight across on Thimble Islands Road, following sign for "Town Dock".
0.6	1.4	Bear left on Thimble Islands Road, following signs for "Town Dock".
0.2	21.6	Bear left on Thimble Islands Road.
0.1	21.7	Tennis courts on right.
0.1	21.8	Large Victorian mansion on right, Wallace Road on left. Don't take this entrance to Wallace Road.
0.1	21.9	Wallace Road on left; Long Point Road on right. Turn left on Wallace Road. Almost immediately there is a small green house with a white picket fence on the left; road forks just beyond this. Left fork goes up hill--do not take this. Take right fork into woods.
0.2	22.1	Track bends sharply to right through marsh. Park in turning circle on left. Follow main track around to right hand side of quarry--continue to far wall (east side) of quarry.

<u>STOP 7</u>.

DANGER--DO NOT CLIMB QUARRY WALLS.

Two old quarries near core of dome contain a garnetiferous facies of SCGI intimately associated with the more typical garnet-free SCGI. Strain is low in both types (cf. STOP 3). The garnetiferous facies is irregularly distributed on a scale ~ 10m; it does not show clear contact relations to SCGI. Enclaves of semi-pelitic material here are assigned to the Middle Plainfield; they show no consistent relation to the development of garnets in SCGI. Both garnet-bearing and garnet-free SCGI are cut by small veins of coarser, random-textured material. The veins in garnet-free SCGI appear to be of SCGIII type, and commonly show a well-developed selvedge (as was seen at STOP 3). Garnetiferous SCGI carries veins which are rich in Kspar+garnet; these veins typically lack a selvedge. Garnets in the veins are up to 5x the grain diameter of those in the host (see sketch). There is no systematic pattern to the orientation of the veins (Plate 3).

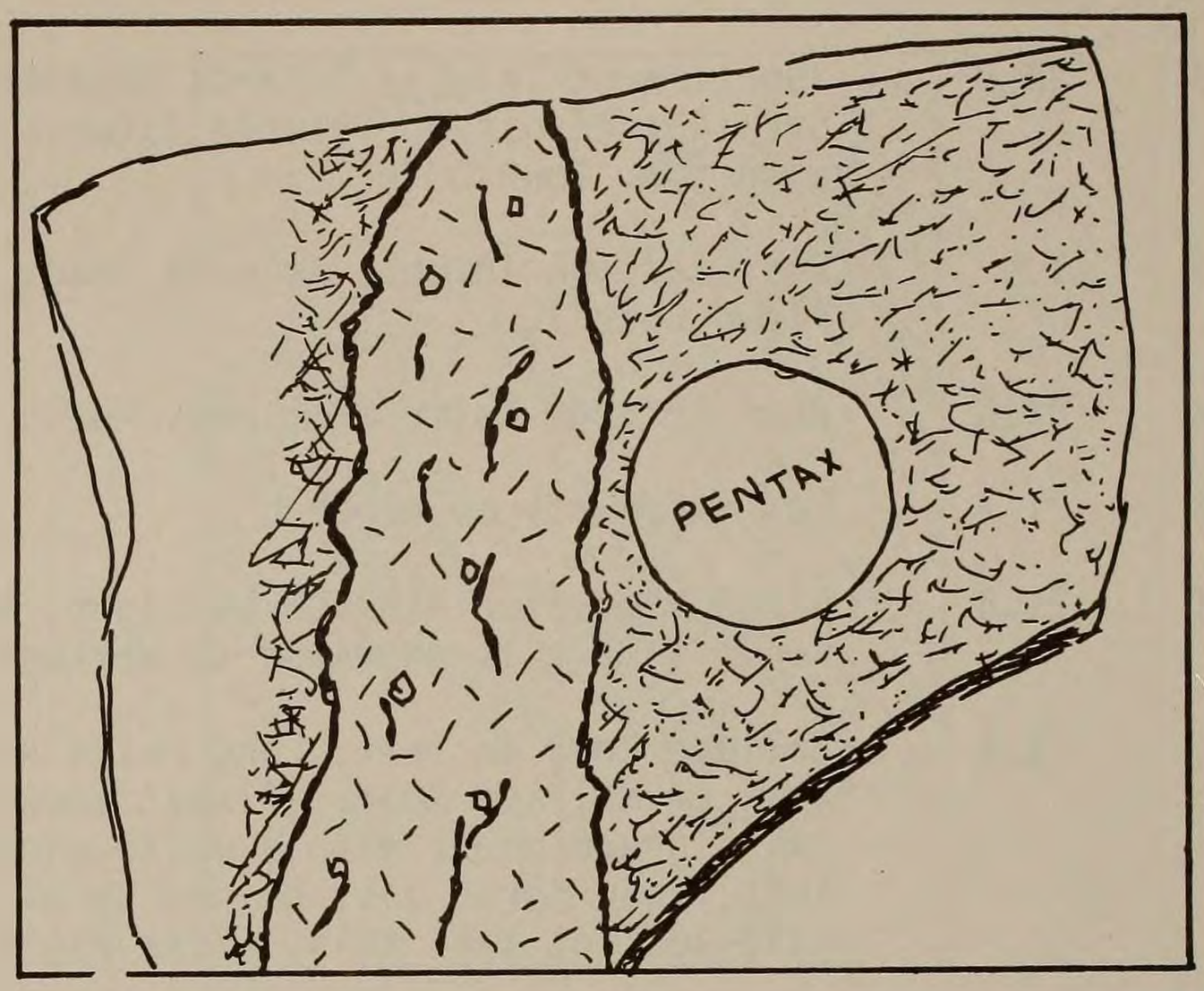

Figure 21 STOP 7. Garnetiferous (?) SCGIII vein in garnetiferous (?) SCGI.

The garnetiferous facies of SCGI has not been found elsewhere in the dome. Samples from these quarries were among those used by Hills and Dasch (1972) in dating the so-called Stony Creek Granite.

Return to vehicles.

0.0	22.1	Drive back down track to Wallace Road.
0.2	22.3	Turn left onto Wallace Road, then almost immediately right onto Thimble Islands Road at stop sign.
0.5	22.8	Thimble Islands Road Tennis Courts. Park by tennis courts, walk through motel grounds to outcrops on shore.

STOP 8.

(At the time of writing, we are unclear whether we will be able to obtain permission to visit this site.)

Outcrops below Stony Creek Pier show extensively migmatised and folded Lower Plainfield Formation (Plate 4 and sketch below). Biotite-gneisses predominate, often carrying veins rich in garnet. Highly aluminous layers consist of biotite + garnet (up to 25% gt)--these do not appear to be restitic, but appear to be

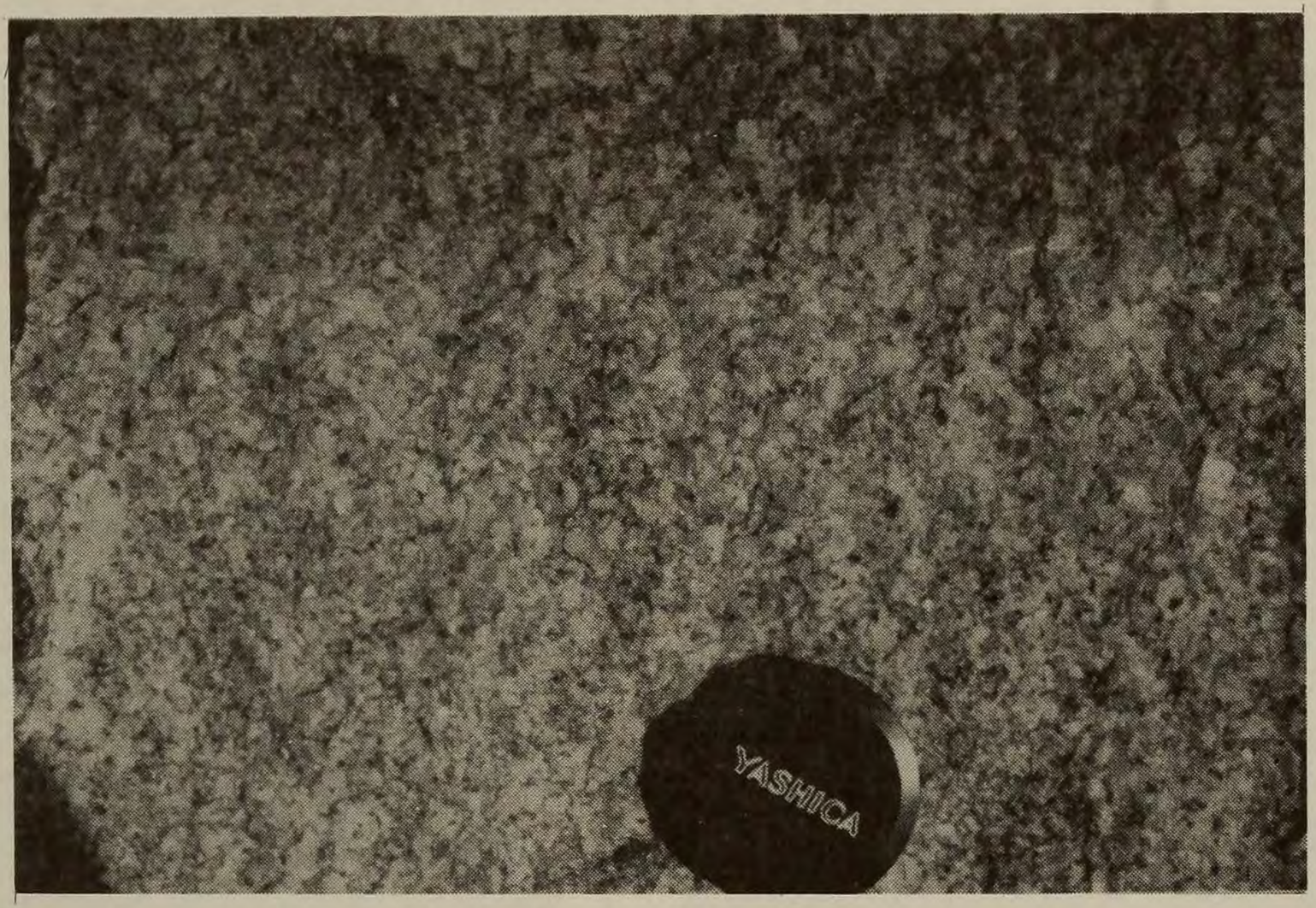

Plate 2 STOP 3. Close-up of SCGIII.

Plate 3 STOP 7. Garnet veins in SCGI.

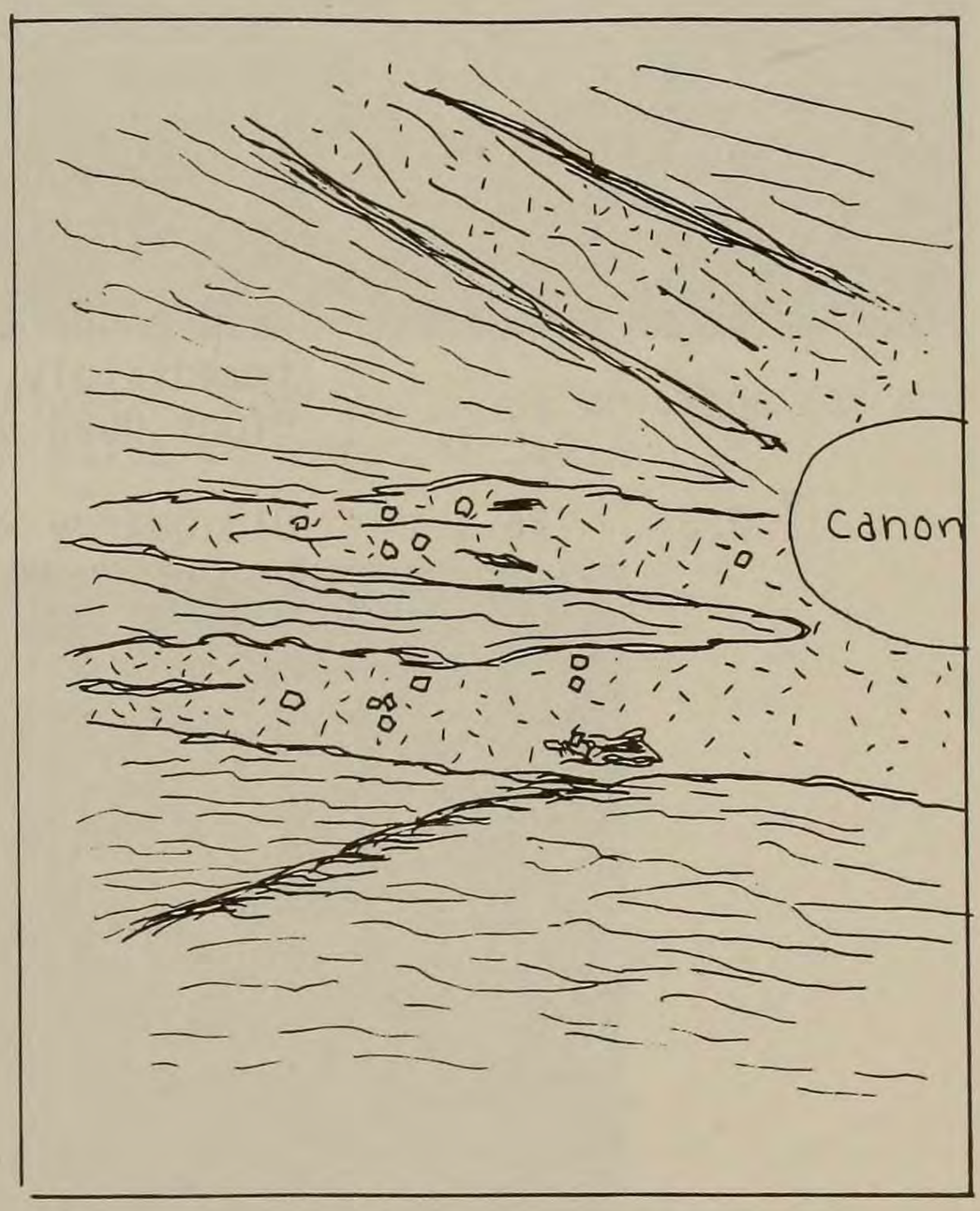

Figure 22 STOP 8. Migmatised L.Pl. with garnet bearing leucosomes.

original compositional layering. There are rare amphibole-rich lenses. Garnet-biotite geothermometry suggests T ~ 770°C here. Migmatite lenses in the Lower Plainfield are warped into open, upright folds; these folds are locally cut by small shears. Many leucosomes are trondhjemitoid, with tiny garnets enclosed in plagioclase crystals. The outcrop is cut by a large vein of massive pegmatite; at first glance this resembles SCGIII pegmatites such as seen at STOP 5, but it seems to be more quartz-rich, Kfeldspar poor. Locally it may contain biotite schlieren, and locally has garnet ± muscovite.

This outcrop is near the core of the dome, and is therefore presumed to be low-strain. At STOP 12 we will see very similiar lithologies to this, but showing more sign of strain. This variation in strain across the dome, and consequently variable fabric, makes correlation of the granitic units very difficult.

Return to vehicles.

0.0	22.8	Turn right at stop sign onto Thimble Islands Road.
0.7	23.5	Turn right at stop sign onto Conn. Rte. 146. This takes us back past the entrance to STOP 3.
1.7	25.2	SLOW--DANGEROUS BRIDGE AGAIN! Wave to those field trip participants stranded at first attempt at this bridge.
0.3	25.5	Road bends to right with New Quarry Road on left, and, immediately afterward, Old Quarry Road on right. Turn right down Old Quarry Road.
0.6	26.1	Old Quarry Road ends in circle. Park here. Walk between stone gate posts into "Yale University--Peabody Museum Field Station".

Walk past house to outcrops on shore. (If doing this subsequent to NEIGC, ask permission at the house.)

LUNCH STOP

STOP 9.

BE CAREFUL ON STEEP ROCKS!

Good exposures of SCGII, showing strong compositional banding defined by stringers of biotite + garnets, also strong shape fabric in quartz and feldspar (Plates 5, 6). Locally this fabric wraps augen of Kfeldspar.

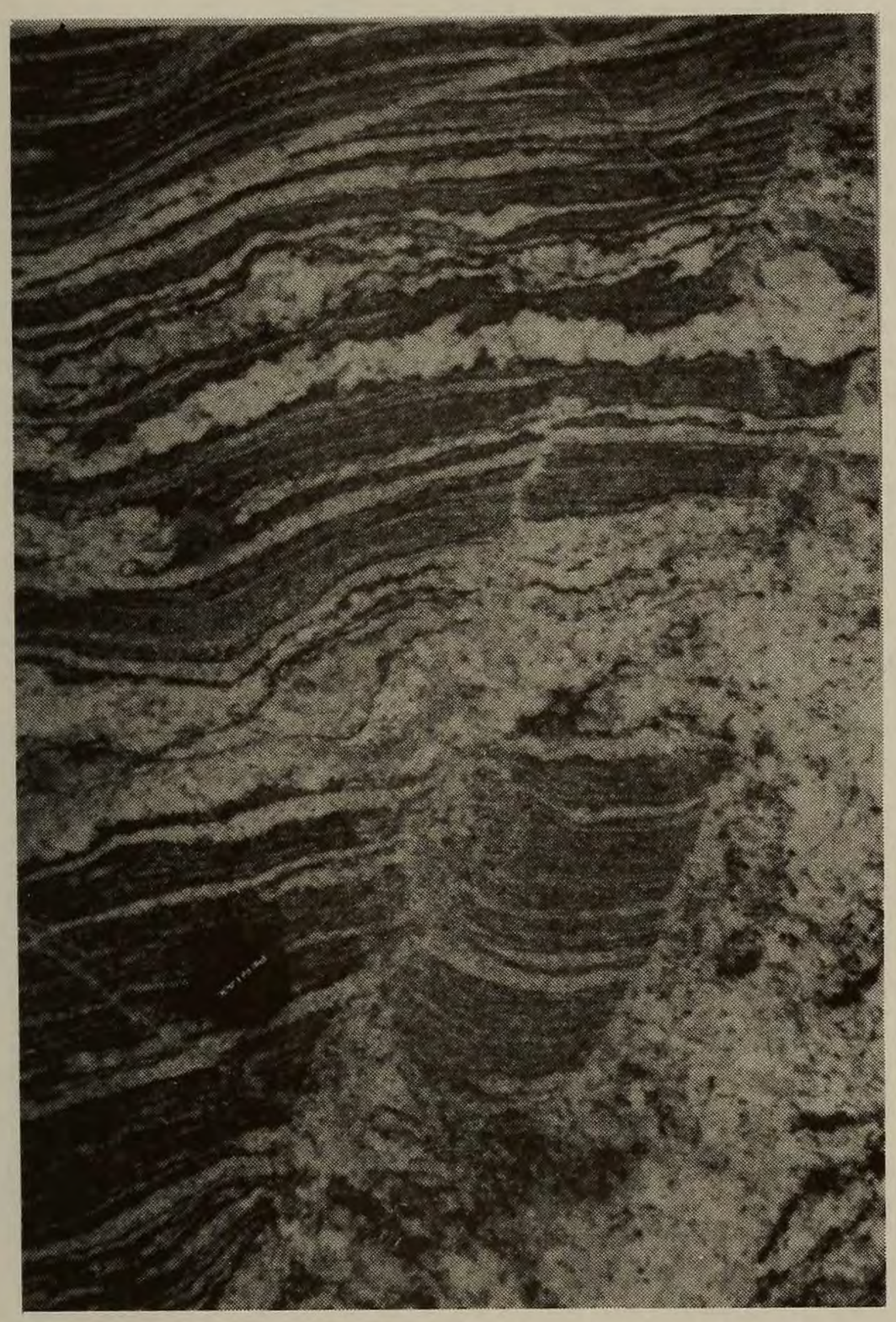

Plate 4 STOP 8. Migmatised L.PL. with selvedges. Note flexures and cross-cut pegmatite veins.

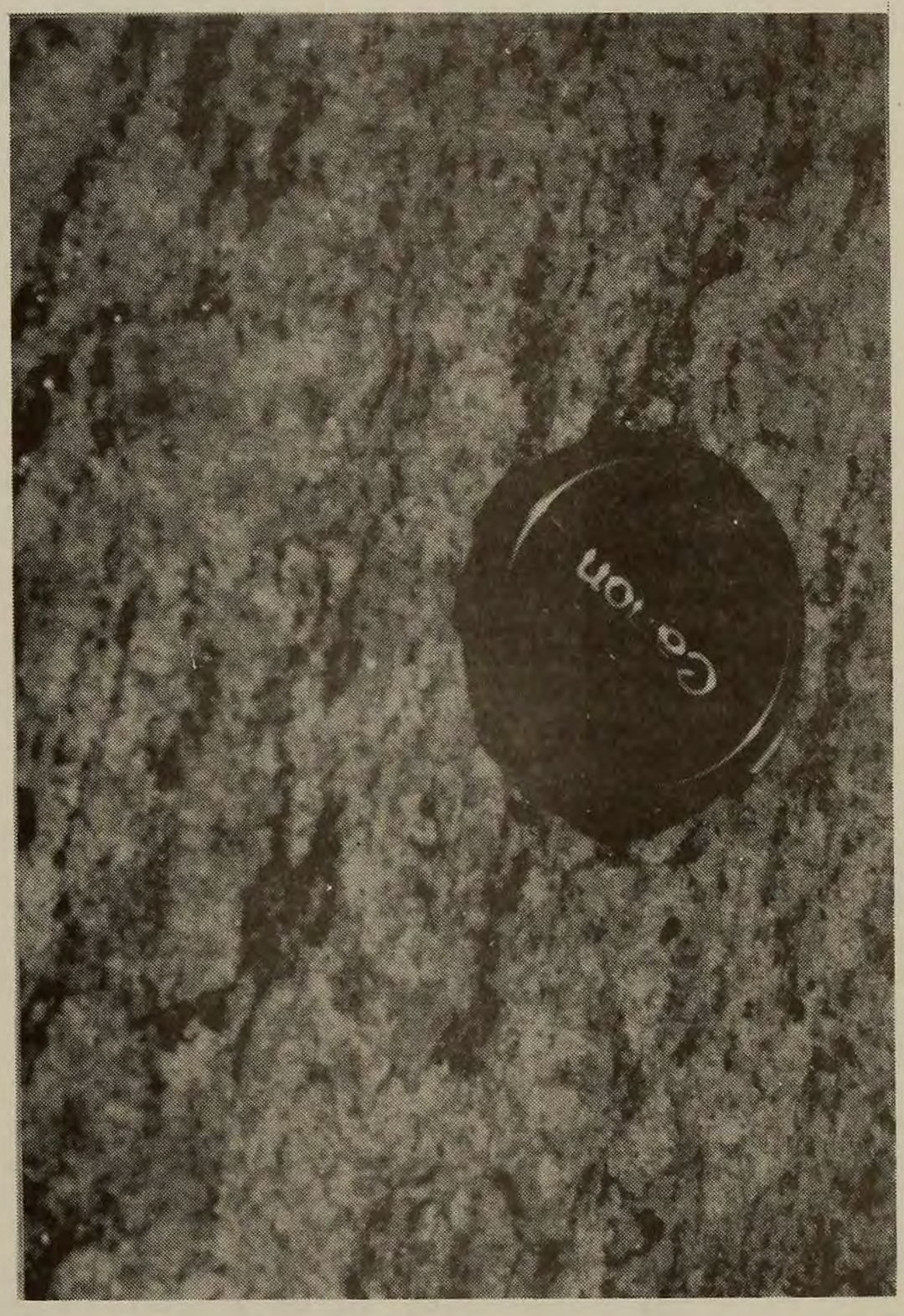

Plate 6 STOP 9. Close up of garnet and biotite stringers in SCGII.

Plate 5 STOP 9. Strongly lineated SCGII. Note flattened aplite.

SCGII is typically associated with Lower Plainfield Formation, but this is rare here. Biotite-rich enclaves of Lower Plainfield are locally rich in garnet; wisps of this material can be traced out into enclosing SCGII, where they form strands of tiny garnets. The biotite + garnet layers may be interpreted as highly strained layers of restite, or as the result of deformation of an original biotite + garnet-bearing granite.

An aplitic unit can be seen within the SCGII, at a low angle to layering; this may be a vein rotated into near-parallelism with layering during deformation. Both the layering in SCGII and the aplitic unit are deformed by shear zones identical to those seen at STOP 3.

0.0	26.1	Return to vehicles and retrace Old Quarry Road back towards Conn. Rte. 146.
0.5	26.6	Bear left, following"one-way" sign. At stop sign turn right on Conn. Rte. 146.
0.4	27.0	Moose Hill Road (leading to STOP 4) on left, Shell Beach Road on right. Turn right down Shell Beach Road.
0.2	27.2	Sign on left reads "Private Beach, Leetes Island Members Only". Park at right, by beach. Obtain permission if necessary. Walk to outcrops on right of beach. DO NOT ENTER GARDEN.

STOP 10.

Migmatised Lower Plainfield, SCGII and SCGIV. Biotite schist horizons of the Lower Plainfield carry very large plagioclases; are these porphyroblasts growing in situ by a metamorphic/anatectic process, or are they porphyroclasts indicating preferential deformation of originally coarser areas? Note the occurrence of isolated very coarse Kfeldspar elsewhere in the outcrop. Garnet-biotite temperatures here are ~ 730°C. As seen at STOP 8, the Lower Plainfield is deformed by early open folds and late shears.

SCGII is apparently interlayered with the migmatised Lower Plainfield, and shows the same shear deformation. This is presumably contemporaneous with that at STOPS 3 and 9. Biotite schlieren are common within masses of SCGII. SCGIV is developed as diffuse patches within shear zones in SCGII, and can be distinguished by its lack of fabric (it cross-cuts layering in SCGII) and by the presence of abundant garnets. These garnets are coarser than those in SCGII.

The outcrop is cut by a huge pegmatite vein (crystals up to 6cm.) bordered by huge biotite crystals. The relationship of this pegmatite to that at STOP 8, and in turn to pegmatitic SCGIII at STOP 5, is unknown. Such pegmatites are very common in this part of the dome, and show similarities to the pegmatites described at "Narragansett Pier Granite of Blackhall type" further east in Connecticut (Lundgren, 1967).

Return to vehicles.

0.0	27.2	Continue along Shell Beach Road.
0.4	27.6	Shell Beach Road bears left; do not take right fork (Point Road--Dead End). Immediately afterwards turn right into Rockledge Circle (one-way) and park.
		Walk back down Rockledge Circle and turn right onto Beach Road. After 0.1 mile road forks; Boulder Road to left and Great Harbour Drive to right. Bear right; first house on right (no 72) sits low by water. Cross garden of no. 72 (obtain permission) and descend steps to water's edge.

STOP 11.

This again shows SCGII and Lower Plainfield, as at the previous stop, but here the contacts between the two are marked by selvedges. Enclaves of very coarsely crystalline bi + plag + qz can be found in SCGII. Are these xenoliths of Lower Plainfield caught up in intrusive SCGII and subsequently deformed, or are they restites produced complementary to SCGII during migmatisation of Plainfield?

This outcrop shows a very strong fabric in SCGII. Note pods of musc + gt-bearing aplite elongate parallel to foliation--this material is similiar to the SCGIV developed in shear zones at STOP 10 and which will be seen again at STOP 12.

Walk round outcrop to front of house. This shows a possible contact between SCGI and SCGII. Granite here has the strong lineations typical of SCGII but lacks the characteristic garnet. Veins here are of the SCGIII type normally found in association with SCGI (as at STOPS 3 and 4). Is this rock transitional between SCGI and SCGII, or can a contact between two distinct types be traced? Could it simply be a high-strain facies of SCGI?

Look at outcrop by seawall. This shows the concordant contacts between Lower Plainfield and SCGII. Migmatised Plainfield has abundant coarse garnet in leucosomes.

Return to vehicles.

0.0	27.6	Drive round Rockledge Circle back to Shell Beach Road. Turn left on Shell Beach Road and drive back past stop 10 to Conn. Rte. 146.
0.6	28.2	Junction of Shell Beach Road and Conn. Rte. 146. Turn right onto Conn. Rte. 146.
1.3	29.5	Conn. Rte. 146 swings sharp left under railroad bridge.
0.4	29.9	Turn right on Mulberry Point Road.
0.4	30.3	Junction of Mulberry Point Road and Chaffinch Island Road; continue straight on Mulberry Point Road.
0.7	31.0	Follow Mulberry Point Road round to left.
0.1	31.1	Park on right.

Turn around, walk 0.1 mile back along Mulberry Point Road to junction with Daniel Avenue. Turn left onto Daniel Avenue.

Walk 0.4 mile up Daniel Avenue; follow the "one-way" sign. Turn right at stop sign onto Indian Cove Road. Walk 0.1 mile on Indian Cove Road, turn left onto Spencer Avenue.

At junction of Spencer Avenue and Prout St., go left down grass slope towards sea, keeping the red house on your right. This is a right-of-way. Turn right at shore and walk ~ 0.5 mile along outcrops.

TAKE CARE ON STEEP SLIPPERY ROCKS.

STOP 12.

The first set of outcrops shows a sharp contact between SCGII and amphibolites of the Lower Plainfield Formation. Folds and shears are well-developed (Plate 7). Garnetiferous leucosomes (SCGIV) occur in shear zones (Plate 8). None of these leucosomes can be traced for more than 3m. across the outcrop; their contacts to SCGII are generally sharp. The leucosomes trend sub-parallel to shears. Note the very strong lineation at this outcrop, marked by extreme elongation of quartz and feldspars.

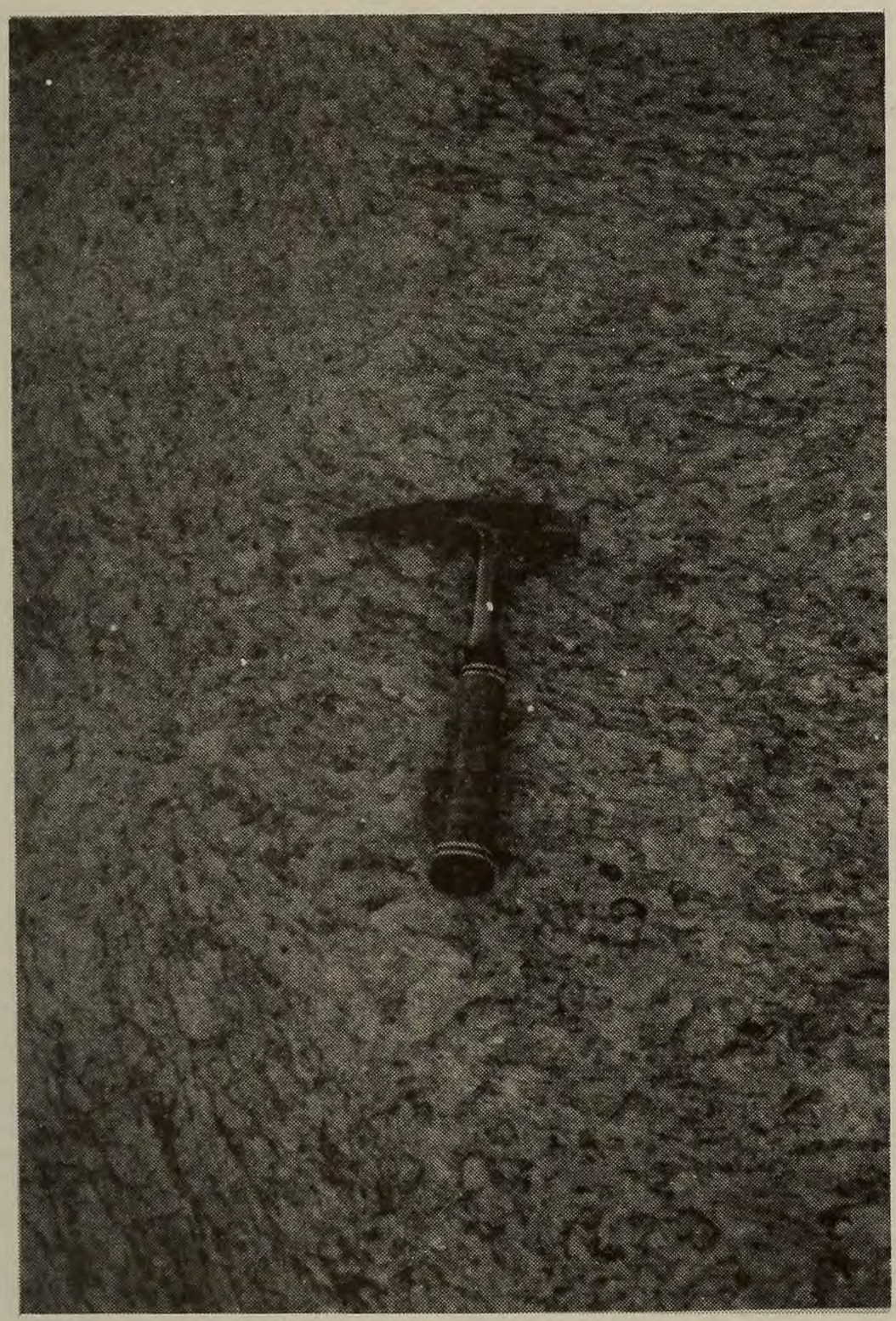

Plate 7 STOP 12. SCGII showing strong augen bent into shear zone at left.

Plate 9 STOP 12. Migmatised L.PL. with pegmatite (?)=SCGIII.

Plate 8 STOP 12. SCGIV concentrated in shear zones in SCGII.

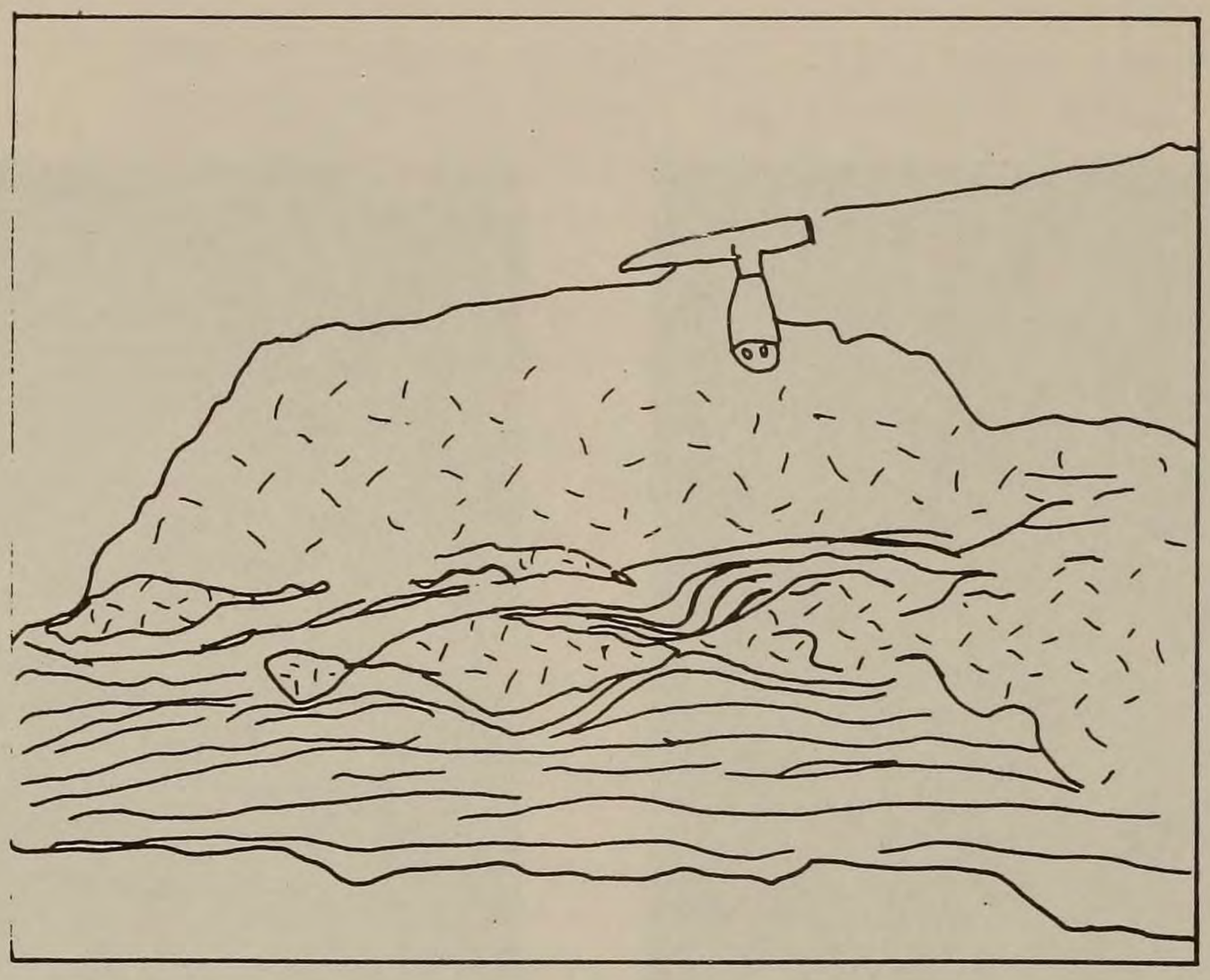

Figure 23 STOP 12. Drag folds around pegmatic boudins in L.PL.

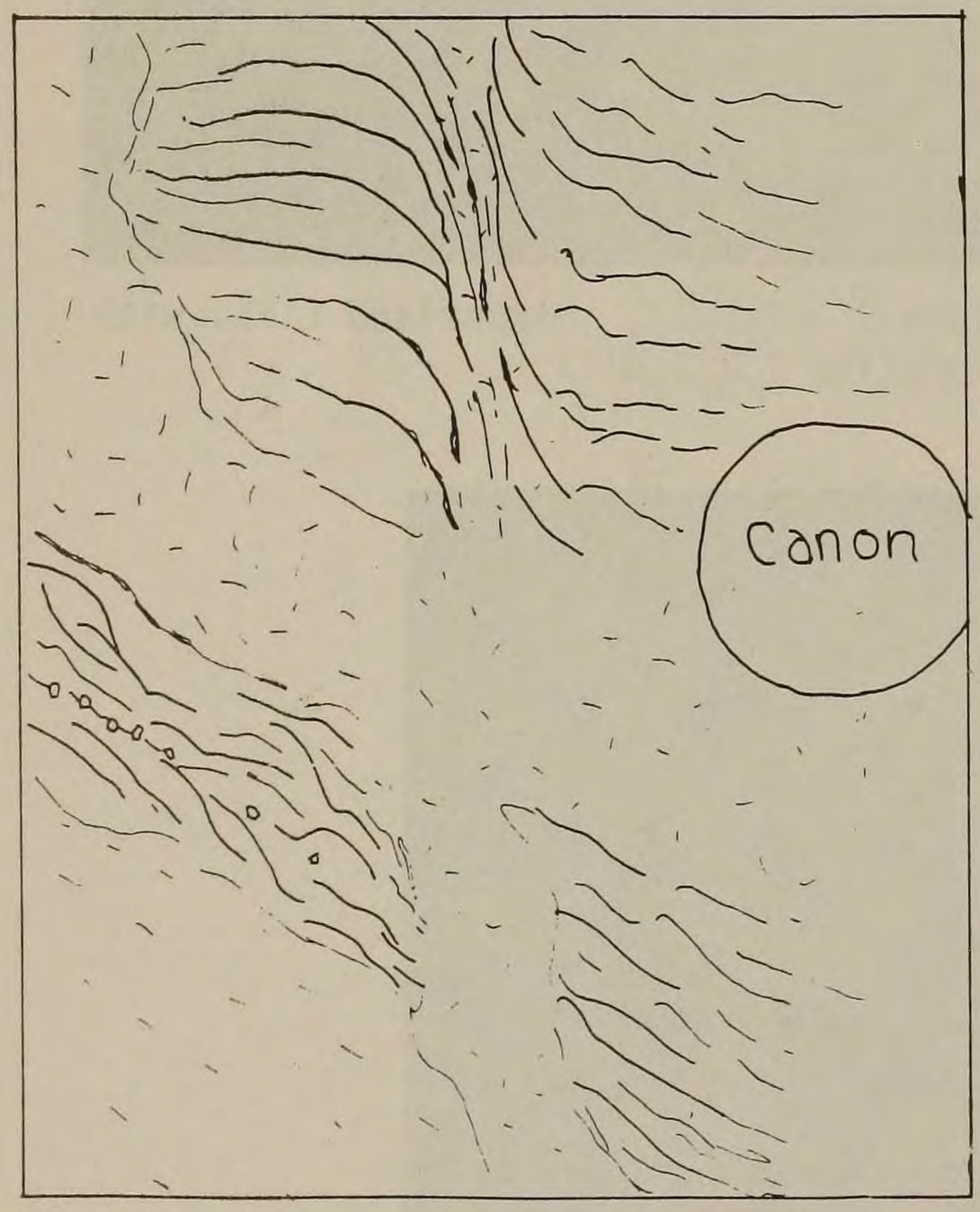

Figure 24 STOP 12. SCGIV concentrated in shear zones in SCGII.

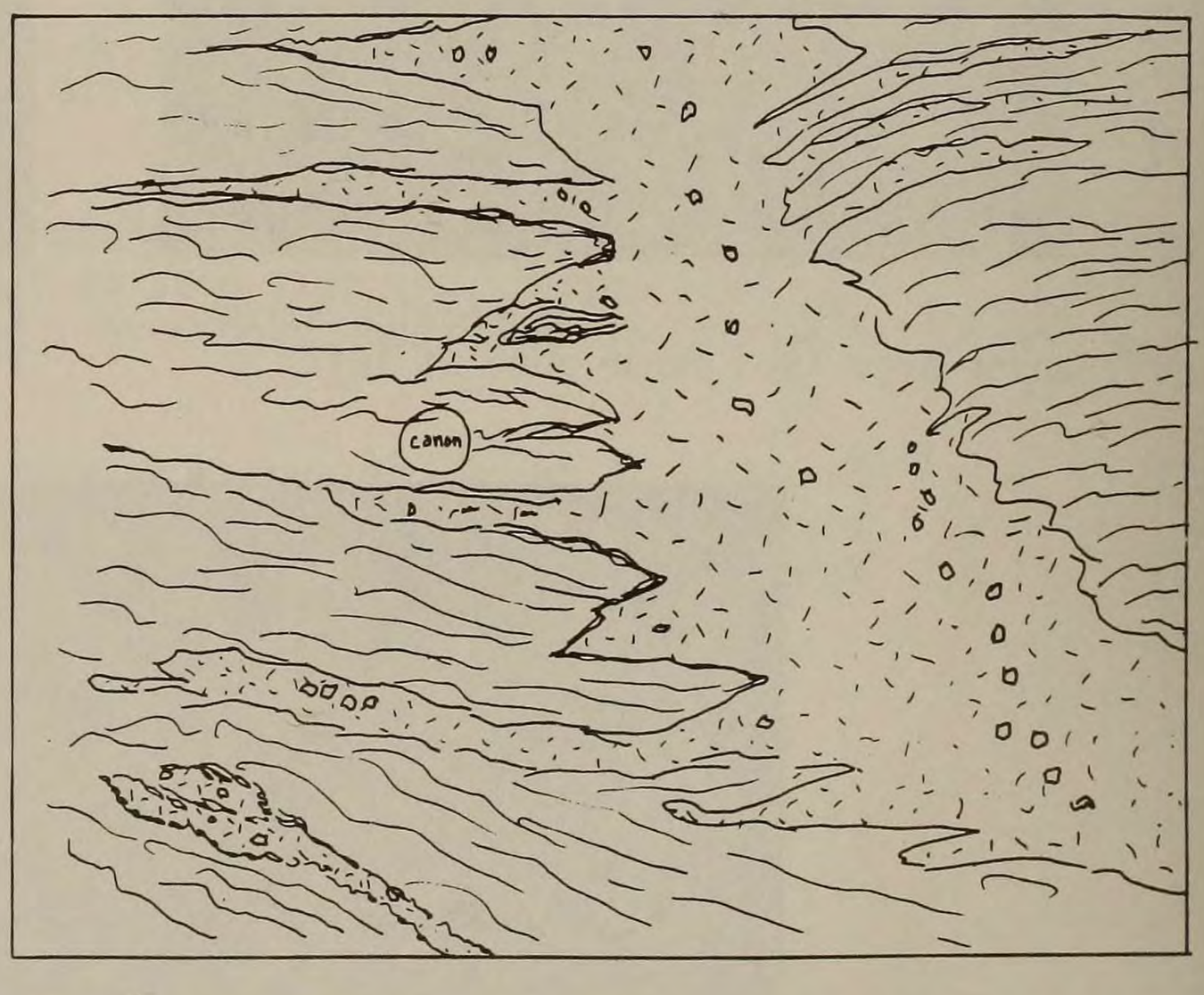

Figure 25 STOP 12. SCGIV forms diffuse patches within SCGII.

After ~ 0.25 mile we reach a very large shear zone just before the house on the point. A pegmatitic granite of the type seen at STOP 10 (possible NPG) occurs in this shear zone; it makes a sharp contact to an aplite which in turn cuts SCGII. A boudinaged vein in the Lower Plainfield here (see sketch) shows drag folds suggestive of top-to-S.E. motion.

Round the point, just below the cairn. Diffuse patches of SCGIV in SCGII have abundant coarse garnet.

50 meters further on, we return to the amphibolite seen at the first outcrop of this stop, veined by coarse Kspar + bi pegmatite of possible NPG-Blackhall type (see Plate 9).

Return to vehicles.

THIS IS END OF TRIP.

We will return to Branhaven Plaza to collect vehicles.

0.0	31.1	Drive back down Mulberry Point Road.
0.1	31.2	Junction of Daniel Avenue and Mulberry Point Road. Turn right onto Mulberry Point Road.
1.1	32.3	Junction of Mulberry Point Road and Conn. Rte. 146. Turn left onto Conn. Rte. 146.
0.7	32.9	SLOW-DANGEROUS BRIDGE
1.7	34.6	Junction of Conn. Rte. 146 and Thimble Islands Road. Turn right on Thimble Islands Road.
1.5	36.1	Turn left onto I-95S (signed for "New Haven and West").
1.0	37.1	Take exit 55 off I-95S. On reaching stop sign, turn right at U.S. Rte. 1 west. Drive 2.8 mile along Rte. U.S. 1 west; turn right at lights into Branhaven Plaza. There is no exit 53 in this direction.

FINAL NOTE: Excellent polished samples of granite from STOP 3 can be found facing the General Post Office in downtown New Haven.

Acknowledgements:

Our thanks to Eric Miller who bravely battled the January snows to aid in the preparation of this roadlog, and whose efforts in sweeping the snow from outcrops will be long remembered. My thanks also to Bob Tracy,

who introduced me to these rocks as part of a more general introduction to the U.S., and who has since offered boundless encouragement and advice. Preparation of this roadlog was partially supported by NSF Grant #EAR83-19673 to Tracy. Thanks also to Vince La Piana for help in sample collection, Tony Creamer for the XRF analyses and to Jeanne Martin for rapid typing of this M.S. Probe data were collected at the Geophysical Laboratory, Carnegie Institute, Washington, D. C.; my thanks for the use of that facility, and to David George for his patient instruction in the use of the probe.

I also wish to thank the wonderful people of Stony Creek, who welcomed me to their gardens, homes and hearts. In particular, I wish to thank Ann Shimuzi, Sonny Wallace, William van Wie, Alison Page, the Leete Family, Mr. & Mrs. Hall, Shirley Belden, Mr. Carter and John Barnes.